RESEARCH PERFORMANCE PROGRESS REPORT
Amended

U.S. Department of Energy National Energy Technology Laboratory

Cooperative Agreement: DE-FE0031558

Project Title: Partnership for Offshore Carbon Storage Resources and Technology Development in the Gulf of Mexico

Principal Investigator: Dr. Susan Hovorka

PH: 512-471-4863
susan.hovorka@beg.utexas.edu

Co-Principal Investigator: Dr. Tip Meckel

PH: 512-471-4306
tip.meckel@beg.utexas.edu

Co-Principal Investigator: Mr. Ramon Trevino

PH: 512-471-3362

ramon.trevino@beg.utexas.edu

Submission Date: October 31, 2019

DUNS Number: 170230239

The University of Texas at Austin
Jackson School of Geosciences
Bureau of Economic Geology
University Station, Box X
Austin, Texas, 78713

Project Period: April 1, 2018 – March 31, 2023

Reporting Period End Date: September 30, 2019

Report Frequency: Quarterly

Signature Submitting Official: ____

EXECUTIVE SUMMARY OF RESEARCH DEVELOPMENTS DURING THIS QUARTER

Project Management

Project PI, Dr. Susan Hovorka, communicated with pending subcontractor, Aker Solutions. Aker's legal department was closely reviewing UT's contract terms & conditions. As of the end of the quarter, the Aker subcontract was pending.

A senior BEG (Bureau of Economic Geology) research scientist associate began characterizing the geology of the middle Texas coast. The researcher is a staff member of the STARR (State of Texas Advanced Resource Recovery) program at BEG. STARR is a state of Texas funded program whose goal is to increase revenue from Texas state lands and state waters. The researcher's work will continue to be funded by STARR, but he will work closely and in conjunction with GoMCarb, as GoMCarb's and STARR's interests overlap in Texas state waters. The researcher's area of interest coincides with the recently leased Texas OBS 3D seismic dataset ("aka offshore OBS_South").

After several months and multiple iterations, the following list of "intellectual property categories and data" were submitted on September 4, 2019 to the NETL contract specialist for the current project. As of the end of the reporting quarter, no negative response had been received. Consequently, the co-PIs assumed that the list was accepted.

The project incorporated approximately 376 wells' formation picks and digital logs LAS into GoMCarb's IHS Petra, "Miocene Offshore CO2" project for well correlation and mapping. The tasks involved combining data from 3 different sources (GBDS (Gulf Basin Depositional Synthesis) database (see also next paragraph), IHS Enerdeq, Lexco OWL, and a pre-existing Petra project).

It was determined that a batch download of usable well log data from (Lexco OWL, https://www.lexco.com/) was not possible. Rather, a well by well interrogation will be necessary. This will most efficiently be accomplished by undergraduate research assistants (URAs). Three were hired and were being trained as of the end of the reporting quarter.

Offshore Storage Resource Assessment

The project incorporated approximately 376 wells' formation picks and digital logs LAS into GoMCarb's IHS Petra, "Miocene Offshore CO2" project for well correlation and mapping

During the reporting quarter, the large, "GalBrazos" Phases 1 and 2 dataset (Figure 2.1.1.1) was released to the public by the Bureau of Ocean Energy Management (BOEM). The dataset was added to the project's seismic database.

The BEG Geologic Data Continuum website (https://coastal.beg.utexas.edu/continuum) was searched for wells with rock data in the area in and near the Texas state water from Port Arthur to Corpus Christi (Figure 2.1.1.2. Twenty-two wells with geological samples (whole core, slabbed core, sidewall core, core chips/plugs; Figure 2.1.1.4) were identified. Results of the database search indicate one well has whole core, two wells have slabbed core, 13 wells have sidewall core, and 6 wells have core chips/ core plugs.

A senior BEG (Bureau of Economic Geology) research scientist associate, began characterizing the geology of the middle Texas coast. The researcher is a staff member of BEG's STARR (State of Texas Advanced Resource Recovery) program. STARR is a state of Texas funded program whose goal is to increase revenue from Texas state lands and state waters. The researcher's work will continue to be funded by STARR, but the results will be useful to GoMCarb, as GoMCarb's and STARR's objectives overlap in Texas state waters.

During this quarter fault interpretation of the Chandeleur Sound 3D seismic dataset was completed. A second iteration of stratigraphic interpretation was conducted cross-referencing the first round of picks, based on nearby picks from 2D seismic lines from ION Geophysical, with biostratigraphy from wells within the 3D survey area. Our current understanding is that no well drilled in the area ever produced hydrocarbons, but more research is required to validate this assumption.

For the deterministic static methodology case using Goodman et al. (2011) equations, an average total P_{50} capacity value of 28.25 Megatonnes [Mt] of CO_2 was estimated for the six reservoir layers in the High Island 10L Field (within structural closures).

Risk Assessment

LBNL (Lawrence Berkeley National Laboratory) finalized revision of a journal paper on the multiscale and multipath channeling of CO_2 flow in a hierarchical fluvial reservoir that is relevant to the GoMCarb storage sites.

Geologic Modeling

Compressibility Effects on Viscous Instability Under Sealing and Partially Sealing Boundaries:

1. The Saffman-Taylor approach analyzed the behavior of perturbation of a displacement front. A perturbation in the front position will grow when M>1 and the front will be unstable. This criterion is equivalent to determining whether the volumetric flux of the fluid increases with distance to the production end.

2. For steady-state flow (transparent outer boundary) adding compressibility always makes displacements more unstable. The simple reason for this is that as flow proceeds downstream, pressure declines, specific volume of the fluid increases and velocity increases. According to finding 1, a displacement will be unstable even if M<1.

3. For semi-steady-state flow (sealed outer boundary) displacements will become more stable as a front approaches a boundary simply because the front velocity must slow down there and average pressure rises.

Monitoring, Verification, and Assessment (MVA)

Research in the MVA effort continued to evaluate the potential of marine DAS (distributed acoustic sensing) for GCS (geological carbon sequestration) monitoring.

Lamar University investigated marine environmental conditions near the High Island 10L Field. Knowing environmental conditions is important for potential pipeline siting and site evaluations.

Infrastructure, Operations and Permitting

Lamar University modeled capacity of compressors needed to deliver CO2 from refineries to a pipeline and then to offshore storage using multiple scenarios.

There appears to be an alignment of interests and incentives to re-use existing oil and gas infrastructure in applications such as CO_2 storage offshore. Trimeric has not yet identified a database that addresses production platform infrastructure in High Island-10L Field area, the area currently considered as an analog for potential future development.

In September, co-PI, Tip Meckel, met with Robert Hatter and George Martin at the GLO (Texas General Land Office) to discuss CCUS developments, including an update of 45Q and implications for developing CCUS projects on lands owned and managed by the GLO. The meeting resulted in a better understanding of leasing concepts for CO_2 storage projects, easements for pipeline development, and comparisons with lease structures for wind and solar projects.

There can be various point sources of CO_2 (i.e. furnaces, boilers, fluidized catalytic crackers, methane steam reformers, and electric power generators). The feasibility of capture from such sources is based on the available amine technology used for CO_2 separation (i.e. capture). Attempting to capture from smaller CO_2 producers could result in higher operating expenses (OPEX). With the current technology, it is predicted that of the total refinery CO_2 emissions, 40% of those emissions occur from these point sources.[1] Aspen Plus™ was used to simulate the various CO_2 point sources. The process models were then used to size compressors needed for CO_2 delivery to a pipeline.

Knowledge Dissemination

In July, a knowledge dissemination team finalized an interview guide and in-depth interviews for the focus groups mentioned in the previous report. The team recruited participants and scheduled meeting times for the interviews. The interviews were carried out over a three-day period from July 30 to Aug. 1 in Beaumont, TX. In September, the team continued to analyze the data from the qualitative interviews, relying on these insights to develop the questions and stimuli for the survey, to be fielded this fall.

Task 1.0 – Project Management, Planning, and Reporting

Project PI, Dr. Susan Hovorka, had a conference call with pending subcontractor, Aker Solutions on September 3, 2019. Aker's legal department was closely reviewing UT's contract terms & conditions. As of the end of the quarter, the Aker subcontract was pending.

On July 19, the co-PIs met with representatives from subcontractor Trimeric Corp. at the Bureau of Economic Geology. Several plans and action items resulted from the meeting. Of note, Trimeric was scheduled to present results to a meeting of the GoMCarb research and outreach team and the GoMCarb advisory committee. The meeting occurred in Pittsburgh as a side meeting to the NETL, "Addressing the Nation's Energy Needs Through Technology Innovation – 2019 Carbon Capture, Utilization, Storage, and Oil and Gas Technologies Integrated Review Meeting."

On August 27, PI, Dr. Susan Hovorka presented, a talk (Figure 6.2.4) summarizing the project's accomplishments during the previous year at NETL's "Addressing the Nation's Energy Needs Through Technology Innovation – 2019 Carbon Capture, Utilization, Storage, and Oil and Gas Technologies Integrated Review Meeting."

A senior BEG (Bureau of Economic Geology) research scientist associate began characterizing the geology of the middle Texas coast. The researcher is a staff member of the STARR (State of Texas Advanced Resource Recovery) project at BEG. STARR is a state of Texas funded program whose goal is to increase revenue from Texas state lands and state waters. The researcher's work will continue to be funded by STARR, but he would work closely and in conjunction with GoMCarb, as GoMCarb's and STARR's interests overlap in Texas state waters. The researcher's work area coincides with the recently leased Texas OBS 3D seismic dataset ("aka offshore OBS_South" in Figure 2.1.1.1).

As a result of meetings co-PI, Dr. Tip Meckel had with Partners, TDI-Brooks and Fugro Marine GeoServices, Inc., in late September, submission of the report for Milestone 4, "Identification of Geologic storage prospects and data gaps," was delayed until November 1 (i.e., in order to incorporate results from the meetings into the report). The due date in the Milestone Table of the Project Management Plan was modified accordingly and submitted to the NETL Project Manager, Mary Sullivan.

The modified order (Figure 1.1) from Geometrics, Inc. for equipment for the HR3D (aka "P-Cable") seismic acquisition system was finalized. On September 26, the order shipped to the BEG Houston Research Center.

GEOMETRICS

Simplify your search

2190 Fortune Drive, San Jose, CA 95131 USA • Tel: (408) 954-0522 • Fax: (408) 954-0902

Sales Invoice	Page 1 of 1
Invoice Number	INV00862
Invoice Date	9/26/19
Sales Order Number	SN030517
Customer PO Number	2019C00518

Bill To	Ship To
UNIVERSITY OF TEXAS AT AUSTIN BUREAU OF ECONOMIC GEOLOGY PO Box X Accounts Payable - BEG AUSTIN, TX 78713 USA	Bureau of Economic Geology 11611 W Little York Road Houston, TX 77041 USA

Credit Terms	N30 (Amount due in 30 days)	**Carrier**	Aeronet (Aeronet Worldwide)
Freight Terms	Prepaid (Prepay and Add)	**Ship Method**	2_Day (2 Day)
F.O.B.	Dest (Destination)	**Ship Date**	9/26/19

Line	Product	Order Qty	UOM	Due Date	Unit Price	Total
1	**860-00137-01** Scoop Proof Upgrade Kit (860-00137-01)	6	EA	9/26/19	3,247.00	19,482.00
2	**860-00113-11** TAIL MODULE, GPS POWER SUPPLY, SP (0057750-50SP)	6	EA	9/26/19	7,831.00	46,986.00
3	**425-00070** *CASE, SHIPPING, BLACK, COLLAPSIBLE 48X45X34/148# (14-416-000)	1	EA	9/26/19	573.00	573.00
4	**425-00071** LID, CASE, SHIPPING, BLACK (14-416-001)	1	EA	9/26/19	0.00	0.00
5	**115-00122** DMS TOW CABLE, 10K BREAK *Note: cable 6 x 280 ft.*	1680	FT	9/26/19	0.00	0.00
6	**810-00118-02** P-CABLE 4 STREAMER NETWORK BOX, Birns NB004	1	EA	9/26/19	15,280.00	15,280.00
7	**900-00401-01** DMS TOW CABLE ASSY 1 WET END 10K BREAK SP (O-RING), Birns TC01252 TC01253 TC01254 TC01255 TC01256 TC01257	6	EA	9/26/19	10,791.50	64,749.00

Notes	Remittance		
Notes: 1) End user: University of Texas at Austin 2) Shipping & Insurance	Remittance ACH/Wire Information: Bank of the West Geometrics Account No. 030729467 Routing ABA # 121100782 Swift BWSTUS66	SubTotal Shipping Tax **Invoice Total**	147,070.00 2,920.00 0.00 **149,990.00**

These items are controlled by the U.S. Government and authorized for export only to the country of ultimate destination for use by the ultimate consignee or end-user(s) herein identified. They may not be resold, transferred, or otherwise disposed of, to any other country or to any person other than the authorized ultimate consignee or end-user(s), either in their original form or after being incorporated into other items, without first obtaining approval from the U. S. government or as otherwise authorized by the U. S. law and regulations.

Figure 1.1 – Invoice from Geometrics, Inc. for equipment needed for the planned HR3D seismic acquisition surveys. Note, this is a list of updated equipment vs. the original equipment list (i.e., after it was discovered that some of the equipment on the original list was incompatible with the existing HR3D system).

After several months and multiple iterations, the following list of “intellectual property categories and data” were submitted on September 4, 2019 to the NETL contract specialist for the current project. As of the end of the reporting quarter, no negative response had been received. Consequently, the co-PIs assumed that the list was accepted.

1. A publicly releasable list of protected data;
    a. Subsurface datasets such as:
        i. structure maps,
        ii. high resolution 3D (HR3D) seismic datasets
        iii. depositional facies maps,
        iv. reservoir models,
        v. geologic interpretations
2. A publicly releasable list of limited rights data;
    a. Proprietary data from Nehring database held by USGS
    b. “TexLa Transition Zone Merge” 3D seismic dataset (owned by SEI, Inc.)
    c. “Chandeleur Sound” 3D seismic dataset (owned by SEI, Inc.)
    d. “Texas Offshore OBS” 3D seismic dataset (owned by SEI, Inc.)
    e. “High Island” 3D seismic dataset (owned by SEI, Inc.)
    f. Proprietary seabed sediments geochemical data from TDI Brooks, Inc.
    g. Proprietary data from Fugro, Inc. (cores and geophysical logs, etc.)
    h. Fluid inclusions data purchased from Fluid Inclusion Technologies, Inc.
    i. Data and reports for the Pledger Field (Brazoria Co., TX) from Petro Tech Associates
    j. UTIG GBDS Consortium datasets:
        i. Gulf of Mexico regional 2D seismic network from ION Geophysics, Inc.
        ii. Gulf of Mexico geologic maps
        iii. Georeferenced images
        iv. Stratigraphic well tops
    k. Paleontological and stratigraphic well tops
    l. Previously acquired Raster and digital wireline well log curves & data files
3. A publicly releasable list of restricted computer software; and
    a. Haliburton Landmark geologic interpretation software package
    b. IHS Petra geologic interpretation software package
    c. RadExPro software from DECO Geophysical, SC
4. A listing of the minimum technical data deliverable with unlimited rights.
    a. Wireline well log curves (e.g., Gamma Ray, SP, resistivity, acoustic, density, etc.) digitized in-house
    b. Techniques developed for new deployment strategies of the HR3D system during 3D acquisition
    c. Depth structure maps of important stratigraphic horizons
        i. based on well tops
        ii. based on seismic interpretations
    d. Knowledge Dissemination (outreach) facts to
        i. To stakeholders
        ii. To technological audiences
    e. Leasing models useful for leasing blocks for CO_2 storage project development
        i. In state waters
        ii. In Federal (OCS) waters

f. Preliminary risk assessment of CO_2 release from truck/barge transfer operations
g. Facts on which to base the feasibility of use of subsea well head installations in the project AOI
h. Techniques and strategies for monitoring key geochemical parameters in the seawater column

Task 2.0 – Offshore Storage Resource Assessment

Subtask 2.1 – Database development:

Subtask 2.1.1 – Geographic Focus Area A - Lake Jackson, Lake Charles, and Lafayette (OCS) districts

Well Database

The project incorporated approximately 376 wells' formation picks and digital logs LAS into GoMCarb's IHS Petra, "Miocene Offshore CO2" project for well correlation and mapping. The tasks involved combining data from 3 different sources (GBDS (Gulf Basin Depositional Synthesis) database (see also next paragraph), IHS Enerdeq, Lexco OWL, and a pre-existing Petra project). We also corrected discrepancies, and validated data quality.

BEG (GCCC – Gulf Coast Carbon Center) staff received and incorporated several hundred, well-related datasets (well log curves, biostratigraphic, aka "paleo," tops and formation tops) from colleagues and GoMCarb Partners at GBDS (Gulf Basin Depositional Synthesis) in BEG's sister organization, the University of Texas at Austin Institute for Geophysics (UTIG). The GBDS datasets provide a significant advantage in GCCC's geologic characterization of the new (to CCS) middle-Texas coast region. The geologic tops result from over two decades of regional geologic interpretation by GBDS, including GBDS founder and world-renowned geologist, Dr. William "Bill" Galloway.

In order to add local geologic detail to the pre-existing GBDS regional well data (mentioned above), it will be necessary to augment the well dataset with commercially available data. It was determined that a batch download of usable well log data from one of the primary well data resources (Lexco OWL, https://www.lexco.com/) was not possible. Rather, a well by well interrogation would be necessary. We decided that this task could most efficiently be accomplished by undergraduate research assistants (URAs). Four students were interviewed for three available positions. Three were hired and were being trained as of the end of the reporting quarter. The URAs' efforts will be devoted mostly to bringing raster images from OWL database into the Petra project and later on to digitize wireline well log rasters (i.e., generate LAS files).

Seismic Database

Available 3D seismic datasets included leased proprietary and publicly available, regional datasets. The latter category continued to be augmented with the release of 1990s vintage 3D surveys in the federal OCS (Offshore Continental Shelf). During the reporting quarter, the large, GalBrazos Phases 1 and 2 dataset (Figure 2.1.1.1) was released to the public by the Bureau of Ocean Energy Management (BOEM). The dataset was added to the project's seismic database.

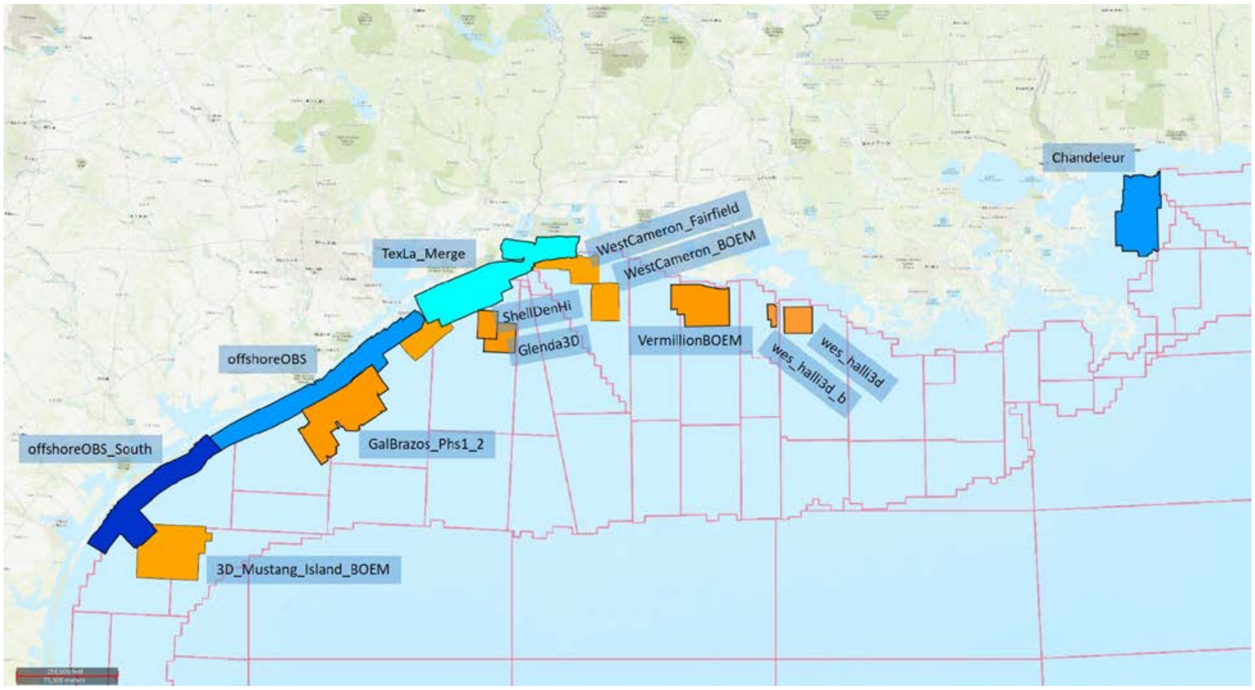

Figure 2.1.1.1 – Basemap of GoMCarb 3D seismic volumes. From left to right: Texas OBS mid-coast 3D ("aka offshoreOBS_South") (Cobalt blue), Texas OBS upper coast 3D (aka "offshoreOBS") (Cerulean blue), TXLA_Merge (Turquoise blue), and Chandeleur Sound 3D (Cerulean blue), and various publicly available NAMSS 3D seismic data sets (Orange).

Rock Samples Database

The BEG Geologic Data Continuum website (https://coastal.beg.utexas.edu/continuum) was searched for wells with rock data in the area in and near the Texas state water from Port Arthur to Corpus Christi (Figure 2.1.1.2). *(Continuum is an application that provides access to the Bureau of Economic Geology's collections of geological samples, geophysical logs, and related materials.)* Wells with geological sample are mostly distributed onshore (Figure 2.1.1.3). Twenty-two wells have geological samples (whole core, slabbed core, sidewall core, core chips/plugs; Figure 2.1.1.4). Results of the database search indicate that there is one well has whole core, two wells have slabbed core, 13 wells have sidewall core, and 6 wells have core chips/ core plugs. The depth ranges of each geological sample still need to be confirmed (Table 2.1.1.1).

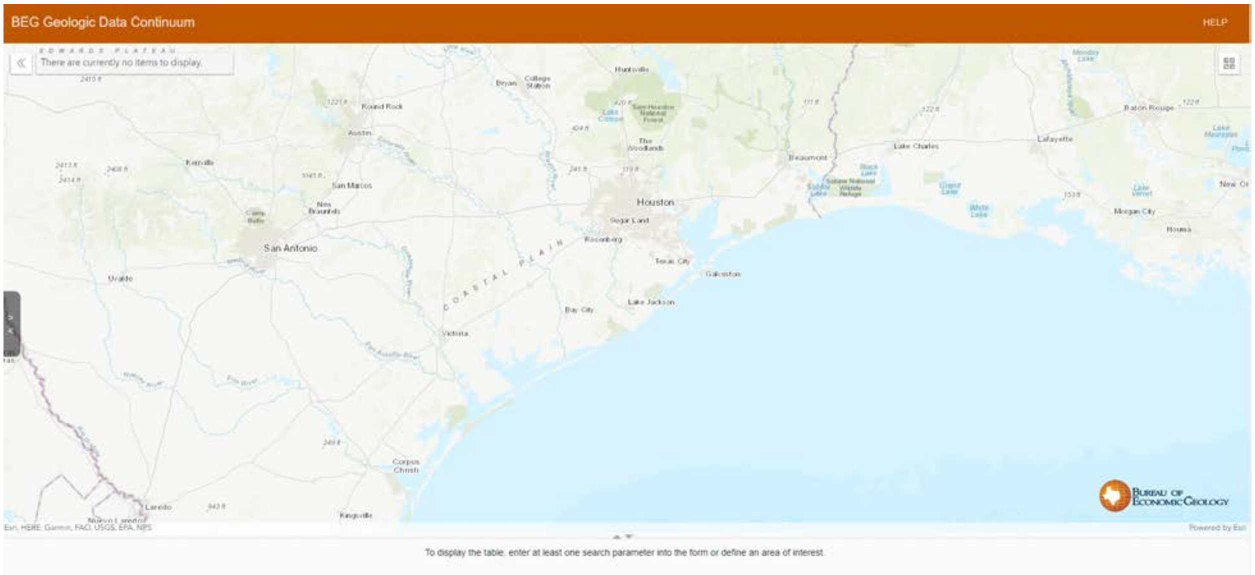

Figure 2.1.1.2 – Overview of the study area in the BEG Geologic Data Continuum website.

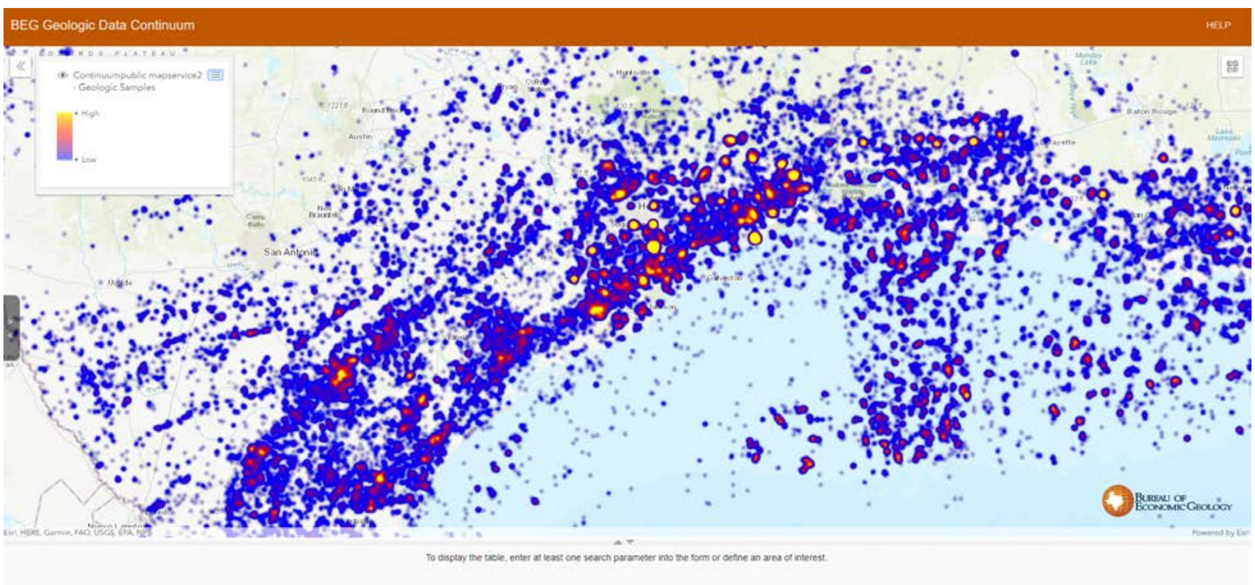

Figure 2.1.1.3 – Distribution of geologic samples (core, cuttings, plugs).

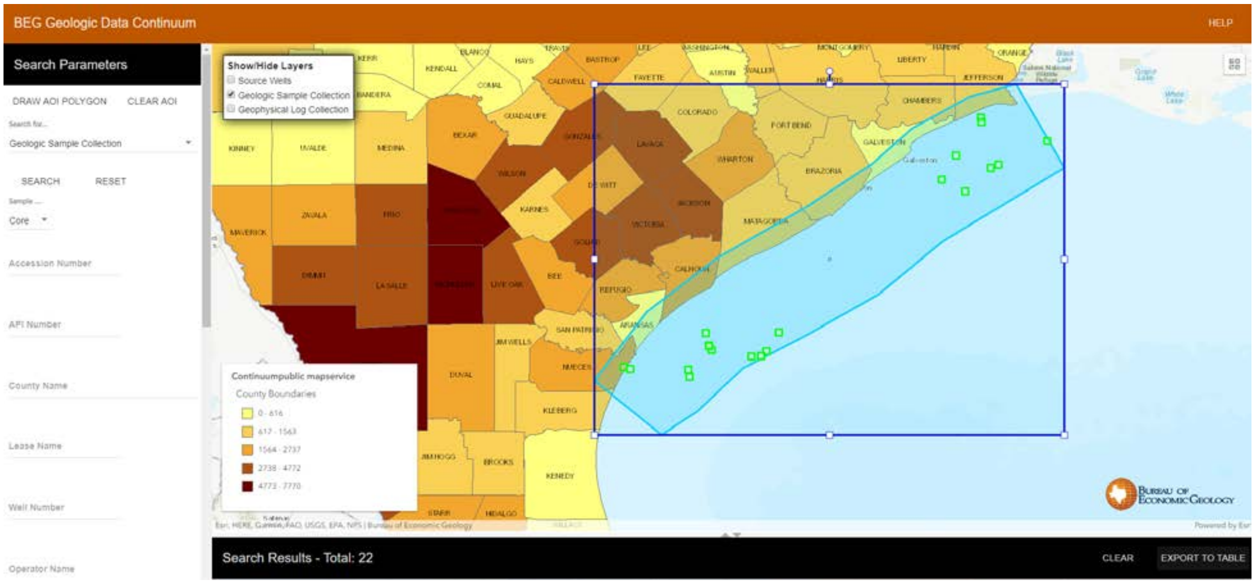

Figure 2.1.1.4 – Map showing the 22 wells (green circles) that have rock samples inside the area of interest (green polygon).

Sample ID	Sample Type	API Number	Lease Name	Well Number	Operator Name	Field Name	County Name	State Name	Country Name	Surface Lo	Surface La	Top Depth	Bottom De	Facility Name
214317	CORE CHIPS/CORE PLUGS	427083029600	STATE TRACT		AMOCO PRODUCTION CO	HIGH ISL BLK 24L				-94.1373	29.58314	1000	14231	Houston CRC
197425	CORE CHIPS/CORE PLUGS	42602000490000	BONER B	12	FUHRMAN PETRO CORP	FUHRMAN - MASCHO	Andrews	Texas	USA	-97.0941	27.72853	496	13870	Houston CRC
217236	CORE CHIPS/CORE PLUGS	427034015800	OCS-G-3733	A-6	ARCO		MATAGORDA		United States	-96.4282	27.89559	1	9882	Houston CRC
161268	CORE CHIPS/CORE PLUGS	177004082100	OCS-G-10549		ARCO					-93.5758	29.41239	600	14400	Houston CRC
192079	CORE CHIPS/CORE PLUGS	427034013400	OCS-G-3733	A-5	VASTAR	703-L				-96.4281	27.89562	980	10200	Houston CRC
172314	CORE CHIPS/CORE PLUGS	427054007100	OCS-G-4183		ARCO OIL & GAS	BRAZOS				-95.941	27.85795	500	18231	Houston CRC
159497	SIDEWALL CORE	427124003900	OCS-G-3927	1	UNKNOWN	Unknown				-96.0709	27.81959	410	10386	Houston CRC
185412	SIDEWALL CORE	427084011600	OCS-G-4730	1	ARCO OIL & GAS CO.		HIGH ISLAND		United States	-94.0555	29.21494	150	15519	Houston CRC
205339	SIDEWALL CORE	427024003500	OCS-G-3019	4	UNKNOWN	MUSTANG ISLAND				-96.6012	27.72231	1040	8560	Houston CRC
158989	SIDEWALL CORE	427084013000	OCS-G-4574	2	UNKNOWN	Unknown				-94.3438	29.30623	300	9634	Houston CRC
208909	SIDEWALL CORE	427084014500	OCS-G-6166	1	ARCO					-94.4669	29.12953	350	14120	Houston CRC
184367	SIDEWALL CORE	427034002400	OCS-G-3733	1	UNKNOWN	MATAGORDA ISLAND				-96.4248	27.90423	400	13310	Houston CRC
171994	SIDEWALL CORE	427054006601	OCS-G-4066	1 ST 1	UNKNOWN	BRAZOS				-95.8404	27.99838	300	17480	Houston CRC
191544	SIDEWALL CORE	427084016000	OCS-G-4731	2	UNKNOWN	Unknown				-93.9854	29.23644	340	15293	Houston CRC
192955	SIDEWALL CORE	427084015700	OCS-G-6178	2	UNKNOWN	HIGH ISLAND				-94.2662	29.04394	370	10120	Houston CRC
176163	SIDEWALL CORE	427054005600	OCS-G-2664	A-1	ATLANTIC RICHFIELD					-95.9896	27.82282	543	17760	Houston CRC
213131	SIDEWALL CORE	427034022000	OCS-G-4547	A-3	UNKNOWN	MATAGORDA ISLAND				-96.4526	27.99314	300	12682	Houston CRC
152337	SIDEWALL CORE	427024004000	OCS-G-3021	2	UNKNOWN	762-L				-96.5897	27.66984	0	9065	Houston CRC
211091	SIDEWALL CORE	427083022800	S/L 59454	B-2	ARCO OIL CO.	HIGH ISLAND				-94.1311	29.54754	1000	8825	Houston CRC
186070	SLABBED CORE	427034012600	OCS-G-4708	1	UNKNOWN	MATAGORDA ISLAND				-96.4046	27.86892	360	11873	Houston CRC
205338	SLABBED CORE	427054007300	OCS-G-2664	A-2	UNKNOWN	BRAZOS				-95.9896	27.82282	460	17153	Houston CRC
172981	WHOLE CORE	423552030100	MUSTANG ISLAND	1	ATLANTIC REFINING CO.		NUECES	Texas	USA	-97.1471	27.74065	2025	16240	Houston CRC

Table 2.1.1.1 Table extracted from the BEG Geologic Data Continuum website.

Subtask 2.1.1.1 Western Louisiana, Lafayette and Lake Charles Districts

No activity this quarter

Subtask 2.1.1.2 Mid-Texas coast offshore Houston to Corpus Christi

Well log correlations in the state waters offshore from Galveston to Matagorda Bay. The intent is to extend correlations of the Miocene interval of interest. There are currently 2523 wells in the study area, 2380 of which have only wireline well log raster data (black dots); 1680 wells have digital SP curves (green dots); 384 have digital gamma ray (red rhombs) and 7 wells have whole core (olive-green squares) (Figure 2.1.1.2.1). A regional stratigraphic cross-section with initial interpretations is shown in figure 2.1.1.2.2. The cross-section's line of section is shown in blue (Figure 2.1.1.2.1). The cross section is flattened on MFS9, which is equivalent to the lower Miocene

Amphistegina B (AMPH_B) biochronozone. The lower depth limit for CO_2 injection (OVERPRESSURE) is determined by the depth at which the hydrostatic pressure in the subsurface is significantly exceeded and is shown on the cross section by the dashed brown line. The top of overpressure is obtained from a U.S. Geological Survey geopressure-gradient model of the regional pressure system spanning the onshore and offshore portions of Texas and Louisiana (Burke et al., 2012; Pitman, 2011).

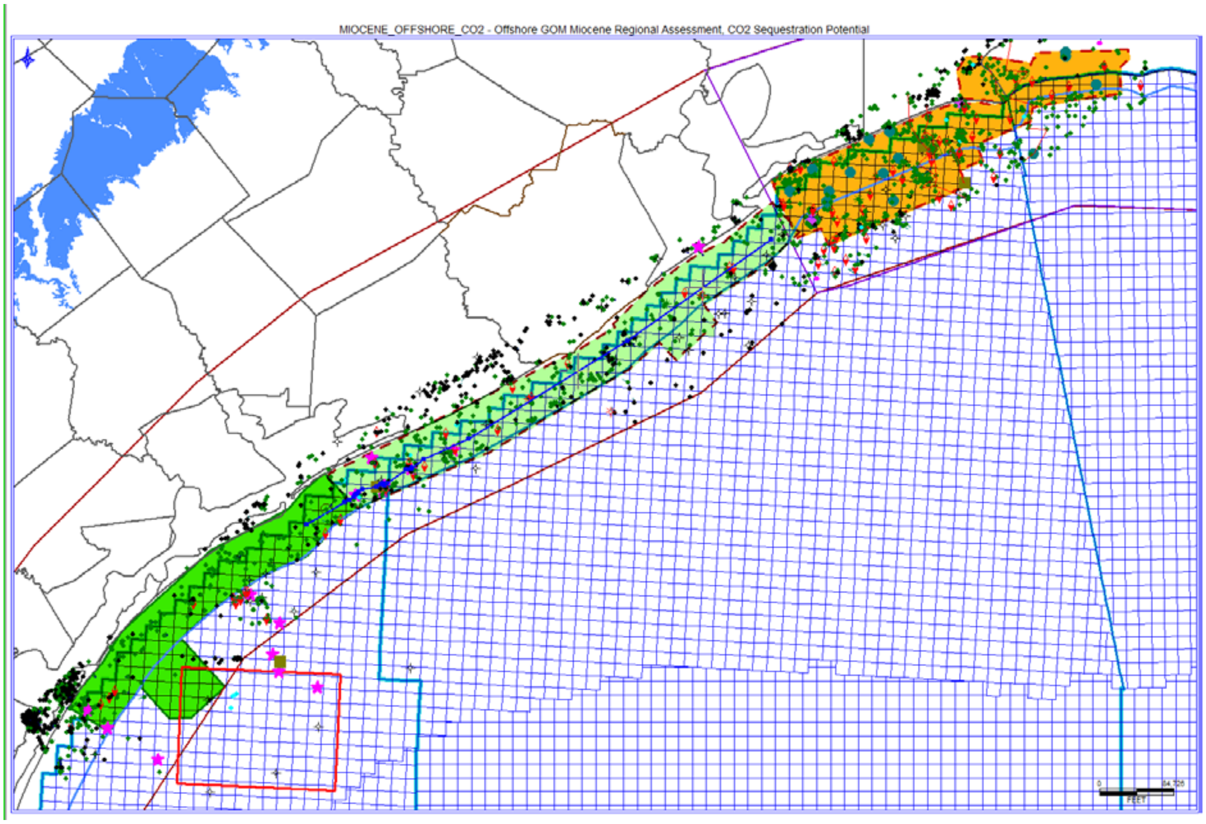

Figure 2.1.1.2.1 – Map of the study area including wells and primary 3D seismic datasets (highlighted in green and orange) The state - federal waters boundary is demarcated by the blue line subparallel to the coast.

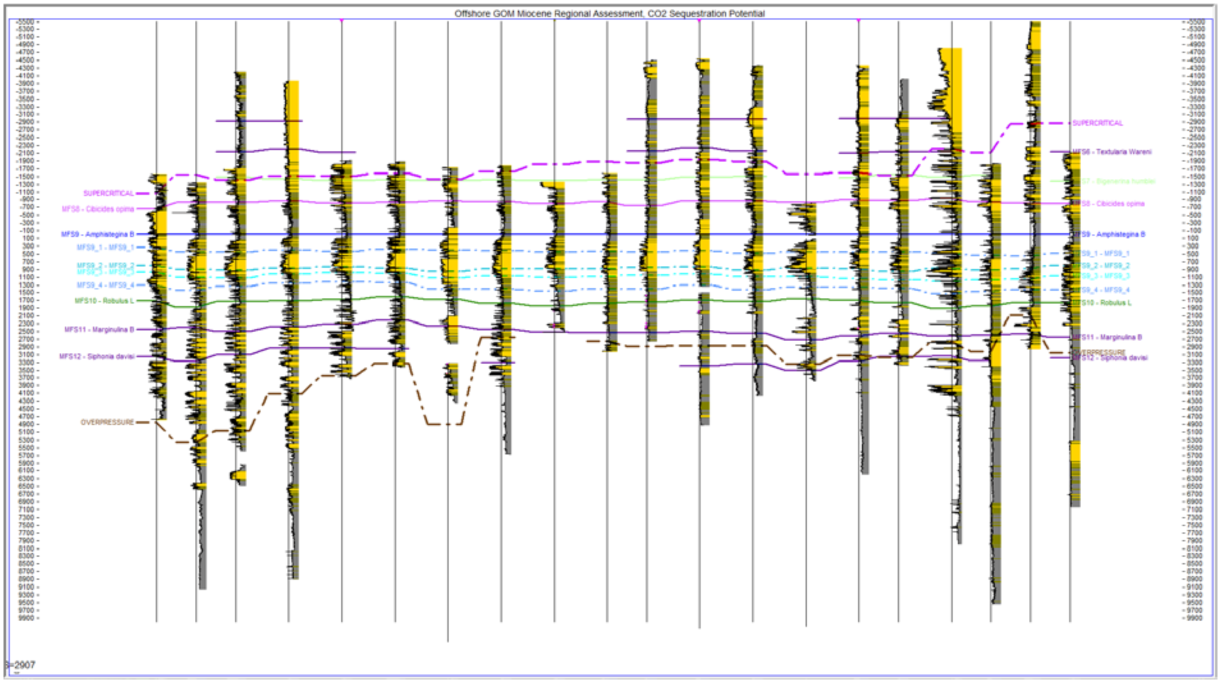

Figure 2.1.1.2.2 – Strike-oriented stratigraphic cross-section, offshore middle Texas coast. The line of section is shown in figure 2.1.1.2.1.

Structural interpretation

Semblance horizon slices were used in the initial structural interpretation phase because this technology allows a mathematical assessment of the 3D seismic data volume without being biased by previous interpretation. Vertical seismic sections of the Texas OBS, oriented in dip direction (Figures 2.1.1.2.3 and 2.1.1.2.4) were then extracted from the 3D seismic amplitude volume for analysis. The fault segments identified from the semblance horizon slices were projected onto these extracted dip seismic sections so fault segments could be correlated to a particular fault line in the vertical seismic section. This process will continue until all identifiable fault planes have been interpreted and correlated. A key stratigraphic horizon (MFS09) has been mapped throughout several 3D seismic volumes (Figure 2.1.1.2.5) and has been subsequently extended to the Texas OBS mid-coast 3D seismic volume. As of September 30th, 2019, over 101 faults planes have been interpreted and triangulated (Figures 2.1.1.2.6 and 2.1.1.2.7) within the Texas OBS upper coast 3D seismic survey.

Figure 2.1.1.2.3. An uninterpreted dip section from the Texas OBS 3D seismic volume.

Figure 2.1.1.2.4 – Interpreted cross-section of the Texas OBS. Faults are in yellow, and the MFS09 horizon is red.

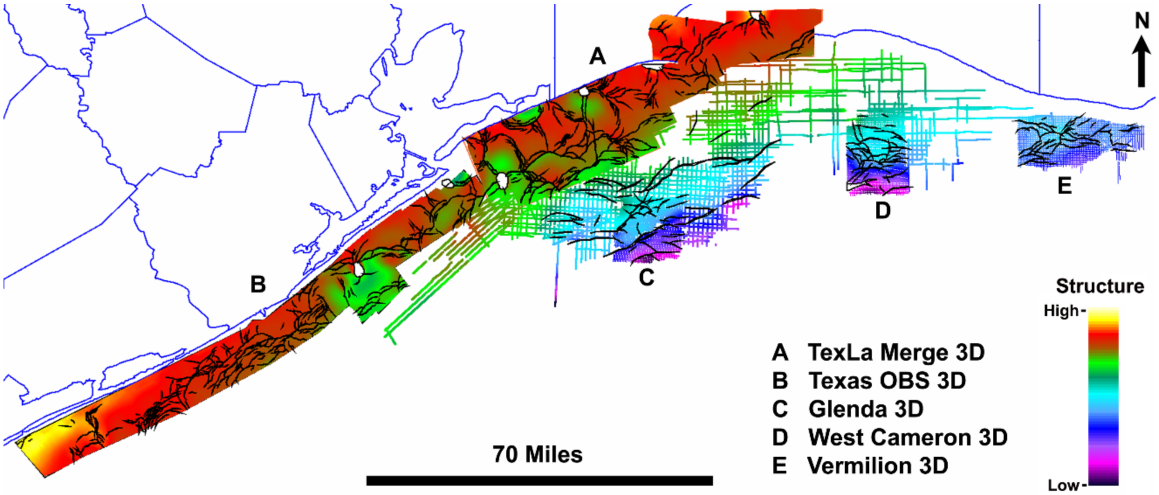

Figure 2.1.1.2.5 – Current status of the regionally interpreted MFS09 surface.

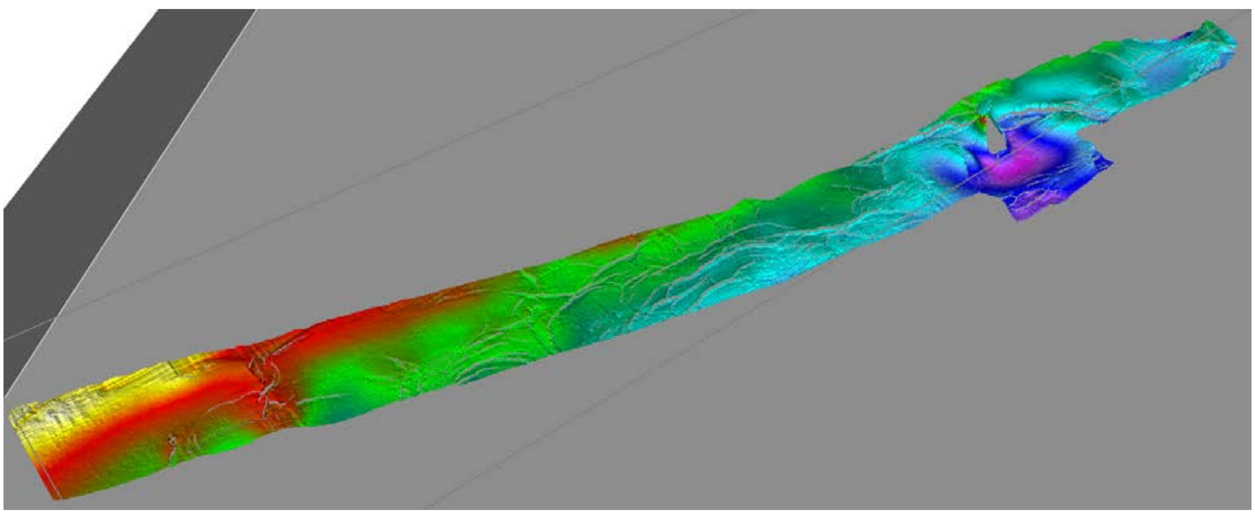
Figure 2.1.1.2.6 – Three-dimensional view of interpreted horizon MFS09 (Offshore OBS), with fault polygons (gray).

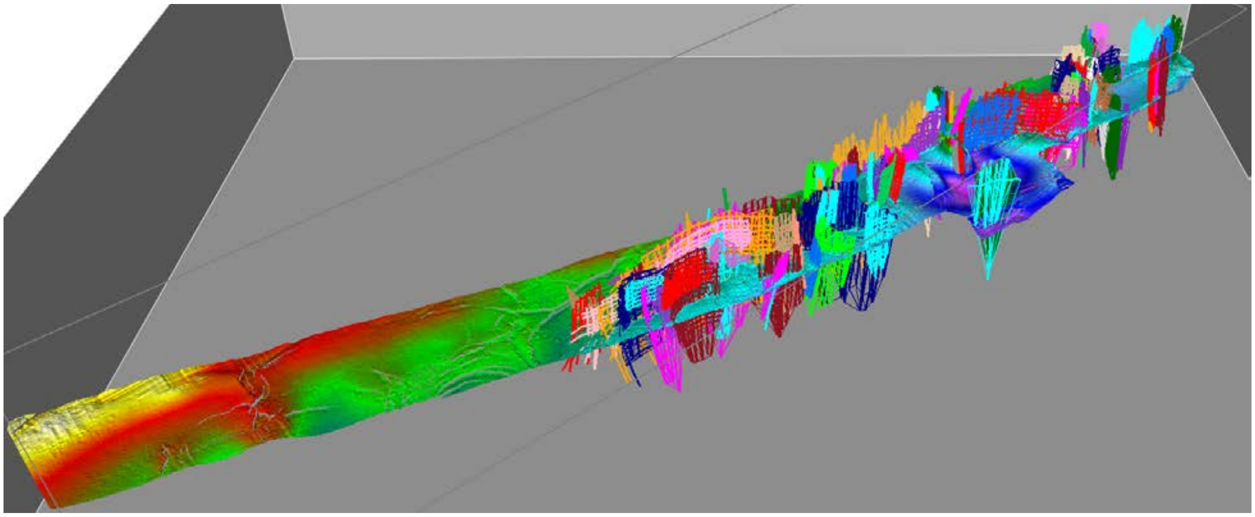

Figure 2.1.1.2.7 – Three-dimensional view of interpreted horizon MFS09 (Offshore OBS), with fault polygons (gray), and correlated fault planes (101 in total).

Subtask 2.1.1.3 Buoyant storage capacity

No activity this quarter

Subtask 2.1.1.4 Fluid inclusion stratigraphy

No activity this quarter

Subtask 2.1.2 – Geologic Characterization of Chandeleur Sound, LA

Fault Interpretation

During this quarter fault interpretation was completed. Faulting is predominant along the continental shelf break and less predominant down the slope. On the continental shelf, north of the shelf break, there is no faulting save a few small faults in the very Northeast corner of the seismic coverage area.

Figure 2.1.2.1 Plan view of all faults in the Chandeleur Seismic Area. Yellow N-S line is section 158.

Figure 2.1.2.3 A Cross-Sectional View of faults along Section 158.

Stratigraphic Interpretation

A second iteration of stratigraphic interpretation was conducted cross-referencing the first round of picks, based on nearby picks from 2D seismic lines from ION Geophysical, with biostratigraphy from wells within the 3D survey area. Once this iteration of stratigraphic interpretation was completed, grids of each surface and thickness maps of each section were produced. In case of any future adjustments, we will wait until a later phase before exporting and formatting these maps to GIS so as not to unnecessarily use our resources.

Figure 2.1.2.4 Cross-sectional view of Iteration 2 stratigraphic horizons. Red, Top cretaceous; Orange, top Oligocene; Yellow, top lower Miocene 1; Green, top lower Miocene 2; Blue, top Middle Miocene; Purple, top Upper Miocene.

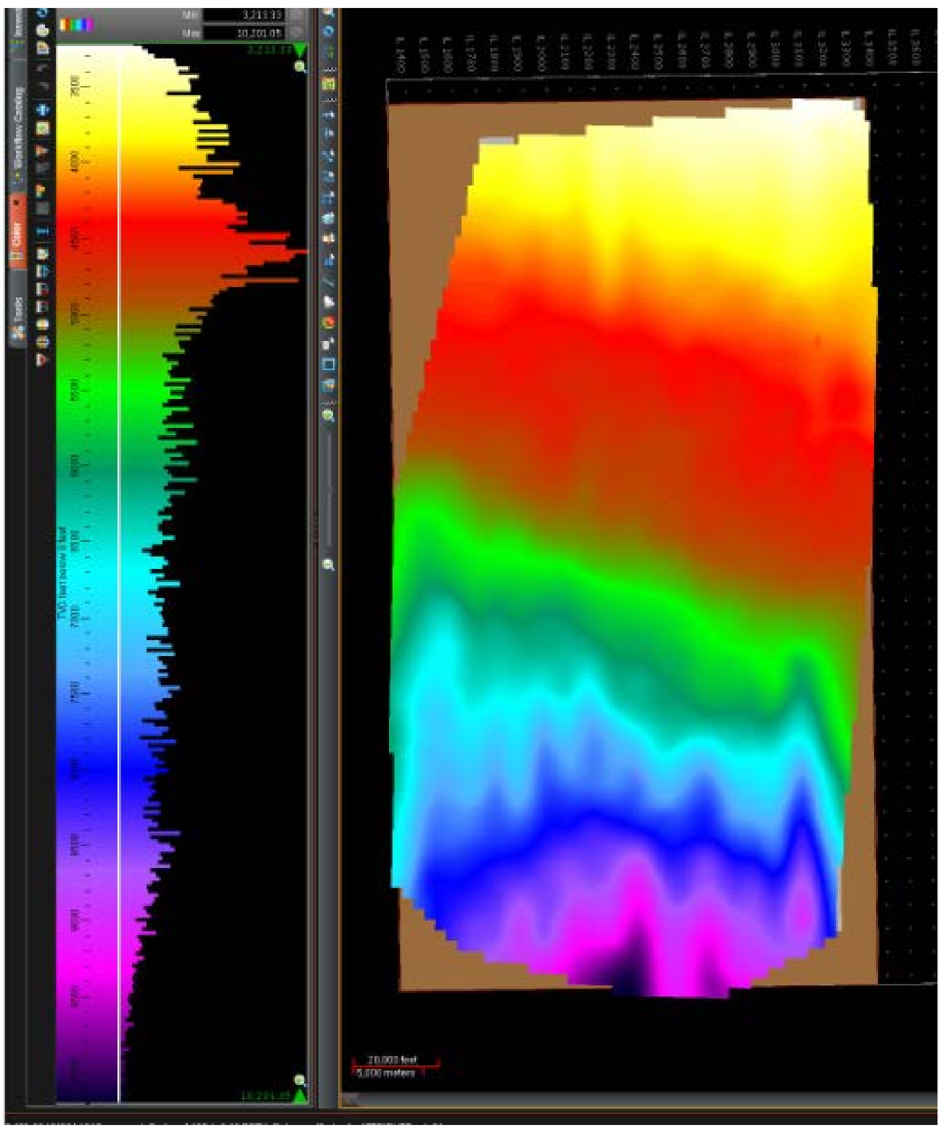

Figure 2.1.2.5 Example of a surface grid, top Middle Miocene

Identification of potential traps/seals

Identification of potential traps and seals will be focused in, but not limited to, the shelf region of the SA, behind (north of) the LM2 shelf break (figure 2.1.2.6). The focus will be on the shelf because it is nearly devoid of faulting decreasing the risk of broken potential seals. The Miocene stratigraphy – particularly that of the Lower and Middle Miocene – are of highest interest. One example is shown below of a sequence of onlapping reflectors bound by a fault on the southern end.

Figure 2.1.2.6 - (right) Plan view of the Lower Miocene
(LM2) shelf break.

Figure 2.1.2.7 - Cross-sectional view of one potential trap/seal (circled in red): onlapping shelf stratigraphy bound by a fault near the shelf break.

Paleoenvironmental Interpretation

Amphistegina B, a benthic foraminifer well-known and highly utilized along the GoM shelf as a marker of a Middle Miocene seal, is conspicuously absent in the Chandeleur SA. There are multiple potential explanations for this. First, only three wells (GBDS 12088, 12089, and 12090, shown below) with available biostratigraphy summaries drilled deep enough to potentially recover samples of this species; therefore, any interpretation will be inherently skewed by limited data. Fortunately, each of these three wells is in a different depositional setting: one on the shelf (shallow, unfaulted), one on the shelf break (deeper and highly faulted), and one off the continental shelf (deep water, moderately faulted). The working hypothesis is that the GoM sea-level was dropping and the paleo shoreline was approximately where the shelf break is interpreted to be meaning the continental slope was subaerially exposed, and the submarine setting was too deep to accommodate this neritic species. This also means that the seal associated with this biohorizon was likely not deposited here. An important side-note is that the neritic-dwelling *Amphistegina* B has a deep-water equivalent, *Globigerinatella insueta*, which also was not observed or annotated in any of the available biostratigraphy summaries.

It should also be noted that through the decades, with the re-calibration of biohorizons and the geologic time scale, the top of *Amphistegina* B is now calibrated at 15.59 Ma, which is closer to marking the top of the Early Miocene (15.97 Ma) than the Middle Miocene (11.62 Ma) according to the 2016 Geologic Time Scale (Ogg et al., 2016).

Well Information

173 wells have been drilled inside the Chandeleur SA (listed in the table below). Target zones appear to have been either the Cretaceous or the Miocene. Currently, we are certain that 76% of these wells were drilled and non-producers. It is unclear whether or not the other 24% were drilled, and if they were what their production status was. At this time, it does not appear that any well drilled in this area was ever producing, but more research is required to validate this assumption. We will be further investigating the Miocene to see what regional geologic aspects may have lent to the lack of success in this area.

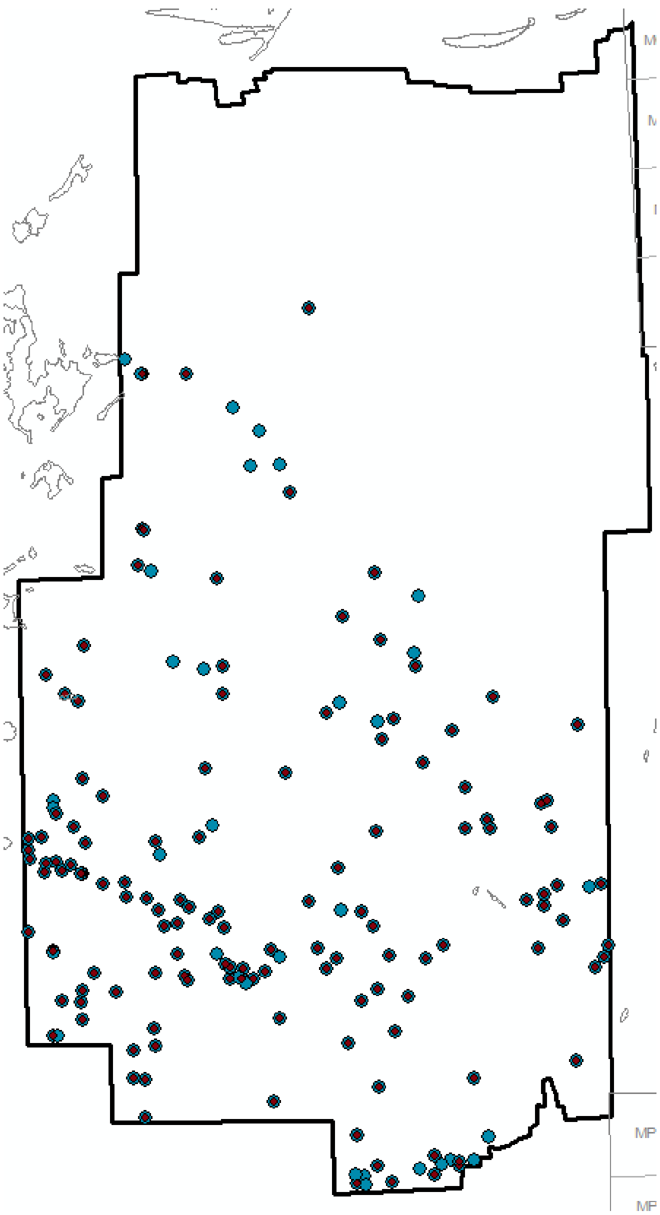

Figure 2.1.2.9 – Map showing all wells drilled in the Chandeleur SA (blue dots). Wells drilled that are definitely dry have a smaller red dot within the blue dot.

Table 2.1.2.1 well list of dry/plugged/abandoned wells in the Chandeleur SA

API	Company	Well	WellNo	Depth	Status
17-726-00229	FOREST OIL CORPORATION	SL 4569	001	9000	ACT 404 ORPHAN WELL-ENG
17-726-00230	FOREST OIL CORPORATION	SL 4570	001	0	ACT 404 ORPHAN WELL-ENG
17-726-00267	ARCO O & G CO-DIV ATL RICH CO	SL 4754	001	9500	ACT 404 ORPHAN WELL-ENG
17-726-20020	PLACID OIL COMPANY	SL 5384	001	9000	ACT 404 ORPHAN WELL-ENG
17-726-20026	KERR-MCGEE CORPORATION	SL 5383	001	9000	Completed
17-726-20027	KERR-MCGEE CORPORATION	SL 5384	001	0	DRY AND PLUGGED
17-726-20028	KERR-MCGEE CORPORATION	SL 5382	001	0	DRY AND PLUGGED
17-726-20029	KERR-MCGEE CORPORATION	SL 5385	001	0	DRY AND PLUGGED
17-726-20030	TERRA RESOURCES, INC.	SL 5384	001	6480	DRY AND PLUGGED
17-726-20097	AMOCO PRODUCTION COMPANY	SL 6689	001	9500	DRY AND PLUGGED
17-726-20243	SUPRON ENERGY CORPORATION	SL 9301	001	7878	DRY AND PLUGGED
17-726-20241	INACTIVE OPERATOR	SL 9177	001	9455	DRY AND PLUGGED
17-726-20264	POGO PRODUCING COMPANY	SL 9446	001	0	DRY AND PLUGGED
17-726-20267	POGO PRODUCING COMPANY	SL 9445	001	0	DRY AND PLUGGED
17-726-20268	SUPRON ENERGY CORPORATION	SL 9300	001	0	DRY AND PLUGGED
17-726-20269	SUPRON ENERGY CORPORATION	SL 9300	002	0	DRY AND PLUGGED
17-726-20270	POGO PRODUCING COMPANY	SL 9445	002	9000	DRY AND PLUGGED
17-726-20276	POGO PRODUCING COMPANY	SL 9446	003	0	DRY AND PLUGGED
17-730-00005	INACTIVE OPERATOR	SL 5110	001	0	DRY AND PLUGGED
17-730-20026	RIPCO	SL 6168	001	5505	DRY AND PLUGGED
17-730-20025	RIPCO	SL 6168	002	5519	DRY AND PLUGGED
17-730-20022	AMOCO PRODUCTION COMPANY	SL 6625	001	9000	DRY AND PLUGGED
17-730-20006	THE SUPERIOR OIL COMPANY	VUA;HA WILKINSON	001	0	DRY AND PLUGGED
17-730-20006	THE SUPERIOR OIL COMPANY	SL 8526	001	0	DRY AND PLUGGED
17-730-20014	PEL-TEX OIL COMPANY, INC.	SL 11778	001	17413	DRY AND PLUGGED
17-730-20015	ARCO O & G CO-DIV ATL RICH CO	SL 11769	001	6702	DRY AND PLUGGED
17-730-20019	INACTIVE OPERATOR	SL 11693	001	6546	DRY AND PLUGGED
17-730-20020	INACTIVE OPERATOR	SL 11694	001	6500	DRY AND PLUGGED
17-730-20021	TENNECO OIL COMPANY, E.G.D.	SL 12825	001	6400	DRY AND PLUGGED
17-730-20023	OPMI OPERATING COMPANY	SL 13547	001	4900	DRY AND PLUGGED
17-730-20030	MANTI EXPLORATION OPERATING LLC	SL 17387	001	5555	DRY AND PLUGGED
17-730-20032	MANTI OPERATING COMPANY	SL 17659	001	6877	DRY AND PLUGGED
17-730-20031	MANTI OPERATING COMPANY	SL 17387	002	7274	DRY AND PLUGGED
17-730-20033	MANTI OPERATING COMPANY	SL 17659	002	10800	DRY AND PLUGGED

17-730-20034	CAPCO OFFSHORE, INC.	SL 17812	001	4800	DRY AND PLUGGED
17-730-20035	CAPCO OFFSHORE, INC.	SL 17388	001	4600	DRY AND PLUGGED
17-730-20036	PXP LOUISIANA L.L.C.	SL 17389	001	5000	DRY AND PLUGGED
17-730-20037	PXP GULF COAST INC.	SL 17388	002	4700	DRY AND PLUGGED
17-730-20038	CAPCO OFFSHORE, INC.	SL 17387	001	5550	DRY AND PLUGGED
17-727-00004	SHELL OIL COMPANY	SL 2254	001	10035	DRY AND PLUGGED
17-727-00058	TEXACO, INC.	SL 2257	001	10315	DRY AND PLUGGED
17-727-00005	PHILLIPS PETROLEUM CO.	SL 2306	001	9500	DRY AND PLUGGED
17-727-00003	INACTIVE OPERATOR	SL 2533	001	9500	DRY AND PLUGGED
17-727-00006	PHILLIPS PETROLEUM CO.	SL 2306	002	9103	DRY AND PLUGGED
17-727-00007	PHILLIPS PETROLEUM CO.	SL 2306	003	9506	DRY AND PLUGGED
17-727-00008	PHILLIPS PETROLEUM CO.	SL 2306	004	9310	DRY AND PLUGGED
17-727-00010	INACTIVE OPERATOR	SL 4135	001	9500	DRY AND PLUGGED
17-727-00104	J. C. TRAHAN DRLG. CONTR INC	SL 4118	002	7500	DRY AND PLUGGED
17-727-00102	INACTIVE OPERATOR	SL 4116	001	10000	DRY AND PLUGGED
17-727-00103	KERR-MCGEE OIL INDUSTRIES INC	SL 4119	001	8500	DRY AND PLUGGED
17-727-00112	INACTIVE OPERATOR	SL 4142	001	8711	DRY AND PLUGGED
17-727-00123	COASTAL STATES GAS PROD. CO.	SL 4119	001	8500	DRY AND PLUGGED
17-727-00176	INACTIVE OPERATOR	SL 4142	001	8600	DRY AND PLUGGED
17-727-00127	KERR-MCGEE OIL INDUSTRIES INC	SL 4119	002	9805	DRY AND PLUGGED
17-727-00128	INACTIVE OPERATOR	SL 4558	001	9728	DRY AND PLUGGED
17-727-00129	INACTIVE OPERATOR	SL 4556	001	10000	DRY AND PLUGGED
17-727-00156	INACTIVE OPERATOR	SL 4548	001	9894	DRY AND PLUGGED
17-727-00157	OCEAN DRILLING AND EXPL.	SL 4546	001	10000	DRY AND PLUGGED
17-727-00155	CONSOLIDATED GAS SUPPLY CORP.	SL 4142	001	8609	DRY AND PLUGGED
17-727-00170	FOREST OIL CORPORATION	SL 4555	001	10300	DRY AND PLUGGED
17-727-00173	GULF OIL CORPORATION	SL 4566 BLK 63	001	10000	DRY AND PLUGGED
17-727-00172	GULF OIL CORPORATION	SL 4567 BLK 62	001	0	DRY AND PLUGGED
17-727-00164	INACTIVE OPERATOR	SL 4119	001	6425	DRY AND PLUGGED
17-727-00169	INACTIVE OPERATOR	SL 4554	001	9500	DRY AND PLUGGED
17-727-00171	GULF OIL CORPORATION	SL 4560	001	10000	DRY AND PLUGGED
17-727-00168	FOREST OIL CORPORATION	SL 4554	002	9000	DRY AND PLUGGED
17-727-00174	INACTIVE OPERATOR	SL 4119	002	6300	DRY AND PLUGGED
17-727-00181	INACTIVE OPERATOR	SL 4546	001	9205	DRY AND PLUGGED
17-727-00196	KERR-MCGEE CORPORATION	SL 4563	001	9500	DRY AND PLUGGED
17-727-00195	CONSOLIDATED GAS-O & G FUTRS.	SL 4559	001	9405	DRY AND PLUGGED
17-727-00184	SOUTHERN NATURAL GAS CO.	SL 4551	001	9036	DRY AND PLUGGED
17-727-00192	FOREST OIL CORPORATION	SL 4555	002	9467	DRY AND PLUGGED
17-727-00193	FOREST OIL CORPORATION	SL 4555	003	9488	DRY AND PLUGGED

17-727-00194	FOREST OIL CORPORATION	SL 4554	003	9000	DRY AND PLUGGED
17-727-00190	INACTIVE OPERATOR	SL 4812	001	8515	DRY AND PLUGGED
17-727-00183	ARCO O & G CO-DIV ATL RICH CO	SL 4753	001	9461	DRY AND PLUGGED
17-727-00218	AMERICAN TRADING & PROD CORP	SL 4554	001	9045	DRY AND PLUGGED
17-727-00225	TEXACO, INC.	SL 4893	001	11623	DRY AND PLUGGED
17-727-00237	INACTIVE OPERATOR	SL 5111	001	0	DRY AND PLUGGED
17-727-00233	SHELL OIL COMPANY	SL 4894	001	15151	DRY AND PLUGGED
17-727-00235	OCCIDENTAL PETROLEUM CORP.	SL 5218	001	16556	DRY AND PLUGGED
17-727-00236	GULF OIL CORPORATION	SL 5114	001	16500	DRY AND PLUGGED
17-727-20000	OCCIDENTAL PETROLEUM CORP.	SL 5289	001	8600	DRY AND PLUGGED
17-727-20007	OCCIDENTAL PETROLEUM CORP.	SL 5411	001	8500	DRY AND PLUGGED
17-727-20023	INACTIVE OPERATOR	SL 5426	001	6715	DRY AND PLUGGED
17-727-20029	DYNAMIC EXPLORATION, INC.	SL 5866	001	6055	DRY AND PLUGGED
17-727-20455	INACTIVE OPERATOR	S/L 5922	001	8501	DRY AND PLUGGED
17-727-20050	GRAHAM ROYALTY, LTD.	SL 6674	001	9005	DRY AND PLUGGED
17-727-20055	OIL AND GAS FUTURES, INC.	S/L 6668	001	9014	DRY AND PLUGGED
17-727-20056	OIL AND GAS FUTURES, INC.	S/L 6671	001	9011	DRY AND PLUGGED
17-727-20059	AMOCO PRODUCTION COMPANY	S/L 6662	001	9000	DRY AND PLUGGED
17-727-20065	OIL AND GAS FUTURES, INC.	S/L 6668	002	7500	DRY AND PLUGGED
17-727-20067	INACTIVE OPERATOR	S/L 6656	001	5670	DRY AND PLUGGED
17-727-20073	LGS EXPLORATION PROGRAM	SL 6657	001	9000	DRY AND PLUGGED
17-727-20074	FMP OPERATING COMPANY, LTD PTN	SL 6674	002	8730	DRY AND PLUGGED
17-727-20075	FMP OPERATING COMPANY, LTD PTN	SL 6678	002	8490	DRY AND PLUGGED
17-727-20085	INACTIVE OPERATOR	S/L 6657	002	9000	DRY AND PLUGGED
17-727-20093	T I P C O	SL 7505	001	7000	DRY AND PLUGGED
17-727-20099	THE STONE OIL CORPORATION	SL 7000	001	9000	DRY AND PLUGGED
17-727-20105	LGS EXPLORATION PROGRAM	SL 7004	001	9000	DRY AND PLUGGED
17-727-20108	MATAGORDA PRODUCTION COMPANY	SL 7984	001	7000	DRY AND PLUGGED
17-727-20114	GULF OIL CORPORATION	SL 7204	001	7500	DRY AND PLUGGED
17-727-20118	C.F. BRAUN & COMPANY	SL 7985	001	7500	DRY AND PLUGGED
17-727-20119	TEXACO, INC.	SL 8323	001	11000	DRY AND PLUGGED
17-727-20108	MATAGORDA PRODUCTION COMPANY	SL 7984	001	7500	DRY AND PLUGGED
17-727-20122	TENNECO	SL 8241	001	13458	DRY AND PLUGGED
17-727-20123	INACTIVE OPERATOR	SL 8242	001	0	DRY AND PLUGGED
17-727-20129	PHILLIPS PETROLEUM CO.	SL 8244	001	19000	DRY AND PLUGGED
17-727-20146	KERR-MCGEE CORPORATION	SL 9170	001	10200	DRY AND PLUGGED
17-727-20147	KERR-MCGEE CORPORATION	S L 9171	001	0	DRY AND PLUGGED
17-727-20148	KERR-MCGEE CORPORATION	S L 9171	002	0	Inactive
17-727-20152	SAMEDAN OIL CORPORATION	SL 9246	001	8839	Inactive

17-727-20153	TEXAS GENERAL PETROLEUM CORP.	SL 8409	001	7586	PERMIT EXPIRED
17-727-20154	KERR-MCGEE CORPORATION	SL 9170	002	0	PERMIT EXPIRED
17-727-20160	SUPRON ENERGY CORPORATION	SL 9441	001	8596	PERMIT EXPIRED
17-727-20161	SUPRON ENERGY CORPORATION	SL 9442	001	0	PERMIT EXPIRED
17-727-20162	POGO PRODUCING COMPANY	SL 9443	001	0	PERMIT EXPIRED
17-727-20163	POGO PRODUCING COMPANY	SL 9443	002	0	PERMIT EXPIRED
17-727-20167	SHELL OIL COMPANY	SL 9169	001	14292	PERMIT EXPIRED
17-727-20162	POGO PRODUCING COMPANY	SL 9443	001	7000	PERMIT EXPIRED
17-727-20163	POGO PRODUCING COMPANY	SL 9443	002	0	PERMIT EXPIRED
17-727-20208	INACTIVE OPERATOR	SL 10700	001	8200	PERMIT EXPIRED
17-727-20249	CARUTHERS PRODUCING CO., INC.	SL 10903	001	6500	PERMIT EXPIRED
17-727-20314	NORTH AMERICAN ROYALTIES, INC.	SL 10903	001	6530	PERMIT EXPIRED
17-727-20329	THE STONE PETROLEUM CORP.	SL 11252	001	9412	PERMIT EXPIRED
17-727-20331	INACTIVE OPERATOR	SL 10258	001	8200	PERMIT EXPIRED
17-727-20338	PHILLIPS PETROLEUM CO.	SL 11580	001	8015	PERMIT EXPIRED
17-727-20346	GAS TRANSPORTATION CORPORATION	SL 10258	001	8200	PERMIT EXPIRED
17-727-20348	PEL-TEX OIL COMPANY, INC.	SL 11766	001	10050	PERMIT EXPIRED
17-727-20420	TORCH OPERATING COMPANY	SL 13307	001	10103	PERMIT EXPIRED
17-727-20423	TORCH OPERATING COMPANY	SL 13307	002	9175	PERMIT EXPIRED
17-727-20425	PELTO OIL CO	SL 13308	001	10587	PERMIT EXPIRED
17-727-20461	MANTI OPERATING COMPANY	SL 14055	001	8100	PERMIT EXPIRED
17-727-20474	DAVIS PETROLEUM CORP.	SL 14592	001	10176	PERMIT EXPIRED
17-727-20475	DAVIS PETROLEUM CORP.	SL 14594	001	8100	PERMIT EXPIRED
17-727-20476	DAVIS PETROLEUM CORP.	SL 14595	001	9000	PERMIT EXPIRED
17-727-20477	DAVIS PETROLEUM CORP.	SL 14596	001	9500	PERMIT EXPIRED
17-727-20478	COCKRELL OIL CORPORATION	SL 14525	001	5326	PERMIT EXPIRED
17-727-20480	SCANA PETROLEUM RESOURCES, INC	SL 14705	001	5962	PERMIT EXPIRED
17-727-20484	SCANA PETROLEUM RESOURCES, INC	SL 14705	002	8000	PERMITTED
17-727-20490	EL PASO PRODUCTION O&G COMPANY	SL 16164	001	10800	PLUGGED AND ABANDONED
17-727-20492	COASTAL OIL & GAS CORP.	SL 16167	001	10600	PLUGGED AND ABANDONED
17-727-20499	MANTI OPERATING COMPANY	SL 16521	001	0	PLUGGED AND ABANDONED
17-727-20500	MANTI OPERATING COMPANY	SL 16525	002	10000	PLUGGED AND ABANDONED
17-727-20501	MANTI OPERATING COMPANY	SL 17393	001	6851	PLUGGED AND ABANDONED
17-727-20503	MANTI OPERATING COMPANY	SL 17397	001	8900	PLUGGED AND ABANDONED
17-727-20504	MANTI OPERATING COMPANY	SL 17398	001	9800	PLUGGED AND ABANDONED
17-727-20505	MANTI OPERATING COMPANY	SL 17400	001	8147	PLUGGED AND ABANDONED
17-727-20506	MANTI OPERATING COMPANY	SL 17403	001	8100	PLUGGED AND ABANDONED
17-727-20507	MANTI OPERATING COMPANY	SL 17401	001	9791	PLUGGED AND ABANDONED
17-727-20508	MANTI OPERATING COMPANY	SL 17403	002	9800	PLUGGED AND ABANDONED

17-727-20508		SL 17403	02	9800	PLUGGED AND ABANDONED
17-727-20510	THE MERIDIAN RES. & EXP. LLC	SL 17554	002	6000	PLUGGED AND ABANDONED
17-727-20509	THE MERIDIAN RES. & EXP. LLC	SL 17554	001	6000	PLUGGED AND ABANDONED
17-727-20511	MANTI OPERATING COMPANY	SL 17405	001	11000	PLUGGED AND ABANDONED
17-727-20514	MANTI OPERATING COMPANY	SL 17394	001	7101	PLUGGED AND ABANDONED
17-727-20516	MANTI OPERATING COMPANY	SL 17558	001	9000	PLUGGED AND ABANDONED
17-727-20517	MANTI EXPLORATION OPERATING LLC	SL 17557	001	9200	PLUGGED AND ABANDONED
17-727-20518	GEMINI EXPLORATIONS, INC.	SL 17558	002	2375	PLUGGED AND ABANDONED
17-727-20519	MANTI OPERATING COMPANY	SL 17390	001	7000	PLUGGED AND ABANDONED
17-727-20520	MANTI OPERATING COMPANY	SL 17399	001	7501	PLUGGED AND ABANDONED
17-727-20521	MANTI OPERATING COMPANY	SL 17628	001	8000	PLUGGED AND ABANDONED
17-727-20522	MANTI EXPLORATION OPERATING LLC	SL 17397	002	8390	PLUGGED AND ABANDONED
17-727-20523	MANTI OPERATING COMPANY	SL 17583	001	9800	PLUGGED AND ABANDONED
17-727-20531	PXP LOUISIANA L.L.C.	SL 17405	001	10330	PLUGGED AND ABANDONED
17-727-20532	PXP LOUISIANA L.L.C.	SL 17390	001	4800	PLUGGED AND ABANDONED
17-727-20533	PXP GULF COAST INC.	SL 17406	001	10800	Unknown
17-727-20534	PALACE OPERATING COMPANY	SL 17986	001	8500	Unknown
17-727-20535	PALACE OPERATING COMPANY	SL 17987	001	10820	Unknown
17-727-20540	ST. MARY LAND & EXPLORATION CO	SL 18333	001	10550	Unknown
17-727-20541	ST. MARY LAND & EXPLORATION CO	SL 18333	002	10800	Unknown
17-727-00005	PHILLIPS PETROLEUM CO.	SL 2306	001	9500	Unknown
17-727-00194	WIGWAM PRODUCTION CO.	S/L 4554	003	9000	Unknown

Updated Well Tops

Subsequent iterations of data integration helped confirm or calibrate originally reported paleontology tops. Below is an updated table (Table 2.1.2.2) showing unit tops and thicknesses by GBDS well ID based on paleontology tops.

Table 2.1.2.2 – Updated table of unit tops and thicknesses.

GBDS Well ID	Unit ID	Top Elevation (ft)	Interval Thickness (ft)	Penetration
12082	UM	-4691	2865	Single genetic unit
12082	MM	-7556	685	Base unit, partial penetration
12083	UM	-3950	1486	Single genetic unit
12083	MM	-5436	4313	Base unit, partial penetration
12084	UM	-5081	3378	Single genetic unit
12084	MM	-8459	2733	Base unit, partial penetration
12085	UM	-4447	3098	Single genetic unit
12085	MM	-7545	2186	Base unit, partial penetration
12086	UM	-4505	3215	Single genetic unit
12086	MM	-7720	2246	Base unit, partial penetration
12087	UM	-4614	3448	Single genetic unit

12087	MM	-8062	1900	Base unit, partial penetration
12088	UM	-3346	1819	Single genetic unit
12088	MM	-5165	2397	Single genetic unit
12088	LM2	-7562	199	Single genetic unit
12088	LM1	-7761	127	Single genetic unit
12088	OF	-7888	3279	Undifferentiated Unit
12088	NT	-11167	479	Undifferentiated Unit
12088	AC	-11167	479	Undifferentiated Unit
12088	EFT	-11646	NA	Base unit, inconsequential penetration
12089	UM	-3704	2336	Single genetic unit
12089	MM	-6040	3075	Single genetic unit
12089	LM2	-9115	128	Single genetic unit
12089	LM1	-9243	117	Single genetic unit
12089	OF	-9360	5340	Undifferentiated Unit
12089	NT	-14700	760	Undifferentiated Unit
12089	AC	-14700	760	Undifferentiated Unit
12089	EFT	-15460	1460	Single genetic unit
12089	PW	-16920	NA	Base unit, inconsequential penetration
12090	UM	-3052	1854	Single genetic unit
12090	MM	-4906	2083	Single genetic unit
12090	LM2	-6989	93	Single genetic unit
12090	LM1	-7082	117	Single genetic unit
12090	OF	-7199	3497	Undifferentiated Unit
12090	MD	-10696	277	Single genetic unit
12090	NT	-10973	363	Undifferentiated Unit
12090	AC	-10973	363	Undifferentiated Unit
12090	EFT	-11336	1200	Single genetic unit
12090	PW	-12536	1670	Single genetic unit
12090	GR	-14206	2960	Undifferentiated Unit
12090	FL	-14206	2960	Undifferentiated Unit
12090	RD	-14206	2960	Undifferentiated Unit
12090	BP	-14206	2960	Undifferentiated Unit
12090	SH	-17166	NA	Base unit, inconsequential penetration
12091	UM	-4810	4983	Single genetic unit
12091	MM	-9793	108	Base unit, partial penetration
12092	MM	-4938	4011	Base unit, partial penetration

Reference Cited

Ogg, J. G., Ogg, G., & Gradstein, F. M. (2016). A concise geologic time scale: 2016. Elsevier. ISBN 978-0-444-63771-0.

Subtask 2.1.3 – Geologic Characterization of High Island, TX

General progress on re-processing and improving the utility of HR3D surveys

(The following work to improve HR3D surveys was conducted in conjunction with DE-FE0026083. The, results, thereof, will be available to the GoMCarb Partnership.) The Partnership has access to three HR3D (high-resolution 3D) survey datasets within the greater High Island area of interest (Figure 2.1.3.1). Internally, the datasets are informally named GOM2012, GOM2013, and GOM2014 because they were acquired in the Gulf of Mexico (GOM) in 2012, 2013 and 2014, respectively.

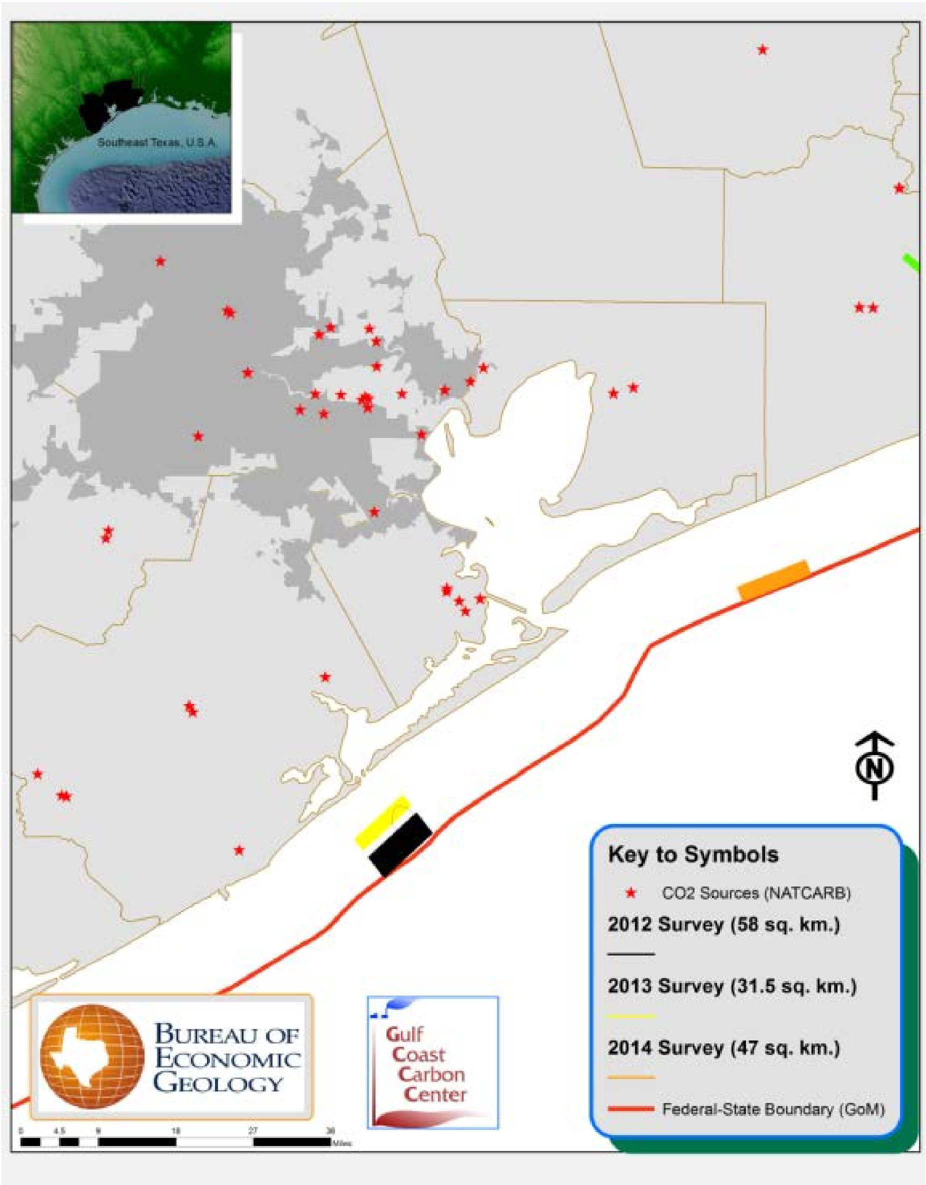

Figure 2.1.3.1 - Map of the southeast Texas coastal region showing the locations of three HR3D (P-Cable) surveys within the study area. The outline of the 2012 survey is shown in black, the 2013 survey in yellow and the 2014 survey in orange. Note the outline of the city of Houston in dark gray and the boundary (red line) between State and Federal waters.

Applied Techniques

1. Weiner type 60, 120 and 180Hz notch filters
2. Phase shifting filters for noise reduction
3. Positional corrections based on linear refractor and offset corrections
4. Stationary noise and minimum phase equivalent transfer function from precursor

noise.

All of the techniques, above, were applied to GOM2012. GOM2013 and GOM2014 did not require Weiner notch filters or Positional corrections to the same extent that GOM2012 did.

Status

GOM2012 was completed and uploaded to the interpretation project in mid-August.

As of August 31, 2019, GOM2013 and GOM2014 were completed with basic time processing. Due to delay in re-activation of the migration software license, pre-stack migration the two datasets was still pending.

	Data QC	Positional Corrections	Signal Processing	3D Statics and Balancing	Migration
GOM2012	Done	Done	Done	Done	Done
GOM2013	Done	Done	Done	Done	
GOM2014	Done	Done	Done	Done	

GOM2012

After pre-stack migration of GOM2012, which interpolated missing data, amplitudes were well balanced and fault features were easily identifiable. There were still unbalanced streaks from some amplitude problems which only occurred in the upper 200-300 ms (milliseconds) of the section. The unbalanced streaks were minimized by the processing but not removed. Pre-stack Kirchhoff time migration worked well on this dataset, infilling gaps and enhancing fault features. In the cross-section view (Figure 2.1.3.2) inline data were enhanced, but slight blurring was visible on the time-slices probably due to the migration data aperture (Figure 2.1.3.3). Aperture was determined to be as small as possible at ~4X the cdp (common depth point) spacing or 25m. It is believed that most of the ray paths are near vertical, and the choice of a short aperture and resulting data support that assumption. The dataset was completed and transferred into the interpretation system (Haliburton Landmark's Decision Space) in mid-August.

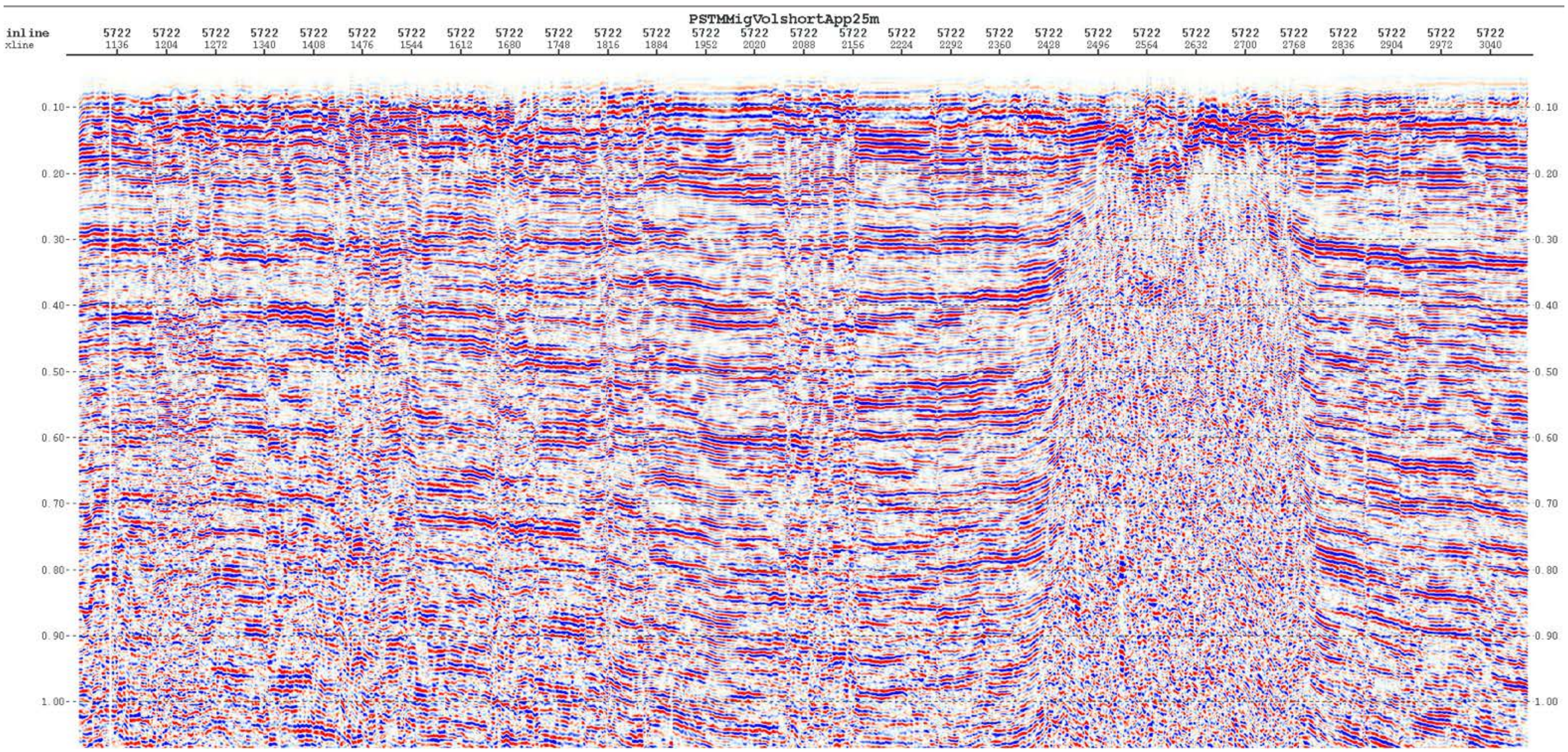

Figure 2.1.3.2 **-** GOM2012 Inline 5722. Pre-stack migration.
Note the clarity of the faults near the center of the section from 0-1000ms.

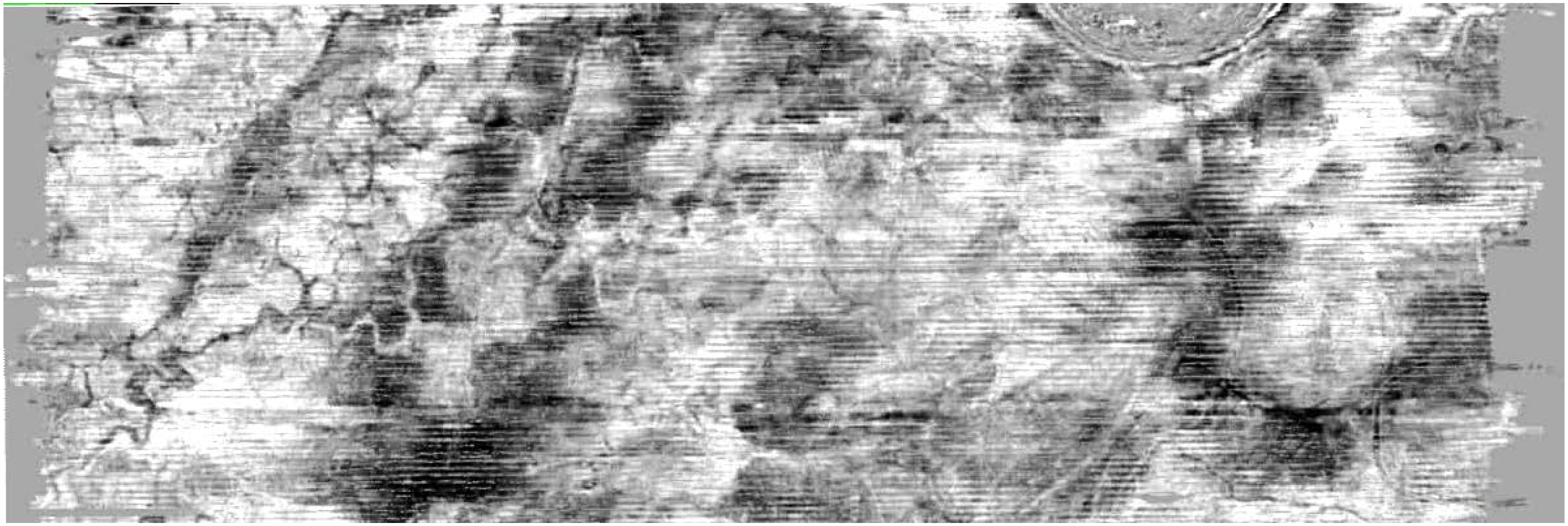

Figure 2.1.3.3 **-** GOM2012 survey timeslice at 197 ms. Numerous channels and other geological features can be seen. Previously noise made interpretation impossible.(see previous reports)

GOM 2013

This dataset did not have the noise or extreme positional problems that GOM2012 did, but applying similar postional and signal processing methods as those applied to GOM2012 did improve the visual appearance of the data. Use of the signal enhancements of phase shift filtering and stationary noise and minimum phase equilvalent transfer function improved the data quality (Figure 2.1.3.4). Applying additonal 3D statics and balancing resulted in marked improvements over previous work (Figure 2.1.3.5).

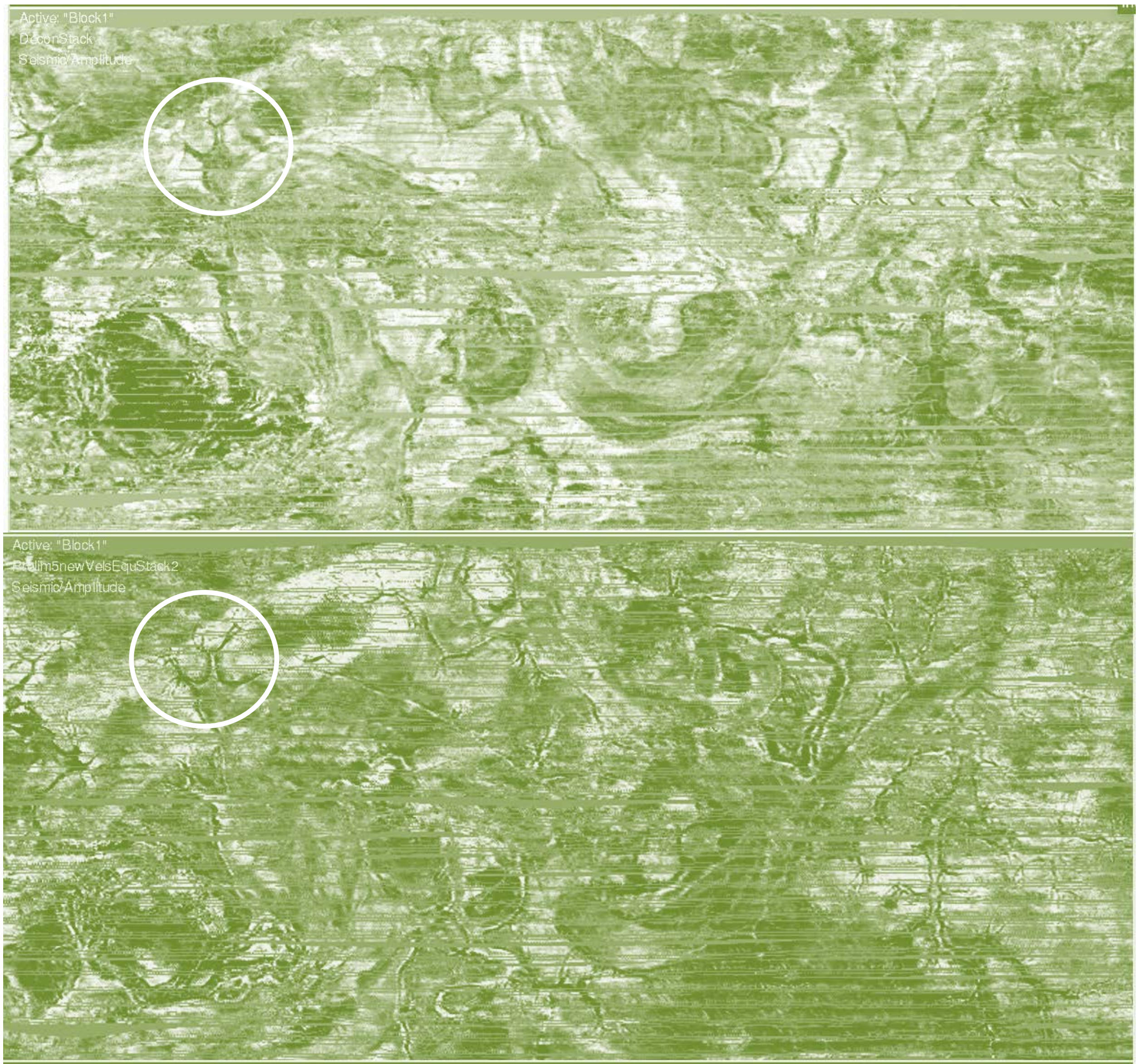

Figure 2.1.3.4 - GOM2013 survey timeslice at 143 ms. Before (above) and after (below) new processing techniques. Note the enhancement of fine channels (white circle) in the re-processed data.

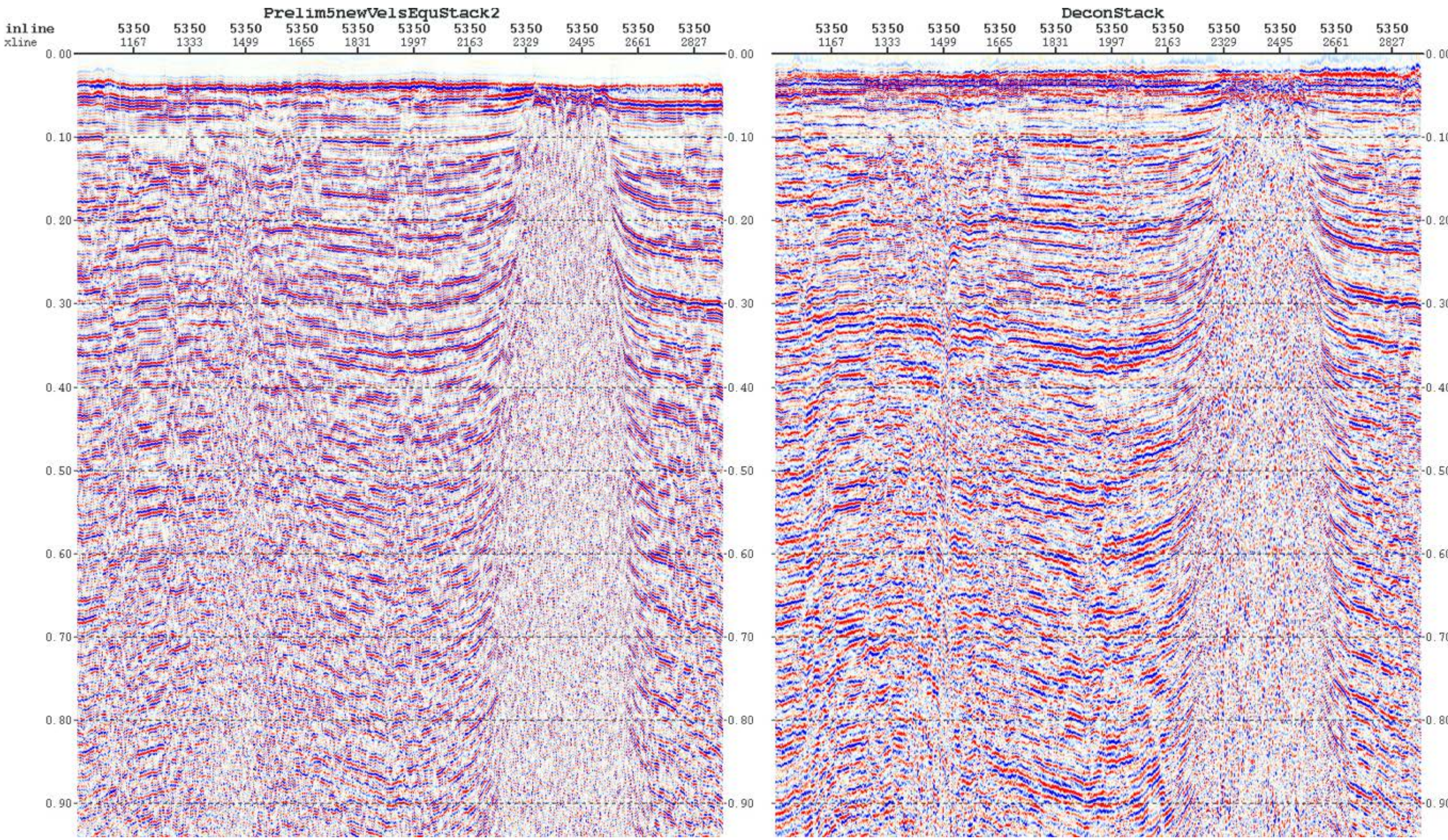

Figure 2.1.3.5 - GOM2013 survey inline 5350 after (left) and before (right) new processing techniques. Note the sharper boundaries of the salt dome and gas chimney.

GOM 2014

As with GOM2013, the techniques for signal processing from GOM2012 were applied to GOM2014 resulting in improved resolution (Figure 2.1.3.6). The GOM2014 data also benefited from little or no positional errors and very little background noise. Additonal 3D statics and balancing were applied and the results show some improvements over previous work (Figures 2.1.3.7).

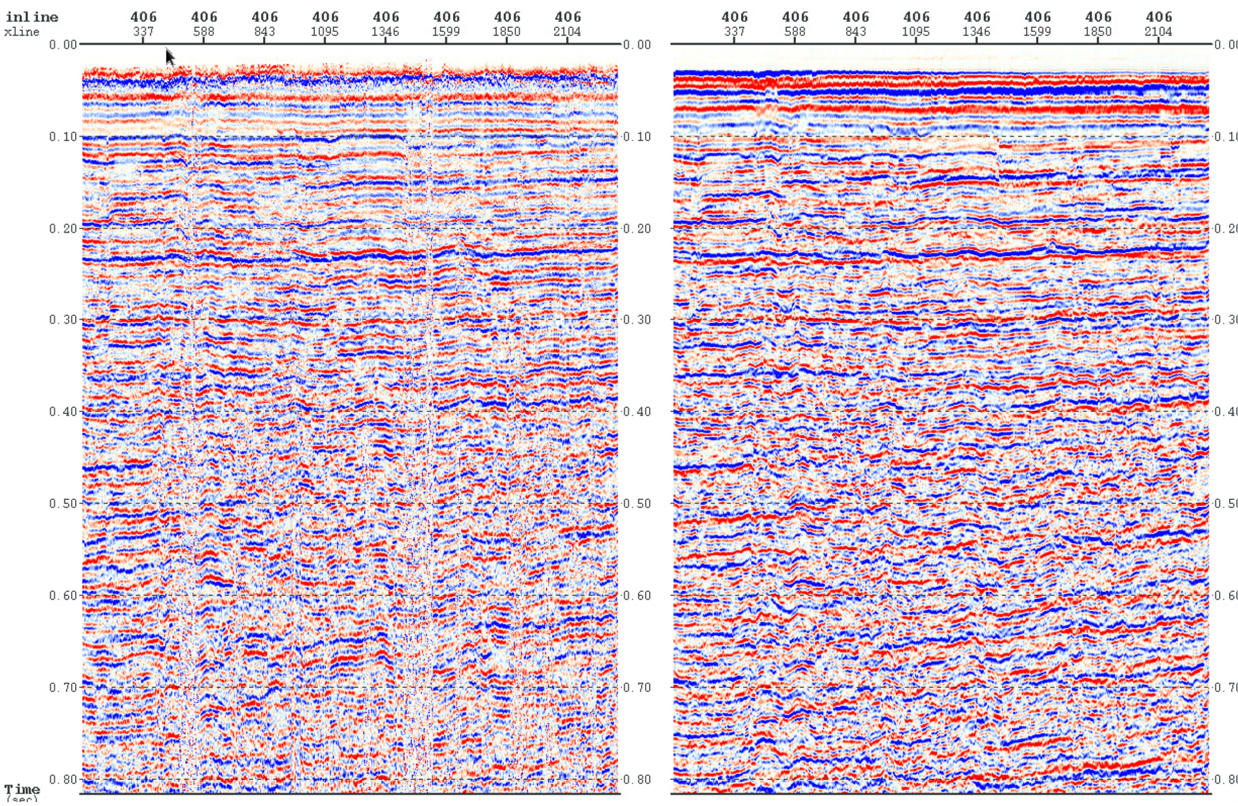

Figure 2.1.3.6 - Inline 406 GOM 2014 showing previous processing (left) and improved resolution from new processing techniques (right).

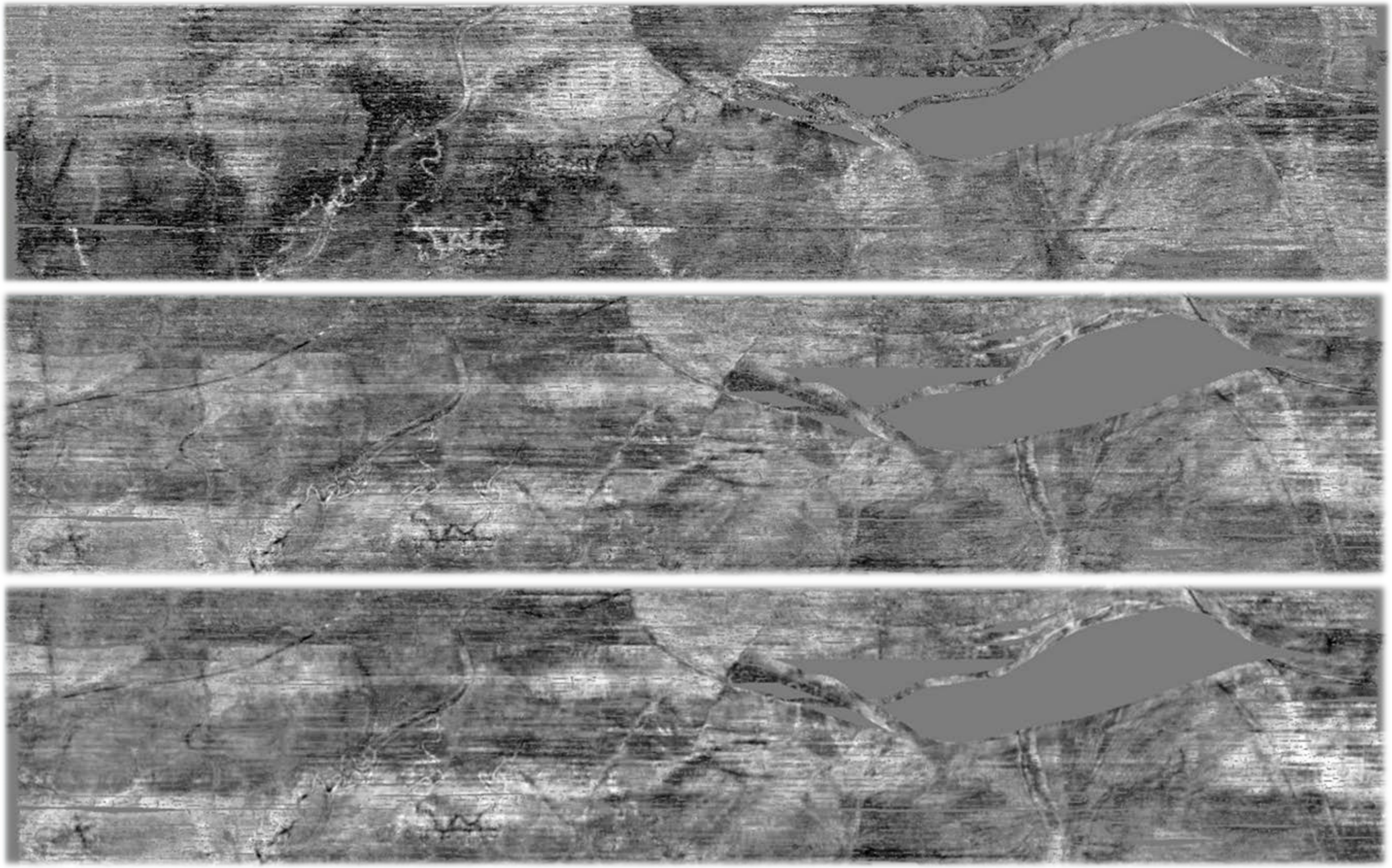

Figure 2.1.3.7 **-** GOM 2014 Time slice at 127ms : Original Processing with no phase shift filter (Top), Phase Shift filters (middle) note the change in features due to shift, Final processing with signal processing and balancing (Bottom)

Subtask 2.2 – Data Gap Assessment

Co-PI Meckel met with Partner, TDI-Brooks, on September 6, 2019. The topic of discussion was generation of a contour map of CO_2 by TDI based on in-house data they have available. In addition, Meckel met with Partner, Fugro, which has extensive experience that they could summarize for high value to the marine CCS community (e.g., technology and monitoring protocols in a variety of environments, including sensitive ones).

Subtask 2.2.1: Data gap assessments will focus on regionally relevant analog settings

No activity this quarter

Subtask 2.3 – Offshore and reservoir storage Enhanced Oil Recovery (EOR) Potential

Per request from the USGS (Partner) PI, two masters degree theses (Ruiz, 2019 and Ramirez Garcia, 2019). (i.e., from recent GCCC graduates,) were made available and downloaded by the USGS PI. The plan was to use the theses to determine available data / datasets that USGS will need to conduct its analog work.

References Cited

Ramirez Garcia, O. (2019). *Geological Characterization and Modeling for Quantifying CO2 Storage Capacity of the High Island 10-L Field in Texas State Waters, Offshore Gulf of Mexico.* (Master of Science), The University of Texas at Austin, Austin, TX.

Ruiz, I. (2019). *Characterization of the High Island 24L Field for Modeling and Estimating CO2 Storage Capacity in the Offshore Texas State Waters, Gulf of Mexico* (Master of Science in Geological Sciences), The University of Texas at Austin, Austin, Texas.

Subtask 2.3.1 Texas (High Island area of Lake Jackson district) and Louisiana (Lake Charles and Lafayette districts)

(The following work was conducted in conjunction with support from DE-FE0026083. The results will be useful and available to the GoMCarb Partnership.)

The High Island 10L Field (Figure 2.3.1.1) is an area of interest as an analog CO_2 injection prospect. The field comprises an area of 50.36 square miles or 130.43 square kilometers, and the depth interval for the lower-middle Miocene in this region ranges from 4,000-8,500 ft (Beckham 2018). This stratigraphic interval of interest falls within the previously mapped regional surfaces of MFS07-MFS10 (maximum flooding surfaces, Galloway et al., 1989), and in particular, the interval considered for this analysis falls between MFS09-MFS10. The interval of interest is located below an easily identifiable regional seal, both in seismic sections as well as in well logs. This seal unit is named *Amphistegina Bigerina* (*Amph B*) due to the fact that it contains the diagnostic *Amphistegina bigerina* faunal assemblage (Miall 2008).

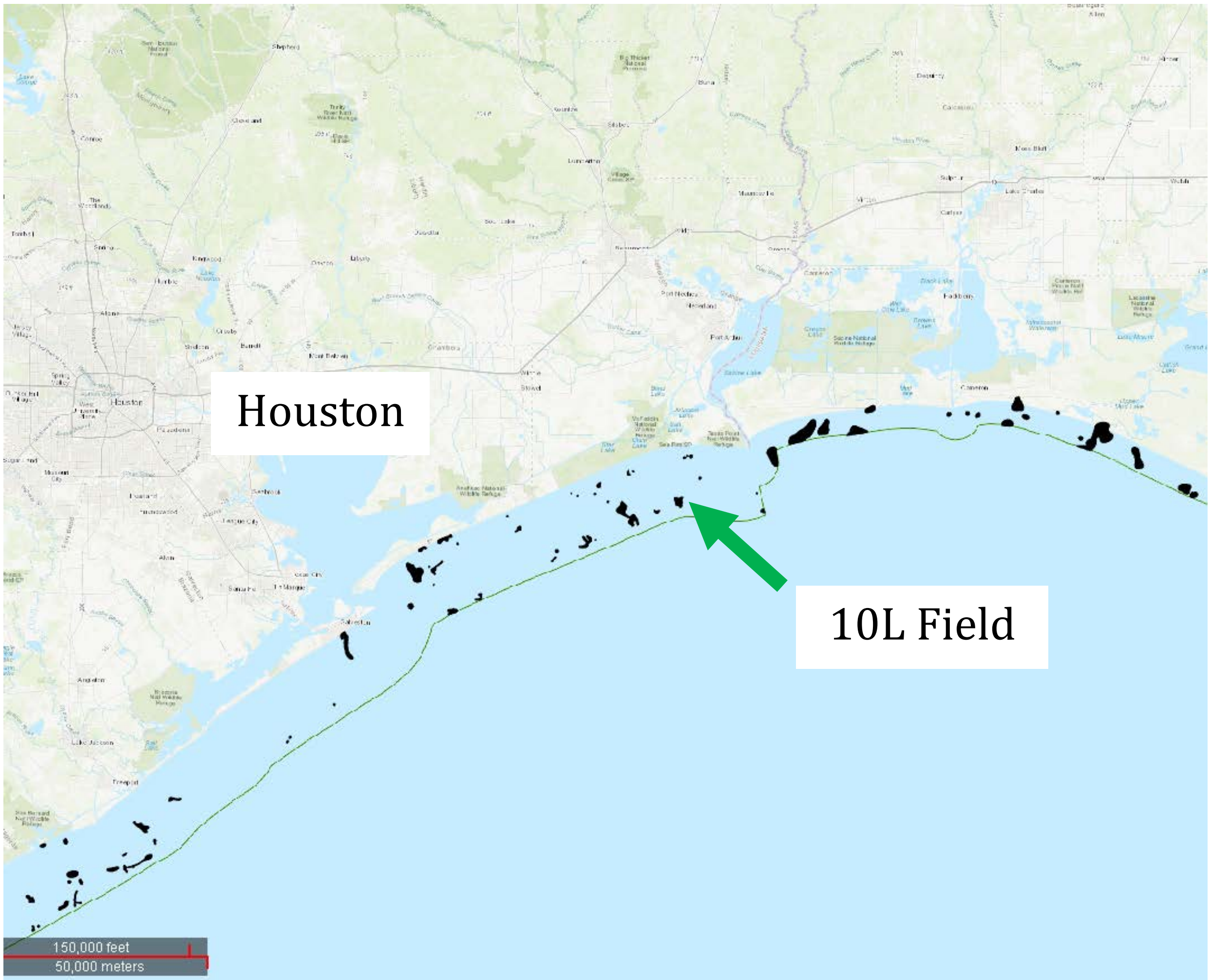

Figure 2.3.1.1 – Location map of the upper Texas and western Louisiana coastal areas showing the locations of historic hydrocarbon fields, including the 10L Field, in the states', respective, state waters.

Structure maps of the 10L field (Figure 2.3.1.2) show two structural highs. The structural high corresponding to the northern region is related to a salt dome located north of the area of interest. The other structural high is located southeast on the downthrown block of a major NE-SW fault and corresponds to a faulted anticline with multiple rollover structures associated with the synthetic and antithetic faults located in that area. The historical High Island 10L hydrocarbon field is located in the faulted anticline, and the structure is of primary interest for carbon storage. An important feature of the faulted anticline structure is the fact that the faults converge with increasing depth (Figure 2.3.1.3, 2.3.1.4, 2.3.1.5). This is important because the structural closure provides the best setting for accumulating and retaining fluids (i.e., hydrocarbons and potentially CO_2). Consequently, structural closure area decreases from the top to the base of the interval of interest.

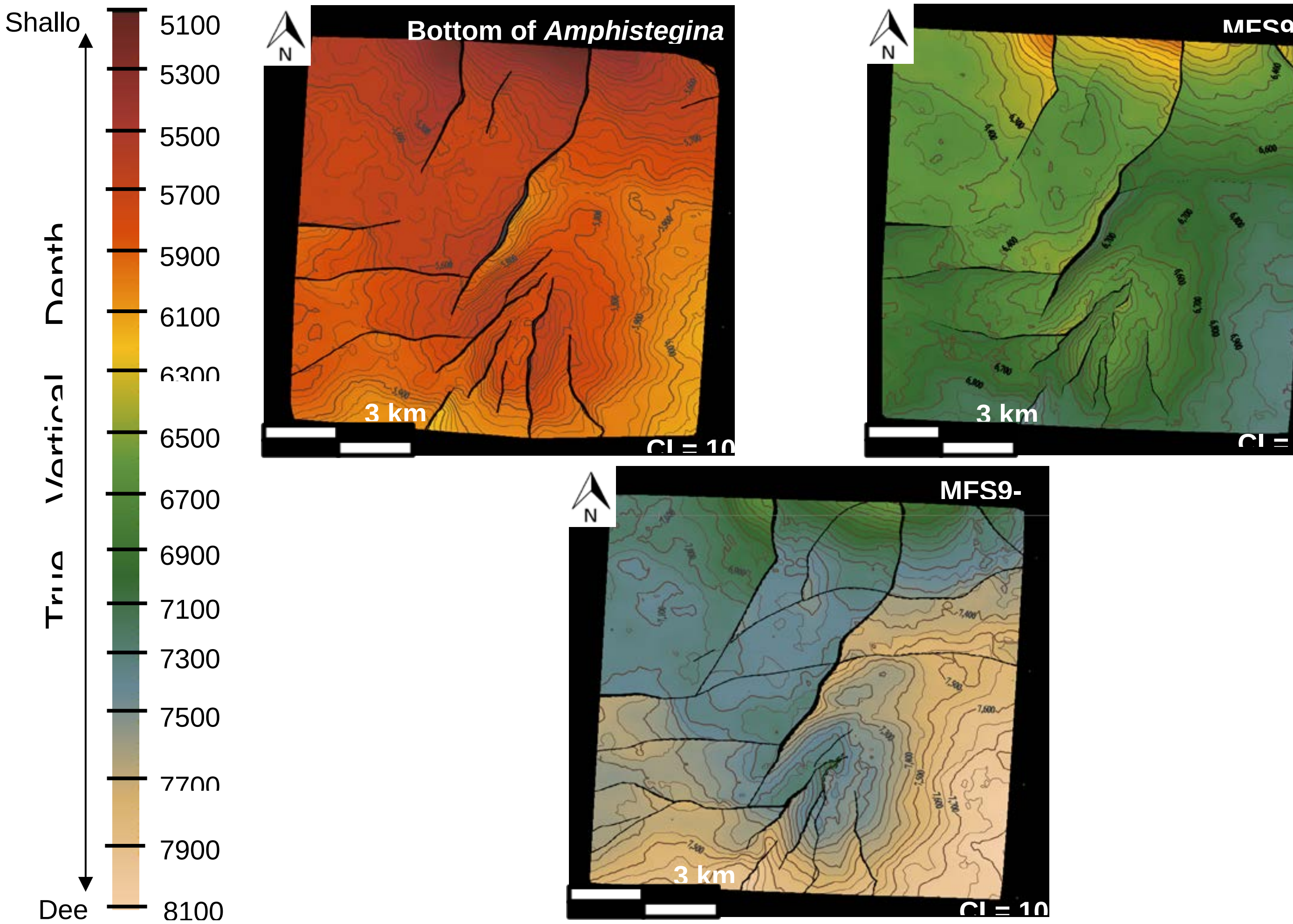

Figure 2.3.1.2 – Depth structure maps showing the structural evolution for the area of interest from the top (upper lef (upper right) to the base of the of the interval of interest (IOI).

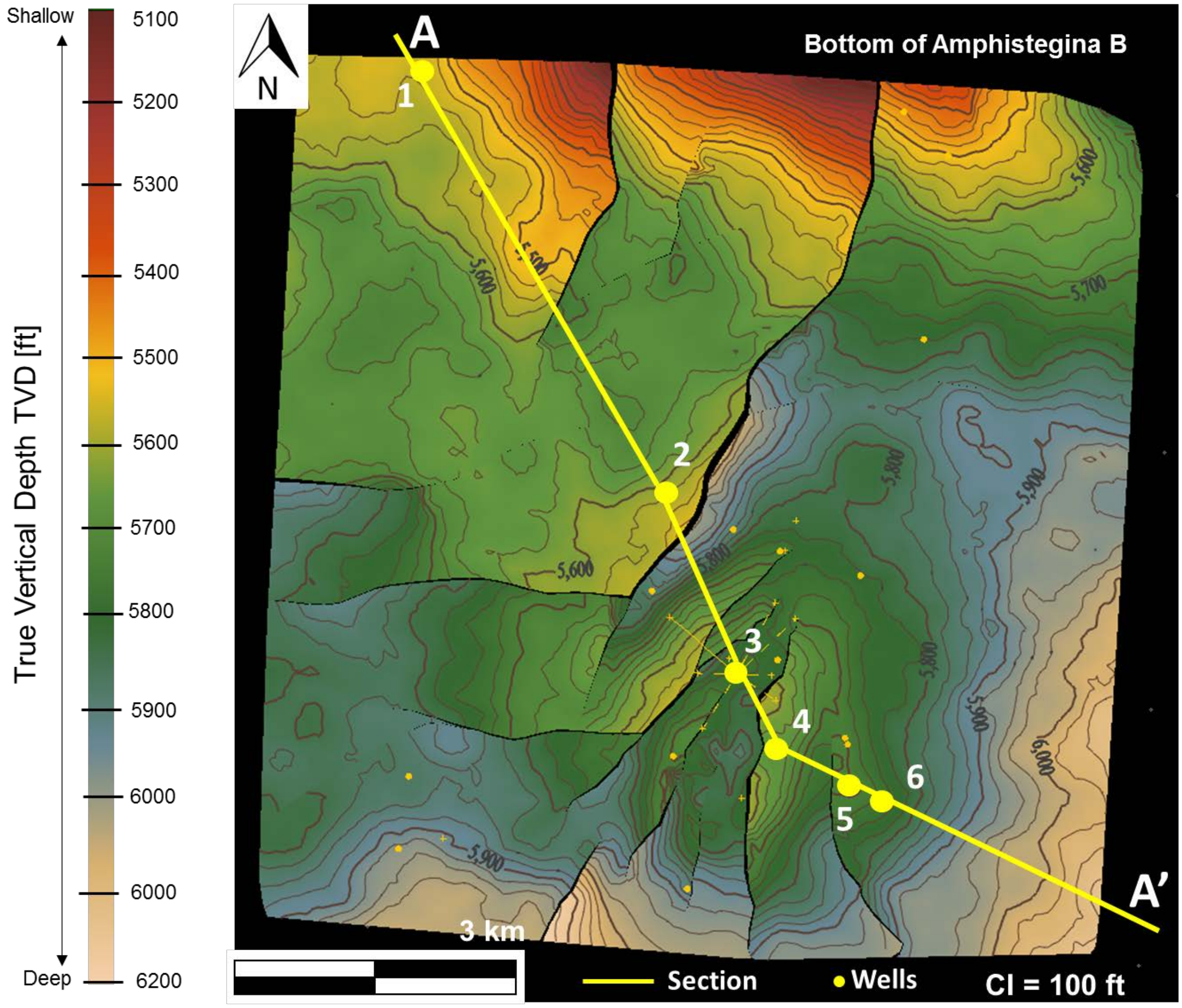

Figure 2.3.1.3 - Structural map of the bottom of the regional seal *Amphistegina B.* The line A-A' corresponds to the seismic section shown in Figure 2.3.1.4. Wells 1-6 correspond to the well panel shown in Figure 2.3.1.5.

Figure 2.3.1.4 - Cross section in dip direction showing the horizons and faults interpreted for the area of interest. This figure also shows the structure of the faulted anticline.

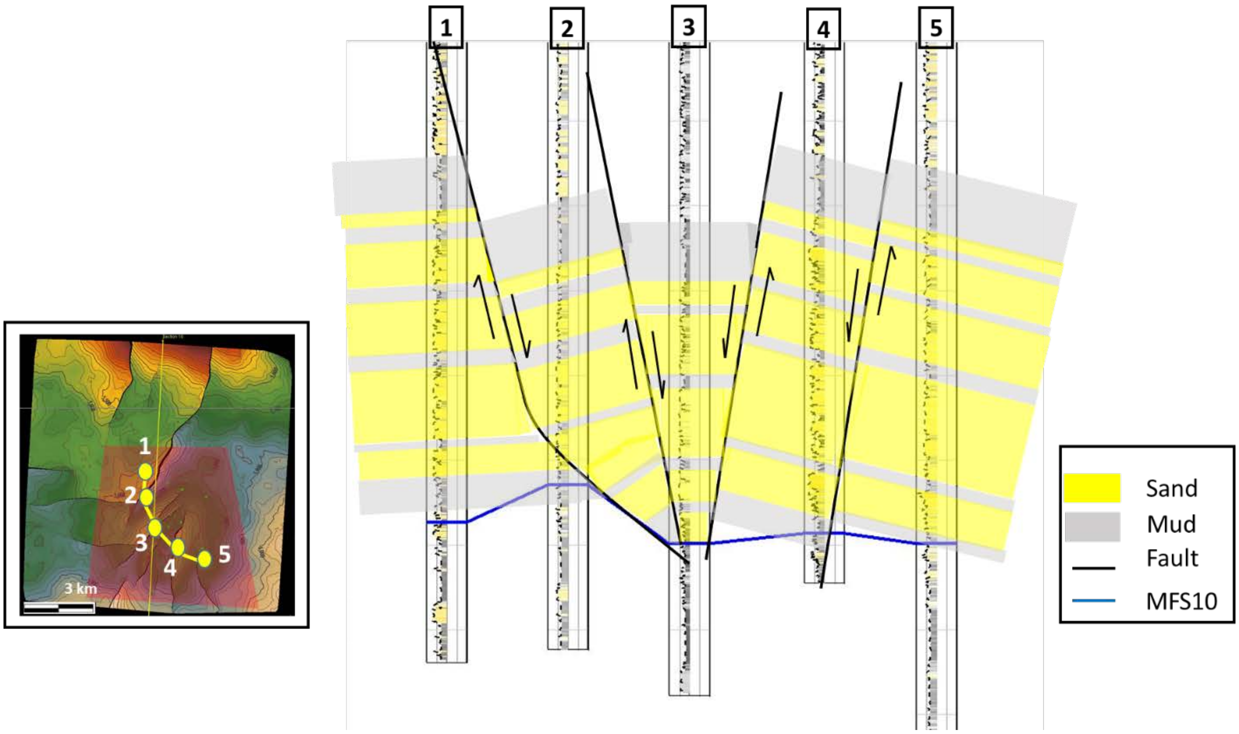

Figure 2.3.1.5: Simplified cross section displaying the main structures in the area of interest. Map on the lower left shows the location of the wells used in the section.

Closure analysis

The traps in the area of interest are structural rather than stratigraphic; so, a closure analysis was performed in order to determine the main traps that will contribute to CO_2 storage volumes, an important step prior to making volumetric estimations. The ten largest closures were determined, with the assumption that the faults present in the area act as seals instead of conduits, and bearing in mind that some of the biggest closures will most likely be associated with the faulted anticline.

Whether the faults seal or not will have a significant impact in fluid flow migration pathways, and the fact that faults might act as conduits rather than as seals represents a risk for potential leakage of CO_2. In addition, the behavior of faults might also contribute to the compartmentalization of the reservoir, which will affect the pressure evolution during injection of CO_2 as well as the management and placement of injection wells.

The closure analysis was performed at the interpreted horizons. The hypothesis was that the closure sizes would decline from the top to the base of the structure, as previously mentioned. Depth maps for the surfaces were generated from the horizons originally interpreted in time using the velocity model from Beckham (2018) and using a refining gridding interpolation method. The surfaces can be used in Halliburton's Permedia™ software to directly determine closure size. However, such depth maps do not integrate the faults that are present in the field, effectively assuming fault zones are conduits. As mentioned above, for the interest of this study, the faults are assumed to act as seals; therefore, they had to be included in the closure analysis.

In order to integrate the faults with the surface maps to determine the closures, a series of polygons (each polygon representing a fault) were created at each surface, and from those polygons a series of maps were created.

The last step was to perform the closure analysis in Permedia™ using as inputs the depth maps as the surfaces from which to compute the closures. The fault maps were barriers, which would represent the sealing effect of the faults. The outcome from the analysis is the surface depth maps with closures, which will be called closure maps (Figure2.3.1.6).

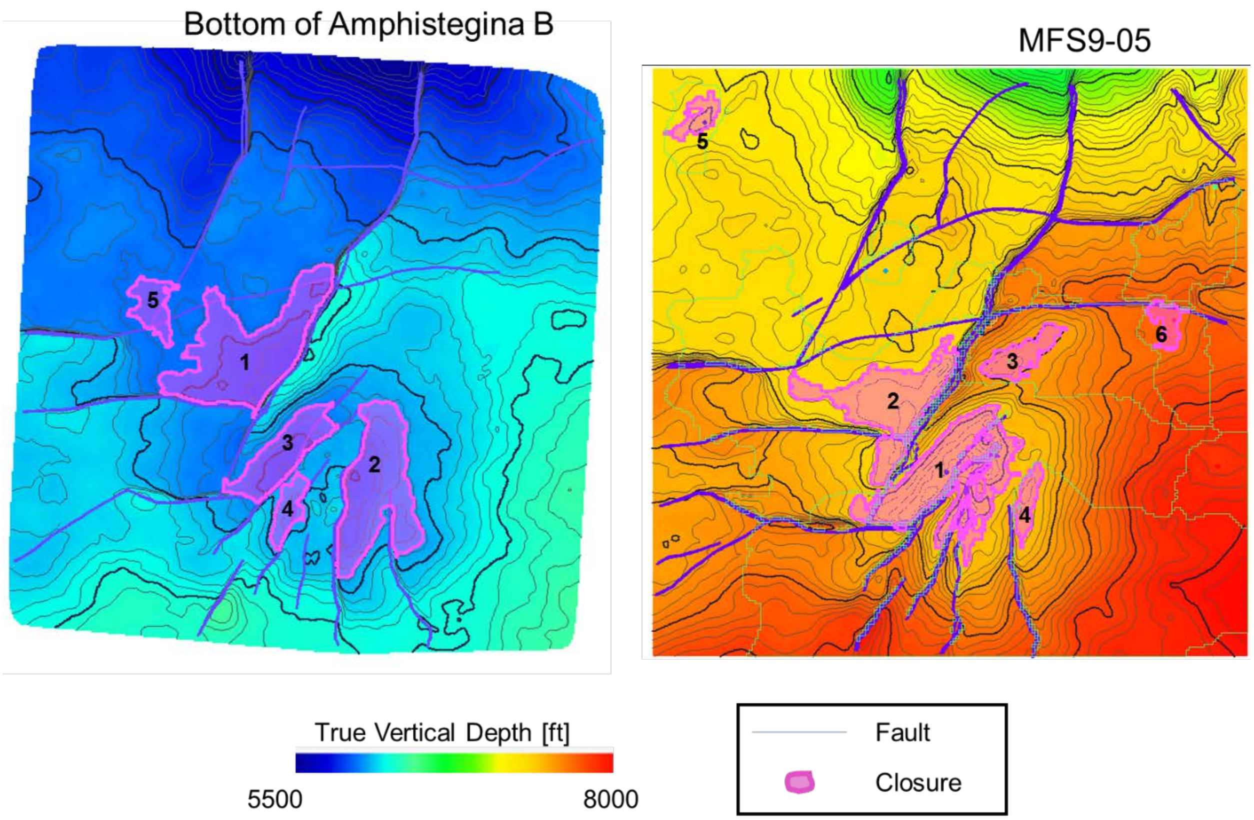

Figure 2.3.1.6 - Structural closure maps of the top of the interval of interest (left) and the bottom of the interval of interest (right). Notice the different areal closures for the two maps.

The closure maps show that three of the five major closures (2, 3 and 5) are associated with the faulted anticline structure, downthrown to the major fault striking northeast-southwest. However, the largest closure (1) is a two-way closure against faults to the south and east. This closure is located in the upthrown (footwall) section of the faults. Note that there has been no production from this footwall trap; so, there are less well data than from the faulted anticline structure. Fewer wells may present less leakage risk and could be a reason to further consider it as a potential target for CO_2 injection. However, it will also be important to determine the reasons why the structure was not charged, and if that represents a potential risk for CO_2 injection.

As expected, the closure areas for the faulted anticline decrease with depth. This is because the faults that form the anticline converge downward (Figures 2.3.1.4 and 2.3.1.5) in the interval of interest. One of the major changes that can be observed comparing the closures at the top of the interval of interest and the closures near the base is that at the top there is a clear compartmentalization caused by the existence of the faults, but near the base of the interval of interest the number of compartments is reduced, generating one larger closure that accounts for roughly half of the faulted anticline (Figure 2.3.1.6). Some of the quantitative results of the closure analysis are shown in table 2.3.1.1, where the area of the closure, the spill depth, the bulk rock volume, among other data, can be found.

Table 2.3.1.1: Quantitative data for the closures shown in Figure 2.3.1.6 for base of Amphistegina B and MFS9-05.

Table 2.3.1.1: Structural Closures Data					
Base of *Amphistegina B*					
Closure ID	Area [mi^2]	Apex Depth [ft]	Spill Depth [ft]	Max Closure Height [ft]	Bulk Rock Volume [ft^3]
1	1.65	5,533	5,644	111	1,897,286,524
2	1.30	5,602	5,734	132	1,789,674,638
3	0.61	5,556	5,671	114	757,326,478
4	0.27	5,616	5,632	16.1	44,071,695
5	0.21	5,684	5,743	58.6	134,922,529
MFS9-05					
Closure ID	Area [mi^2]	Apex Depth [ft]	Spill Depth [ft]	Max Closure Height [ft]	Bulk Rock Volume [ft^3]
1	1.54	6,984	7,274	289	6,848,493,141
2	1.15	6,956	7,153	197	3,263,543,698

3	0.29	7,262	7,312	50.3	167,524,375
4	0.17	7,144	7,207	62.9	88,283,659
5	0.17	6,971	6,999	27.5	50,881,714
6	0.15	7,477	7,500	22.6	35,608,115

Based on Goodman et al. (2011), a deterministic approach was used to calculate the CO_2 storage capacity based on the following equation:

$$G_{CO_2} = A_t h_g \phi_{tot} \rho E_{saline} \qquad (2.3.1.1)$$

where,

G_{CO_2} = CO_2 storage resource mass estimate

A_t = Total area being assessed for CO_2 storage

h_g = Gross formation thickness

φ_{tot} = Total porosity

ρ = CO_2 density at reservoir conditions

E_{saline} = CO_2 storage efficiency factor for saline aquifers

The term in equation 2.3.1.1 that corresponds to the CO_2 storage efficiency factor (E_{saline}) accounts for the fact that not all the pore volume calculated will be available for CO_2 storage; therefore, it reflects the pore volume that can be occupied by the injected CO_2. The efficiency factor is calculated using the following equation (Goodman et al., 2011):

$$E_{saline} = E_{An/At} E_{hn/hg} E_{\phi e/\phi tot} E_A E_L E_g E_d \qquad (2.3.1.2)$$

where:

E_{saline} = CO_2 storage efficiency factor for saline aquifers

$E_{An/At}$ = Net-to-total area ratio

$E_{hn/hg}$ = Net-to-gross thickness ratio

$E_{\varphi e/\varphi tot}$ = Effective-to-total porosity ratio

E_A = Areal displacement

E_L = Vertical displacement

E_g = Gravity displacement

E_d = Microscopic displacement

The first three terms of equation 2.3.1.2 are associated with the uncertainty of static or geologic parameters, such as the net-to-gross thickness result from facies analysis, or effective porosity. The remaining terms are displacement components associated with uncertainty of the characteristics of the multiphase fluid flow in the subsurface (brine-CO_2 system) and the fluid-rock interactions. Net-to-total area refers to the fraction of the total region that is suitable for CO_2 storage, net-to-gross thickness to the fraction of the reservoir unit that meets minimum petrophysical requirements for optimal CO_2 storage, and effective-to-total porosity refers to the fraction of the pore volume that contributes to the fluid flow. The first three displacement terms of equation 3.2.2 refer to the fraction of the pore space surrounding the injection well that can be contacted by CO_2, and they can be integrated into a single term E_v, or volumetric displacement efficiency. The last term of the equation, E_d, is the fraction of the pore volume that can be replaced by CO_2, and it is directly related to irreducible water saturation for the case of saline aquifers (Gorecki et al., 2009; Goodman et al., 2011).

The efficiency terms related to static parameters can be addressed by detailed knowledge of the site geology. The detailed geologic characterization and subsequent geostatistical modeling performed in this work is therefore applicable to the calculation of such efficiency coefficients. In fact, because a 3D geocellular grid covering the reservoir area was created, and properties such as facies and porosity were distributed throughout the grid in the geostatistical modeling, actual values of net area, net thickness and effective porosity can be accounted for by calculating the net pore volume (NPV) of the reservoir from the 3D grid properties. Bearing in mind that there are six different reservoirs within the interval of interest for this work, the equation to calculate CO_2 storage capacity for the site of interest is as follows:

$$G_{CO_2} = \sum_{i=1}^{n} NPV_i \rho_i E_{saline_i} \qquad (2.3.1.3)$$

where:

G_{CO_2} = CO_2 storage resource mass estimate

NPV_i = Net pore volume of reservoir i

ρ_i = CO_2 density at pressure and temperature conditions of reservoir i

E_{saline_i} = CO_2 storage efficiency factor for reservoir i n = Number of reservoirs within the interval of interest

The density term of equation 2.3.1.3, ρ, is calculated as a function of depth using a depth-CO_2 density transform (Nicholson, 2012) to the midpoint of every reservoir. Such depth-CO_2 density transform was derived from empirical pressure-temperature-depth relationships (Figure 2.3.1.7) and comprises two equations, each applicable depending on the depth at which the reservoir is located. Because the interval of interest for this project is located below 5500 ft, for simplicity the equation presented here is that one applicable to the depth of interest:

$$\rho_d = 0.475(\frac{z_d}{1000})^3 - 14.27(\frac{z_d}{1000})^2 + 147.71\left(\frac{z_d}{1000}\right) + 154.92 \quad (2.3.1.4)$$

where,

ρ_d = CO_2 density [kg/m^3] from 5,000 to 10,000 feet of depth

z_d = Depth (between 5,000 and 10,000 feet)

Considering that the net pore volume accounts for the product of the net area, net thickness and effective porosity of each reservoir, their corresponding efficiency terms from equation 2.3.1.2 ($E_{An/At}$, $E_{hn/hg}$ and $E_{\varphi e/\varphi tot}$) can be considered to be equal to one. Therefore, equation 2.3.1.2 can be rewritten as:

$$\mathrm{E_{saline}} = \mathrm{E_v} E_d \quad (2.3.1.5)$$

where,

E_{saline} = CO_2 storage efficiency factor for saline aquifers

E_v = Volumetric displacement

E_d = Microscopic displacement

In order to calculate the efficiency factor associated with the displacement terms, numerical simulations of multiphase fluid flow in the subsurface for the brine-CO_2 system are required. Alternatively, a range of values (Goodman et al., 2011) are used to represent the uncertainty of E_{saline}. Such values were estimated as a result of a combination of data from different clastic reservoirs. Table 2.3.1.2 summarizes the different inputs used to quantify CO_2 storage capacity utilizing the method of Goodman et al. (2011). Clearly the NPV will be different depending on the model result used. Table 2.3.1.2 shows the NPV values for the first realization of the porosity model (facies 1, porosity 1).

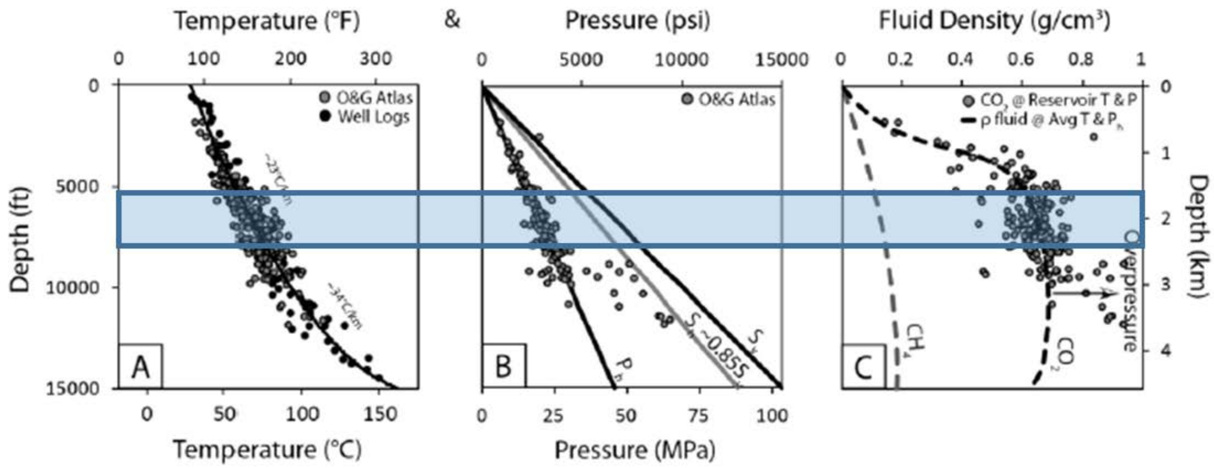

Figure 2.3.1.7: Temperature, pressure and density trends with depth, highlighting the interval of interest for this project. Modified from Nicholson, 2012.

Table 2.3.1.2: Summary of Input Data for Quantifying CO_2 Storage Resources					
	NPV [m^3]	ρ [kg/m^3]	E_{saline}		
			P_{10}	P_{50}	P_{90}
Interval 2	8.28×10^7	626.1	7.4%	14%	24%
Interval 3	4.47×10^7	633.3	7.4%	14%	24%
Interval 4	2.85×10^7	641.5	7.4%	14%	24%
Interval 5	3.02×10^7	648.8	7.4%	14%	24%
Interval 6	7.46×10^7	655	7.4%	14%	24%
Interval 7	4.94×10^7	660.4	7.4%	14%	24%
Total	3.1×10^8				

For the deterministic static methodology case using Goodman et al. (2011) equations, an average total (P_{50}) value of 28.25 Megatonnes [Mt] of CO_2 was estimated for the six reservoir layers in the area of interest (within closures). This result is an average value for 25 generated porosity models, summing the results for each of the 6 reservoirs. Results are summarized in Table 2.3.1.3.

Table 2.3.1.3: Summary Results for Deterministic Methodology using Goodman et al. (2011) Equations			
	P_{10} [Mt]	P_{50} [Mt]	P_{90} [Mt]
SGS_F1_P1	11.86	23.73	40.67
SGS_F1_P2	12.41	24.83	42.56
SGS_F1_P3	11.90	23.81	40.81
SGS_F1_P4	12.13	24.26	41.59
SGS_F1_P5	12.02	24.04	41.20
SGS_F2_P1	12.12	24.23	41.54
SGS_F2_P2	12.20	24.40	41.82
SGS_F2_P3	12.02	24.04	41.21
SGS_F2_P4	12.10	24.20	41.48
SGS_F2_P5	11.97	23.95	41.06
SGS_F3_P1	11.76	23.51	40.31
SGS_F3_P2	11.82	23.64	40.52
SGS_F3_P3	11.71	23.41	40.14
SGS_F3_P4	11.65	23.29	39.93
SGS_F3_P5	11.72	23.44	40.18
SGS_F4_P1	11.92	23.83	40.86
SGS_F4_P2	12.08	24.17	41.43
SGS_F4_P3	12.07	24.13	41.37
SGS_F4_P4	11.95	23.90	40.97
SGS_F4_P5	12.02	24.05	41.23
SGS_F5_P1	12.27	24.54	42.06
SGS_F5_P2	12.36	24.72	42.38
SGS_F5_P3	12.15	24.29	41.64
SGS_F5_P4	12.13	24.27	41.60
SGS_F5_P5	12.21	24.42	41.87
Average	12.02	24.04	41.22
Efficiency Factor	0.074	0.14	0.24

Table 2.3.1.3 – Summary results for the deterministic methodology using DOE's equations. SGS stands for Sequential Gaussian Simulation, F# represents the facies model number of and P# represents the porosity model number.

References

Beckham, E. C. (2018). CO_2 storage in deltaic environments of deposition: integration of 3-dimensional modeling, outcrop analysis, and subsurface application (Master's Thesis).

Galloway, W. E. (1989). Genetic stratigraphic sequences in basin analysis I: architecture and genesis of flooding-surface bounded depositional units. AAPG bulletin, 73(2), 125-142.

Goodman, A., Hakala, A., Bromhal, G., Deel, D., Rodosta, T., Frailey, S., & Huerta, N. (2011). US DOE methodology for the development of geologic storage potential for carbon dioxide at the national and regional scale. International Journal of Greenhouse Gas Control, 5(4), 952-965.

Gorecki, C. D., Sorensen, J. A., Bremer, J. M., Knudsen, D., Smith, S. A., Steadman, E. N., & Harju, J. A. (2009, January). Development of storage coefficients for determining the effective CO_2 storage resource in deep saline formations. In SPE International Conference on CO_2 Capture, Storage, and Utilization. Society of Petroleum Engineers.

Miall, A.D., Sedimentary Basins of the World, Elsevier: Amsterdam, 2008.

Nicholson, A. J. (2012). Empirical analysis of fault seal capacity for CO_2 sequestration, lower Miocene, Texas Gulf Coast (Master's Thesis).

<u>Task 3.0 – Risk Assessment, Simulation and Modeling</u>

Subtask 3.1 – Risk Assessment and Mitigation Strategies

<u>Subtask 3.1.1 Assess the adaptation of existing tools to offshore settings</u>

No activity this quarter.

<u>Subtask 3.1.2 Extend geomechanical assessment to additional areas of the basin</u>

No activity this quarter.

<u>Subtask 3.1.3 Dissolution and bubbling in water column</u>

LBNL (Lawrence Berkeley National Laboratory) reports,

We simulated a hypothetical major CO_2 well blowout in shallow water of the Texas Gulf Coast. We used a coupled reservoir-well model (T2Well) to simulate the subsea blowout flow rate for input to an integral model (TAMOC) for modeling CO_2 transport in the water column. Bubble sizes are estimated for the blowout scenario and used as input to TAMOC. Results suggest that a major CO_2 blowout in ≥50 m of water will be almost entirely attenuated by the water column due to CO_2 dissolution into seawater during upward rise. In contrast, the same blowout in 10 m of water will hardly be attenuated at all. This primary result is shown in Figure 3.1.3.1. We present the simulation results in a manuscript entitled, “Major CO_2 blowouts from offshore wells are strongly attenuated in water deeper than 50 m,” that we submitted to journal, *Greenhouse Gases: Science and Technology*.

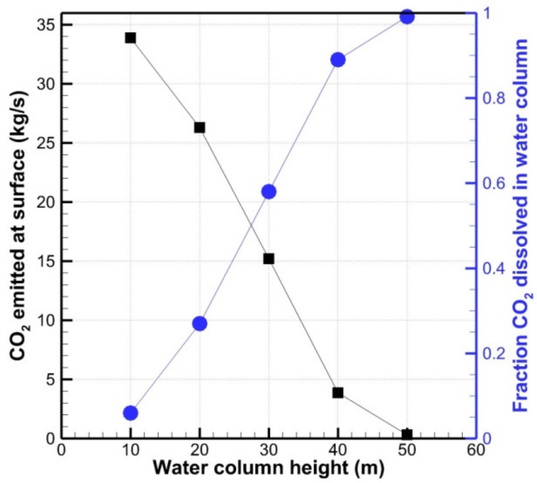

Figure 3.1.3.1 - CO_2 flow rate (squares) at the sea surface and fraction of CO_2 dissolved in the water column (circles) as a function of water column height (depth of wellhead below sea surface) for a major CO_2 blowout at the sea floor.

<u>Subtask 3.1.4 Numerical modeling of heterogeneous reservoirs</u>

LBNL finalized the revision of the journal paper on the multiscale and multipath channeling of CO_2 flow in a hierarchical fluvial reservoir that is relevant to the GoMCarb storage sites.

Subtask 3.2 – Geologic Modeling

Compressibility Effects on Viscous Instability Under Sealing and Partially Sealing Boundaries

Aura N. Araque-Martinez and Larry W. Lake, *Hildebrand Dept. of Petroleum and Geosystems Engineering, Cockrell School of Engineering, The University of Texas at Austin*

The effects of instability and heterogeneity on displacements, primarily enhanced oil recovery and carbon dioxide storage, has been long studied (Homsy, 1978), though they remain difficult to predict. The usual recourse to modeling these effects is through numerical simulation. Simulation remains the gold standard for prediction; however, its results lack generality being case specific. Analytical methods, the type covered here, are more informative than simulation results There are several analytical models, among them the Buckley-Leverett, Koval, Stiles, Dykstra-Parsons and Hearn methods. However, these analytical methods apply to steady-state, incompressible flow. Combining the effects of instability and heterogeneity with compressible flow was the objective of this work.

Carbon dioxide storage uses compressible fluids, and, in the absence of producing wells (Yun et al., 2017), will not be steady-state flow. Consequently, is unlikely that CO_2 storage occur in reservoirs of open boundaries. Flow of compressible fluid, such as CO_2 necessitates the use of closed or partially sealed boundaries, a factor that is consistent with compressible flow. It was the object of this work to investigate the effect of how partially sealed boundaries and compressible fluids affects the displacement behavior in CO_2 storage.

The well-known criterion for the onset of viscous fingering is based on the so-called Saffman-Taylor (ST) instability work (Saffman and Taylor, 1958). Derived from incompressible fluids under steady-state flow, the ST criterion states that a steady state flow will exhibit front displacement instability (an arbitrary perturbation in the front will grow) if the driving fluid is less viscous than the displaced fluid (e.g. mobility ratio M > 1).

Results show that adding compressibility always (even for M<1) makes displacements more unstable for compared steady-state flows. For semi steady-state flow (sealed outer boundary) displacements will become more stable as a front approaches the boundary.

Problem Definition

This work deals with a 1D linear compressible flow as presented in Figure 3.2.1. Flow is from left to right.

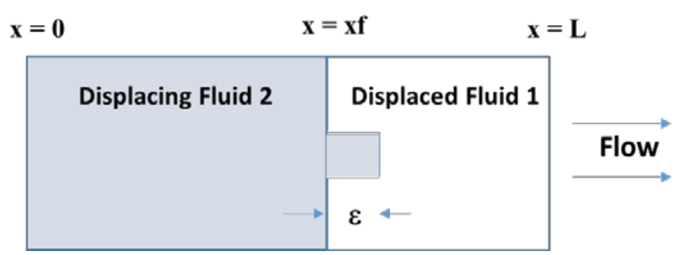

Figure 3.2.1 - Schematic of a 1-D linear displacement, showing the perturbation,

Fluid 2 is displacing fluid 1 with no transition zone between them; the two components are locally segregated or piston like. The absence of a transition zone means that the results apply to both miscible and immiscible displacements, absent dispersion or local capillary pressure. The main displacement boundary is at location x_f and moves with velocity $\frac{dx_f}{dt}$. We imagine an arbitrary perturbation $\boldsymbol{\varepsilon}$ on the front that moves with velocity $\frac{d\varepsilon}{dt}$. The displacement is stable if the perturbation dies out with time ($\frac{d\varepsilon}{dt} < \mathbf{0}$) and unstable ($\frac{d\varepsilon}{dt} > \mathbf{0}$) or neutral ($\frac{d\varepsilon}{dt} = \mathbf{0}$), otherwise.

The condition for stability is necessary and sufficient; the condition for instability is only necessary inasmuch as there are several factors that would make a displacement, classified here as unstable, for which a perturbation would die out.

An important novelty here is the nature of the external boundary at x=L. Because our work considers compressible flow, this boundary may range from sealing (no flow) to completely transparent (no barrier to flow) according to a pre-specified parameter in the problem. These definitions play a role in the problem according to Figure 3.2.2.

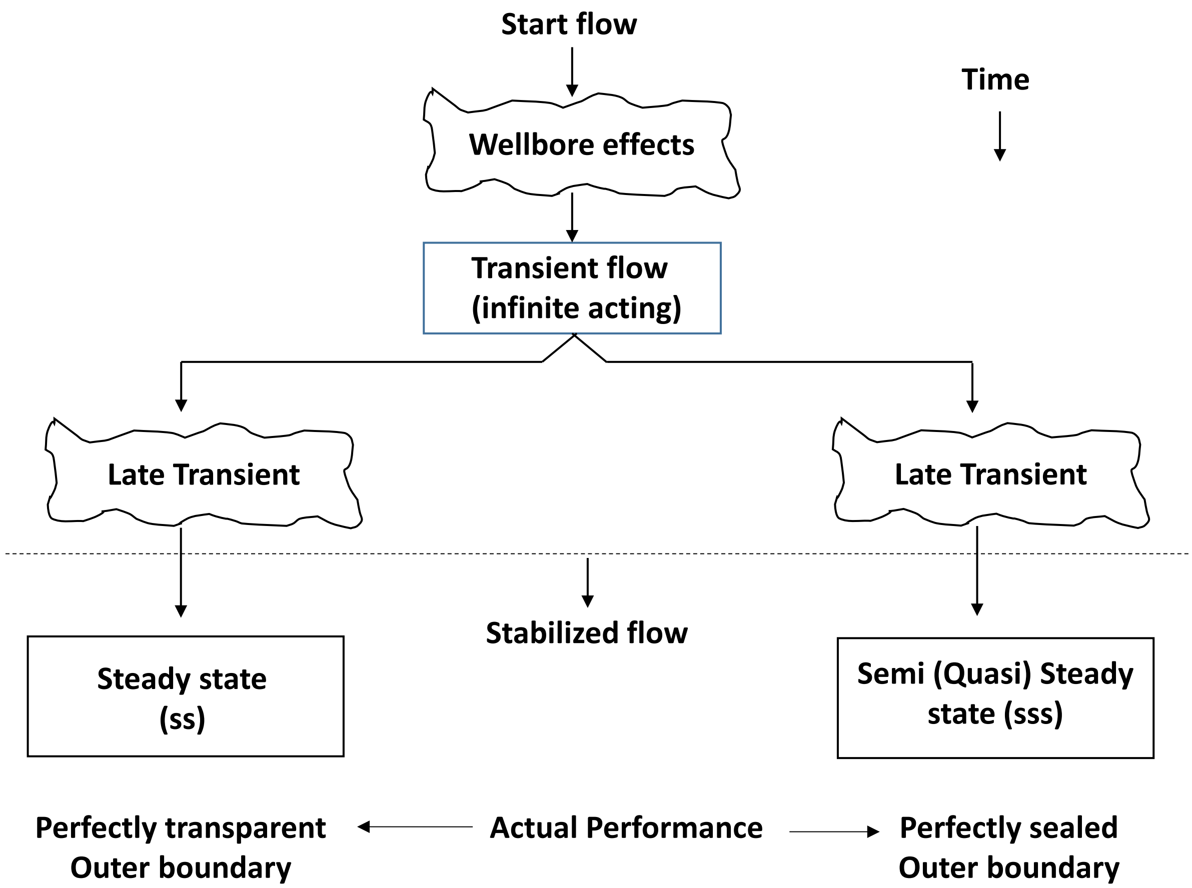

Figure 3.2.2 - Schematic of flow regimes for constant flow rate (taken from Walsh and Lake, 2003)

When flow begins at the left boundary x=0, there is a period of time when the pressure caused by the flow does not reach the external; this flow regime is canned transient or infinite acting because the location of the boundary is unimportant to the flow. At late time (stabilized in Fig. 3.2.2), the nature of the external boundary dominates the flow. If the boundary is transparent, the flow is steady-state and does not depend on time; if the boundary is sealed, as though there is no source of fluid offtake, the flow is semi steady-state. Flow under both conditions is said to be boundary dominated or *stabilized*.

The analytical work presented below deals entirely with stabilized flow, under most conditions the longest period of flow. This means that we are letting the background flow of fluid 1 become stabilized before introducing fluid 2.

Analytic Solutions

The formulations discussed in this section correspond to the solutions to the diffusivity equation:

$$\frac{\partial}{\partial x}\left(\rho \frac{\partial P}{\partial x}\right) = \frac{\rho}{\alpha}\frac{\partial P}{\partial t}$$

Different solutions are derived from the above equation depending on boundary conditions (inlet and outlet) and compressibility combinations. Here, we follow the $c_f \Delta p$ cut-off to differentiate the compressibility regime. In this regard, incompressible flow corresponds to cases where $c_f \Delta p = 0$, while small and constant and large and constant compressibility regimes correspond to the cases where $c_f \Delta p < 0.1$ and $c_f \Delta p > 0.1$ respectively. Some of the solutions are presented in Table 3.2.1 for large and constant compressibility. The term f in those is the outlet to inlet mass flux ratio. For steady-state flow cases f=1 (transparent outer boundary) and for the unsteady-state flow cases (sealed boundary) f=0, Figure 3.2.2 .

Table 3.2.1 – Pressure solutions for large compressibility and different boundary conditions

Compressibility	Inlet	Outlet	Pressure Solution
Large and constant, $c_f \Delta p>0.1$	Mass flux	Mass flux	$e^{c_f P(x,t)} = \frac{c_f}{\rho_R}\frac{\dot{m}_o \mu}{kL}(1-f)\frac{x^2}{2} - \frac{c_f}{\rho_R}\frac{\dot{m}_o \mu}{k}x + e^{c_f P_o}$
large	Volumetric flux	Mass flux	$e^{c_f P(x,t)} = \frac{c_f}{\rho_R}\frac{\dot{m}_o \mu}{kL}(1-f)\frac{x^2}{2} - \frac{c_f}{\rho_R}\frac{\dot{m}_o \mu}{k}x + e^{c_f P_o}$
large	pressure	Mass flux	$e^{c_f P(x,t)} = \frac{c_f}{\rho_R}\frac{\dot{m}_o \mu}{kL}(1-f)\frac{x^2}{2} - \frac{c_f}{\rho_R}\frac{\dot{m}_o \mu}{k}x + e^{c_f P_o}$
large	Mass flux	Volumetric flux	$e^{c_f P(x,t)} = \frac{c_f}{\rho_R}\frac{\dot{m}_o \mu}{kL}(1-f)\frac{x^2}{2} - \frac{c_f}{\rho_R}\frac{\dot{m}_o \mu}{k}x + e^{c_f P_o}$
large	Volumetric flux	Volumetric flux	$e^{c_f P(x,t)} = \frac{c_f}{\rho_R}\frac{\dot{m}_o \mu}{kL}(1-f)\frac{x^2}{2} - \frac{c_f}{\rho_R}\frac{\dot{m}_o \mu}{k}x + e^{c_f P_o}$
large	pressure	Volumetric flux	$e^{c_f P(x,t)} = \frac{c_f}{\rho_R}\frac{\dot{m}_o \mu}{kL}(1-f)\frac{x^2}{2} - \frac{c_f}{\rho_R}\frac{\dot{m}_o \mu}{k}x + e^{c_f P_o}$
large	Mass flux	pressure	$e^{c_f P(x,t)} = \frac{c_f}{\rho_R}\frac{\dot{m}_o \mu}{kL}(1-f)\frac{(x^2-L^2)}{2} - \frac{c_f}{\rho_R}\frac{\dot{m}_o \mu}{k}(x-L) + e^{c_f P_L}$
large	Volumetric flux	pressure	$e^{c_f P(x,t)} = \frac{c_f}{\rho_R}\frac{\dot{m}_o \mu}{kL}(1-f)\frac{(x^2-L^2)}{2} - \frac{c_f}{\rho_R}\frac{\dot{m}_o \mu}{k}(x-L) + e^{c_f P_L}$
large	pressure	pressure	$e^{c_f P(x,t)} = \frac{c_f}{\rho_R}\frac{\dot{m}_o \mu}{kL}(1-f)\frac{(x^2-xL)}{2} + \left(\frac{e^{c_f P_L} - e^{c_f P_o}}{L}\right)(x-L) + e^{c_f P_L}$

Validation Against Numerical Simulation

We validate results from analytical solution using numerical simulations under equivalent flow properties. Pressure profile results are compared for different fluid compressibility and different outlet-inlet mass flux ratio (f). The steady-state (f=1) results are in Figure 3.2.3, while the unsteady-state (f=0) results are in Figure 3.2.5. Figure 3.2.4 includes the results for an in-between case (f=0.5) in order to show the generality of the formulation developed in this work. In general, CO_2-EOR would be $f = 1$ while CO_2-Storage would be $f = 0$.

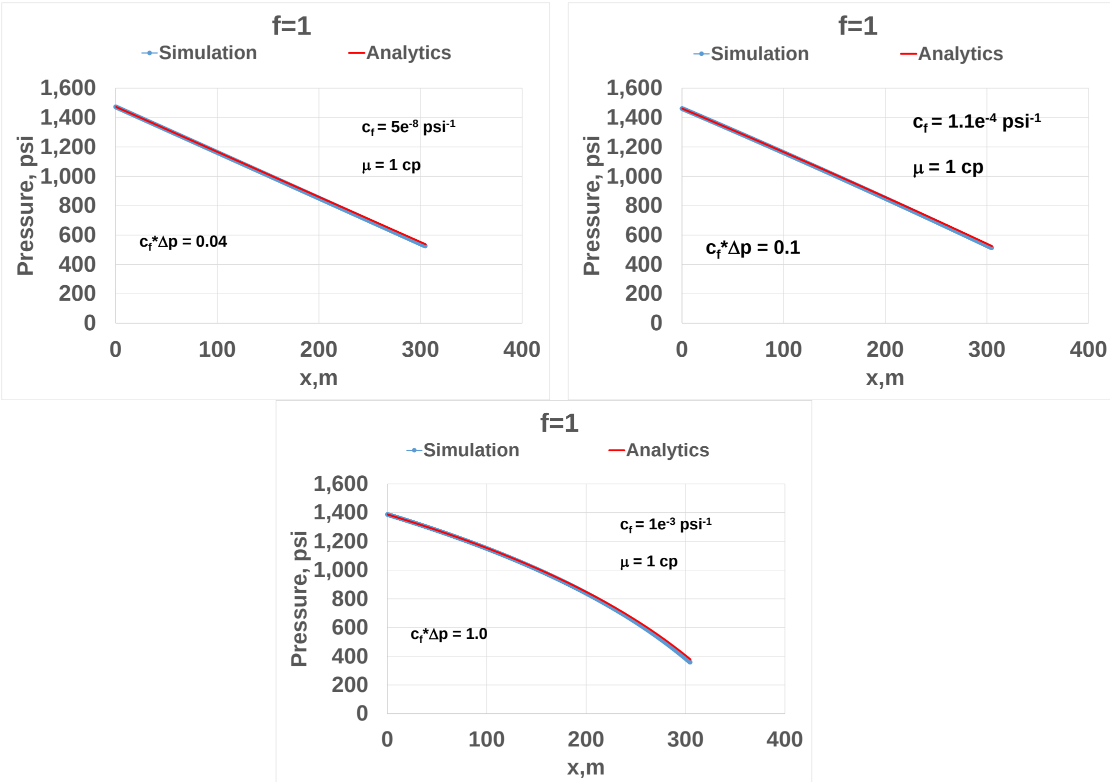

Figure 3.2.3 – Analytical and simulation pressure results comparison for single fluid under different compressibility (f=1, steady-state flow).

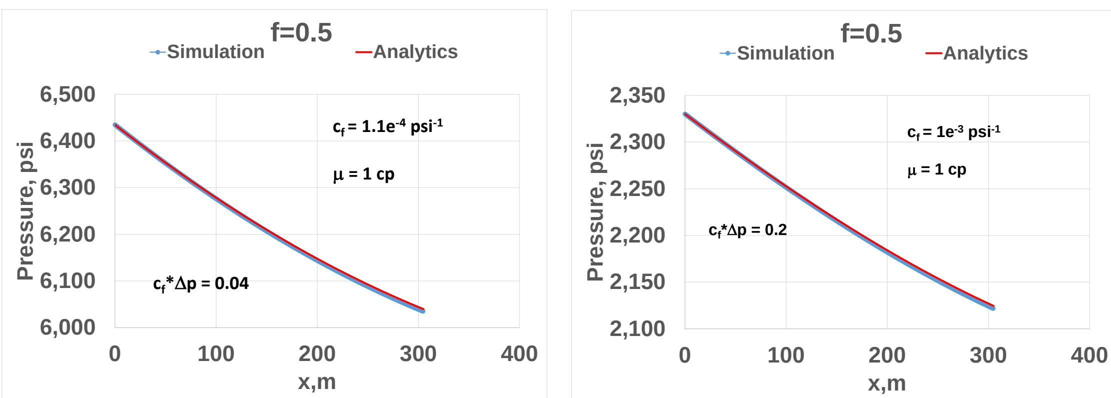

Figure 3.2.4 – Analytical and Simulation pressure results comparison for single fluid under different compressibility (f=0.5).

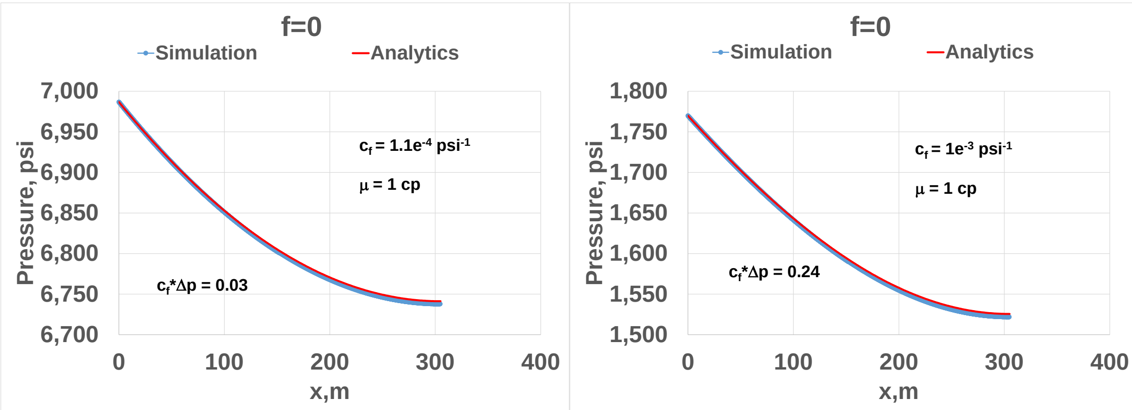

Figure 3.2.5 – Analytical and simulation pressure results comparison for single fluid under different compressibility (f=0, semi-steady-state flow.

All these cases include inlet and outlet volumetric fluxes as boundary conditions, the inlet pressure as known. Results show a perfect agreement between simulation work and the work proposed here.

Instability Analysis

We performed perturbation analysis of the solution of the diffusivity equation by adding a tracer to the flow. Figure 3.2.6 and Figure 3.2.7, a comparison of these results between simulations and analytic solution, show very good agreement for the front position history. The slope (first derivative) of those plots corresponds to the front velocity, while the second derivative of the front position history corresponds to the perturbation velocity. Figure 3.2.6 includes three different outer boundary conditions (f=1, 0.5 and 0) for small and constant compressibility.

For these cases, the displacement is neutral $\frac{d\boldsymbol{\varepsilon}}{d\boldsymbol{t}} = \mathbf{0}$ for f=1 and stable $\frac{d\boldsymbol{\varepsilon}}{d\boldsymbol{t}} < \mathbf{0}$ for f=0.5 and f=0.

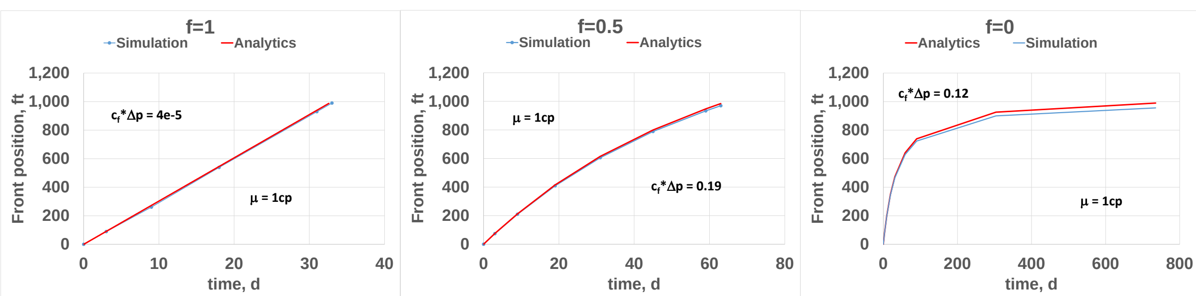

Figure 3.2.6 – Outer boundary effect on front position under small and constant compressibility conditions.

Figure 3.2.7 includes three different outer boundary conditions (f=1, 0.5 and 0) for large and constant compressibility. In this case, the displacement is unstable $\frac{d\boldsymbol{\varepsilon}}{d\boldsymbol{t}} > \mathbf{0}$ for f=1 and stable $\frac{d\boldsymbol{\varepsilon}}{d\boldsymbol{t}} < \mathbf{0}$ for f=0.5 and f=0.

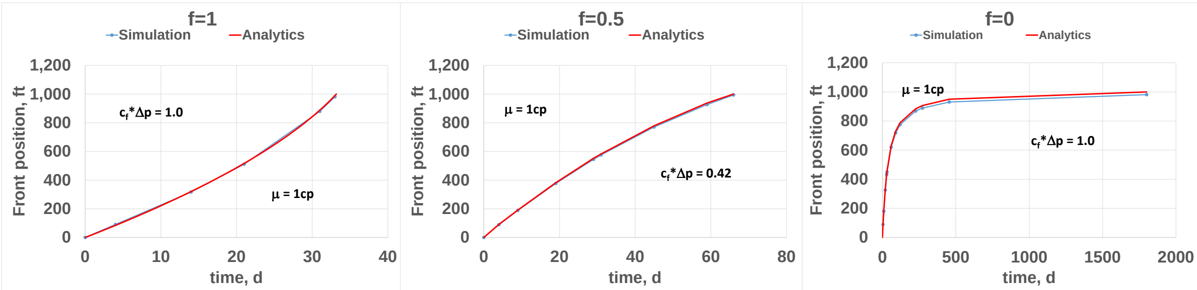

Figure 3.2.7 – Outer boundary effect on front position under large and constant compressibility conditions.

Conclusions

1. The Saffman-Taylor approach analyzed the behavior of perturbation of a displacement front. A perturbation in the front position will grow when M>1 and the front will be unstable. This criterion is equivalent to determining whether the volumetric flux of the fluid increases with distance to the production end.

2. For steady-state flow (transparent outer boundary) adding compressibility always makes displacements more unstable. The simple reason for this is that as flow proceeds downstream, pressure declines, specific volume of the fluid increases and velocity increases. According to finding 1, a displacement will be unstable even if M<1.

3. For semi-steady-state flow (sealed outer boundary) displacements will become more stable as a front approaches a boundary simply because the front velocity must slow down there and average pressure rises.

References

Homsy, G. M. Viscous Fingering in Porous Media. Ann. Rev. Fluid Mech. 1987. 19, pp. 271-311.

Saffman P. G., Taylor S. G., The penetration of a fluid into a porous medium or Hele-Shaw cell containing a more viscous liquid. *Proc. R. Soc. London Ser. A 245 :312-329, 1958.*

Walsh, Mark P. and Lake, Larry W. *Primary Hydrocarbon Recovery*, Elsevier, 2004.

Wu, Yun, Bryant, Steven L., and Lake, Larry W., “Pressure Management of CO_2 Storage by Closed-loop Surface Dissolution”, Energy Procedia 114, 2017, pp. 4811-4821.

NOMENCLATURE

c_f: fluid compressibility, m2/kgf
f: outlet to inlet mass flux ratio, unitless
k: absolute permeability, m2
L: total length of the system, m
$\dot{m}$ mass flux, kg/m2-s

P: pressure, kgf/m2
P_L: outlet pressure, kgf/m2
P_o: inlet pressure, kgf/m2
P_R: reference pressure, kgf/m2
q: fluid rate, m2/s
t: time, s
u: Darcy's velocity – volumetric flux, m/s
x: flow direction, m
x_f: front position, m
u_f: front velocity, m/s

Symbols

α: diffusivity constant, m2/s
ε: perturbation, m
ϕ: porosity, fraction
μ: fluid viscosity, kgf-s/m2
ρ: fluid density, kg/m3
ρ_R: reference fluid density, kg/m3

Lawrence Livermore National Laboratory (LLNL)

LLNL has finished building a gridded model for the High Island 24L site, and we have run some simple single-phase flow simulations on it to confirm it works. We are now testing out CO_2/brine simulations. We will start coordinating with BEG soon to decide on representative well configuration and injection scenarios to consider.

We have reasonable constraint on hydrologic properties based on the attribute maps provided by BEG, but poor constraint on mechanical properties. We are exploring what datasets are available that can narrow the range of mechanical and state-of-stress conditions to explore. We will also develop recommendations for additional site characterization steps if a GoM storage project were to move forward.

LLNL has initiated a task on available state-of-stress indicators for the area of interest. We are reviewing available datasets and previous work on this topic. This work will feed into our geomechanical risk assessment recommendations.

Subtask 3.2.1 – Reservoir modeling

A portion of the High Island-24L area (Figure 3.2.1.1) was modeled using Schlumberger's PETREL® software (aka "sector model"). The sector model was generated in order to correct an issue with fault plane integrity of the previously generated static geologic model that was generated in Haliburton Landmark's DecisionSpace®. The improved fault plane from the sector model will allow for improved reservoir flow simulation to be performed. The dimension of the sector model is 4 km in width and 7 km in length (Figure 3.2.1.1).

Four horizons and two faults were integrated into the sector model (Figure 3.2.1.2). In a pillar gridding process, the pertinent geologic strike (i.e., azimuth trend) of faults was used as the trend for the orientation of the model's grid cells (Figure 3.2.1.3). The result was smooth fault planes in the model instead of the zig-zagging fault planes, which the DecisionSpace® model generated.

Three zones were generated using 10 layers in the upper interval, 20 layers in the middle interval, and 50 layers in the lower interval (Figure 3.2.1.4). The middle interval represents the Amph-B shale interval. The total number of grid cells in this sector model is 413,440 cells with cell dimension 100x100 m. The average layer thickness is approximately 6 feet. Preliminary porosity model was also built based on the average porosity values based on wells in the HI-24L (Figures 3.2.1.2 - 3.2.1.5).

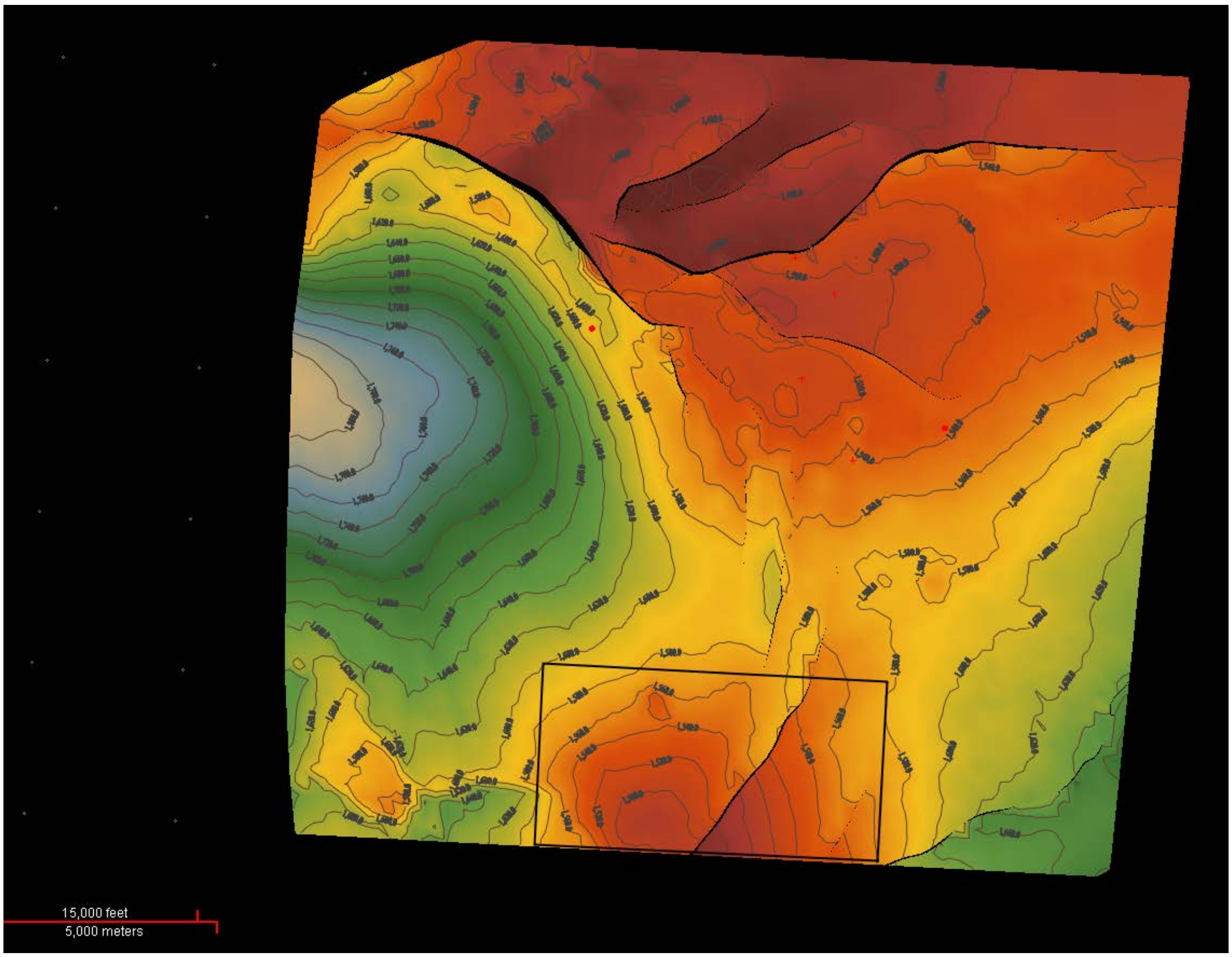

Figure 3.2.1.1 – Map view of the MFS 9 horizon in the High Island 24L Field area. Note, the small rectangle in the bottom center (southern portion) of the map outlines the portion of the area that was modeled in PETREL® shown in figures.

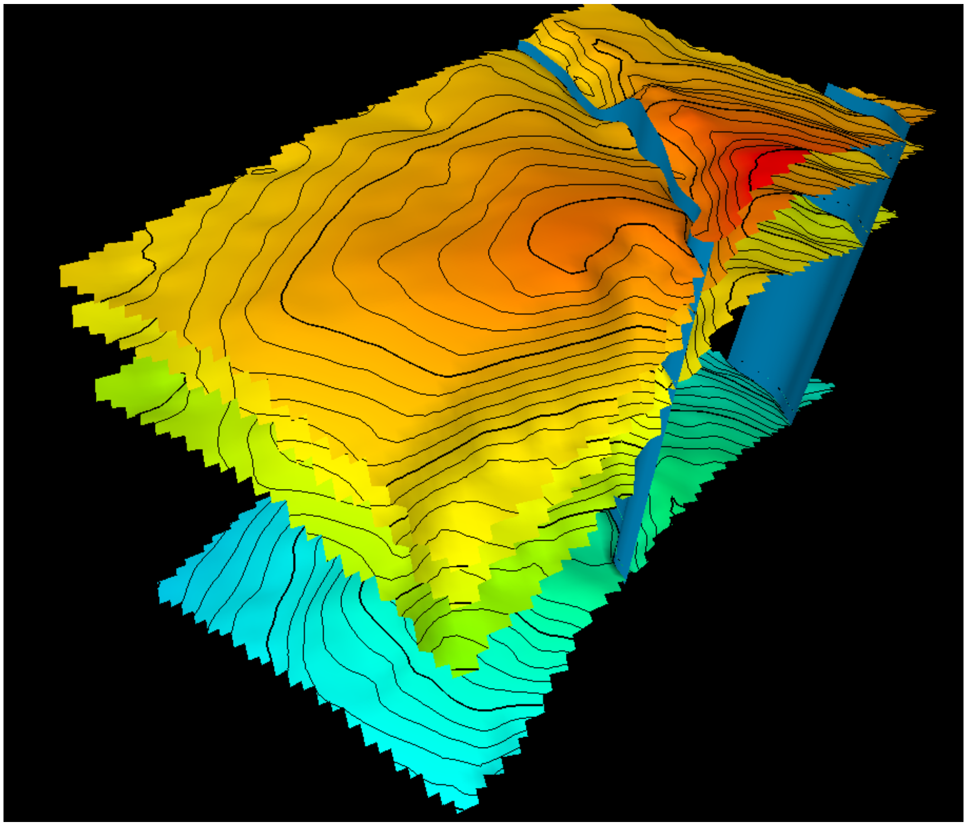

Figure 3.2.1.2. Four horizons and two faults were used in building the PETREL sector model.

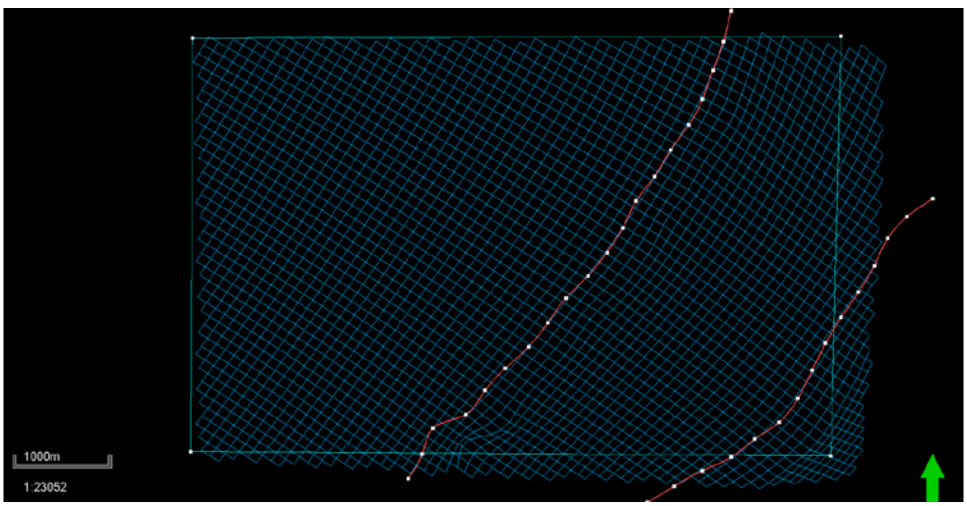

Figure 3.2.1.3. Pillar gridding process allowed the grid cells' orientation to follow the faults' orientations vs. the more problematic zig-zag fault plane model.

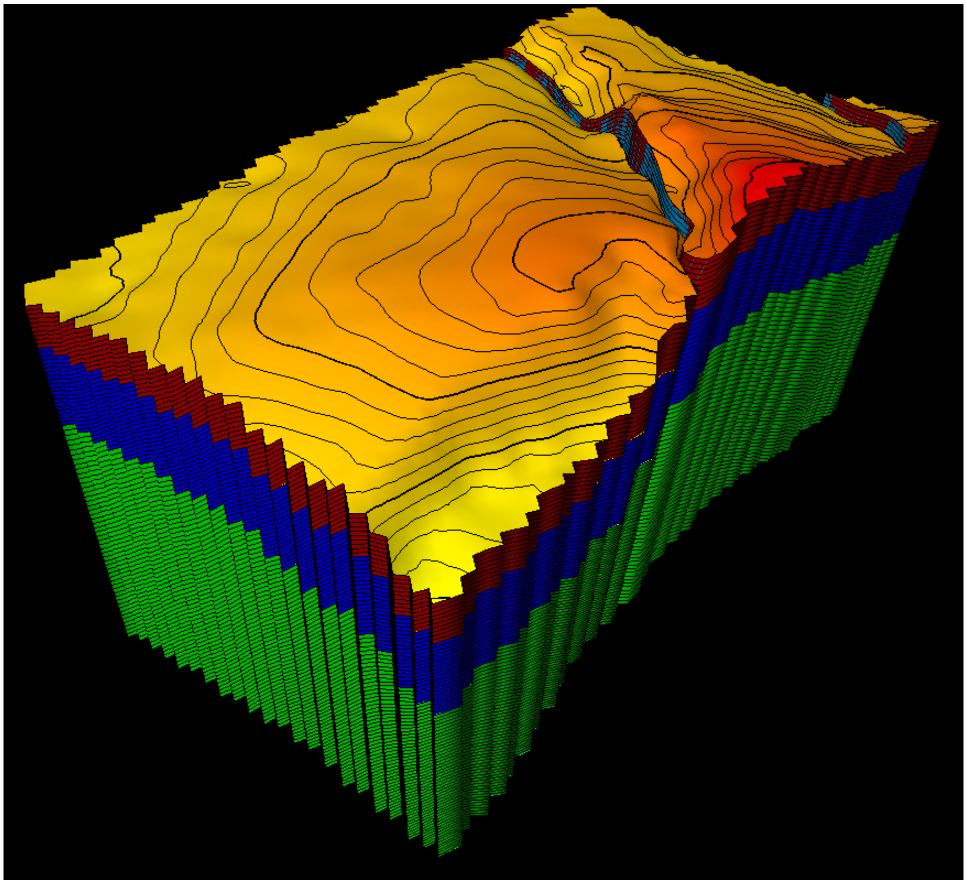
Figure 3.2.1.4 – A total of 80 layers were generated within the upper, middle, and lower intervals.

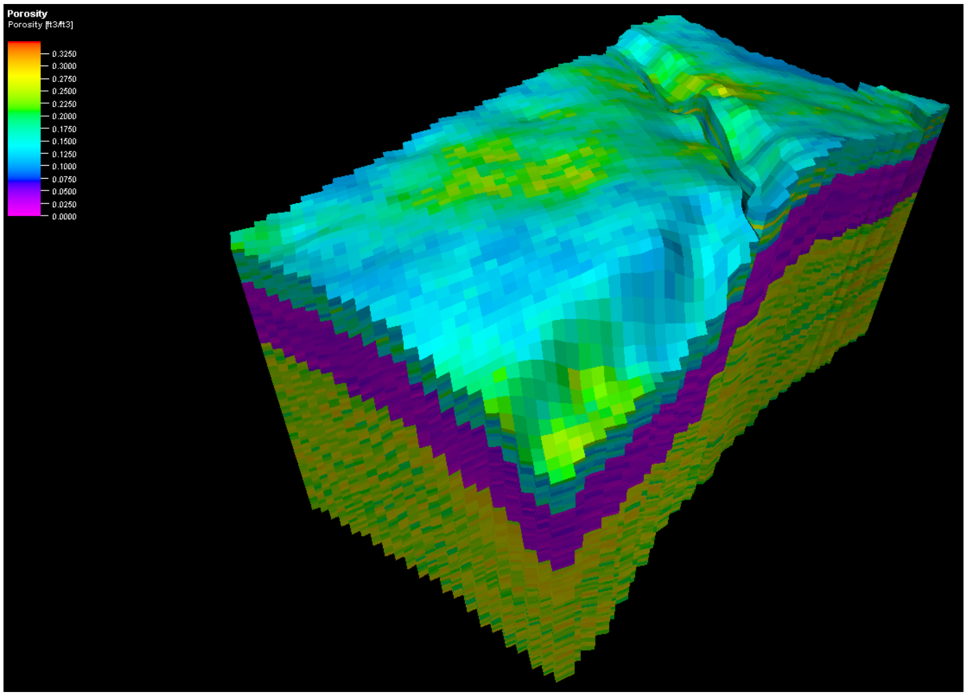

Figure 3.2.1.5 – Preliminary porosity model. Note the lower porosity values in the middle (i.e., *Amphistegina B*) interval, which comprises the mudrocks of the proposed seal (aka caprock) unit.

Subtask 3.2.2 Sub-basinal scale modeling

No activity during this quarter.

Subtask 3.2.3 History matching experiment via modeling

No activity during this quarter.

Subtask 3.2.4 Economic modeling

No activity during this quarter.

TASK 4.0: Monitoring, Verification, and Assessment (MVA)

Subtask 4.1: MVA Technologies and Methodologies

No activity during this quarter.

Subtask 4.1.1 Geochemical Monitoring of Seabed Sediments

No activity during this quarter.

Subtask 4.1.2 Geochemical Monitoring of Seawater Column

No activity during this quarter.

Subtask 4.1.3 UHR3D Seismic

No activity during this quarter.

Subtask 4.1.4 Distributed Acoustic Sensors

FY19, Q4 Quarterly Contribution : GoMCARB, MVA, LBNL/Rice (J. Ajo-Franklin & N. Lindsey)

During the last quarter, the LBNL/Rice MVA effort focused on Subtask 3 and completed analysis of an existing seafloor Distributed Acoustic Sensing (DAS) dataset previously acquired in Monterey Bay. The focus of this analysis was to better understand the noise characteristics of DAS acquisition in a marine environment as well as to understand the utility of passive seismic acquisition using DAS in a near-shore environment for eventual incorporation into a GCS MVA system.

As mentioned previously, the DAS dataset is a *dataset of opportunity* acquired on a seafloor observatory umbilical cable, stretching from Moss Landing, CA, to a deeper environment above the Monterey Canyon. The cable and observatory (MARS) are managed and maintained by the Monterey Bay Aquarium Research Institute. The cable includes both single mode fibers (for telemetry) as well as power for the MARS observatory and was trenched at depths of ~1m beneath the seafloor. During periods when the MARS cable is de-energized for maintenance, the single mode fibers were available for DAS measurements; we have now acquired close to 7 days of ambient noise DAS data on the initial ~20 km of the cable. One interesting aspect of the fiber path is that it passes directly over several mapped faults, which are part of the Aptos Fault Zone, and the cable is in close proximity (20-30 km) to the seismically active San Gregorio and Calaveras Faults.

One interesting opportunity provided by this dataset was a chance to examine the signature of the existing faults when illuminated by both ambient noise (e.g. Scholte waves) as well as arriving body waves generated by regional earthquakes. If detection, mapping, and monitoring of such faults were possible, applications in GCS (geological carbon sequestration) would be numerous, particularly if time-lapse repeatability could be demonstrated. Figure 4.1.4.1 provides an example of the arrival of an M3.4 earthquake as recorded by the seafloor DAS array. A first observation is that such a dense 20 km record with 2 m sampling is effectively unprecedented in the context of seafloor seismology where only sparse OBS (ocean bottom seismometers) are typically available. As can be seen in Fig. 4.1.4.1, panel A, all of the primary EQ phases are resolved including the P, S, and SS arrivals; although the P components are weak because of the broadside incidence angle with respect to the cable. The most interesting observation is the conversion of body waves to scattered surface waves at the seafloor in zones with mapped faulting as can be seen in Panel B. As can be seen in Panel D, these scattering points are coincident with a pull-down in the SS arrival suggesting a zone of lower Vs in the near-seafloor regime, consistent with a fault system. Several other zones with similar scattering features were identified as can be seen in panel C, suggesting that DAS coupled to ambient noise sources could be used to map zones of faulting.

Moving forward, we are examining approaches for imaging the surficial sediment column using high-density DAS datasets, in particular targeting converted surface waves; if successful, similar approaches could be useful at several stages in the characterization and MVA stages of a near-offshore GCS effort. While the resolution of passive imaging methods would be significantly lower than a high-quality 3D dataset, the continuous availability could be advantageous in providing MVA data between repeat time-lapse acquisition. Additionally, such data could be fused with active seismic data generated by the water column CASSM source under development.

The analysis of the MBARI dataset is currently under review and should be published over the next quarter. In the next several months, we anticipate more focused work on Subtasks 1 and 2 which focus on source development and testing for continuous active source DAS acquisition.

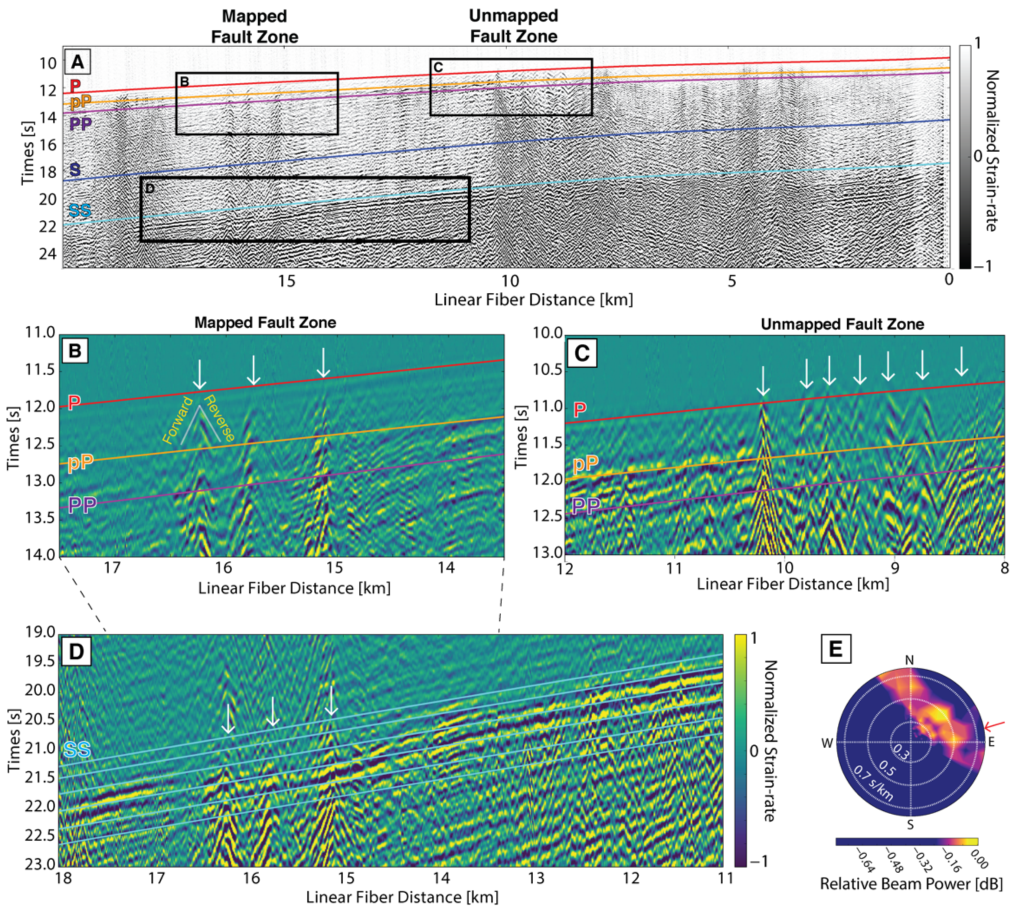

Figure 4.1.4.1: M3.4 2018-Mar-11 Gilroy earthquake wavefield observed by the MBARI DAS array (A) Full array observation (0=shore) with predicted seismic phase arrivals (colored lines). (B) Inset shows scattering with recently-mapped submarine fault locations (white arrows). (C) Same as (B) for an unmapped fault zone. (D) Observed 0.25 s wave front delay in mapped fault zone from (B). Lines show predicted constant phase arrivals immediately following the first SS wave front. (E) Time-domain beamforming solution shows energy arriving from ENE azimuths, while red arrow shows predicted back azimuth.

<u>Subtask 4.1.5 Pipeline MVA</u>

Co-PI, Dr. Daniel Chen, (Project Partner Lamar University)

1. High Island 10L

Lamar University investigated marine environmental conditions near the High Island 10L Field. Knowing environmental conditions is important for potential pipeline siting and site evaluations.

High Island 10L, a historic hydrocarbon field potentially suitable for CO_2 storage, is located in the Gulf of Mexico, long-94.00 and lat 29.554, Figure 4.1.5.1.

Figure 4.1.5.1 Location of the High Island 10L [1]

Three stations in the High Island 10L region are used to collect environmental conditions. The stations are located at the Sabine Pass, Sabine Bank Channel, and the Galveston Bay Entrance, Figure 4.1.5.2.

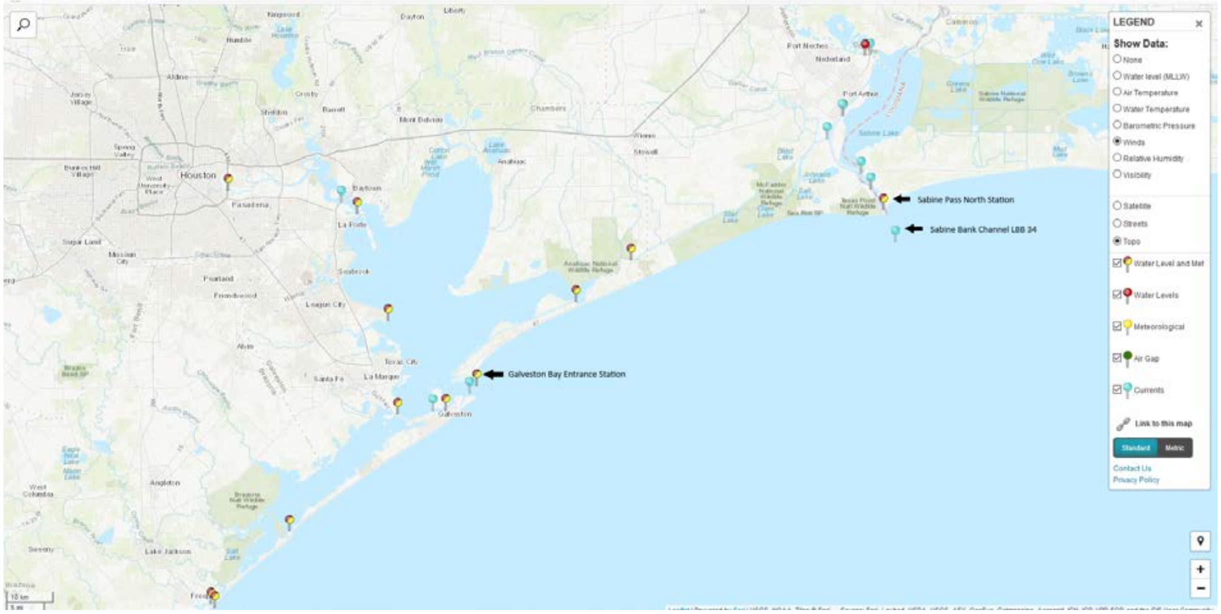

Figure 4.1.5.2 Location of Stations[2]

2. **Environmental Data for High Island 10L**

The data available from each station is summarized in Figures 4.1.5.3 and 4.1.5.4. The speed and direction of surface sea currents are monitored only in the Sabine Bank Channel LBB 34. The stations data can be exported to Excel.

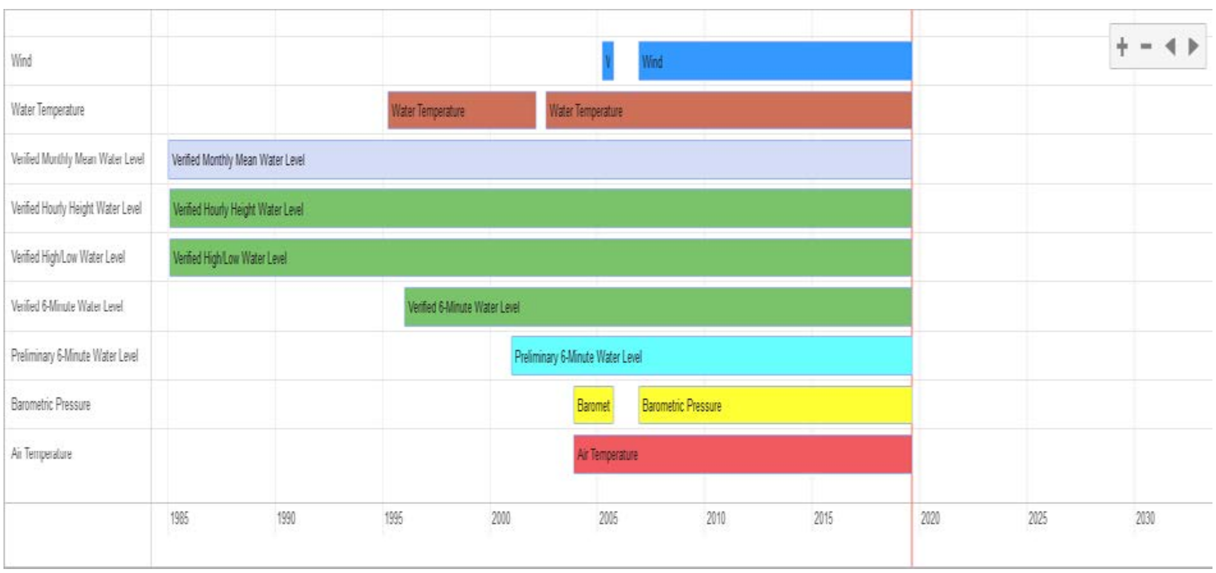

Figure 4.1.5.3 Sabine Pass North Station available data

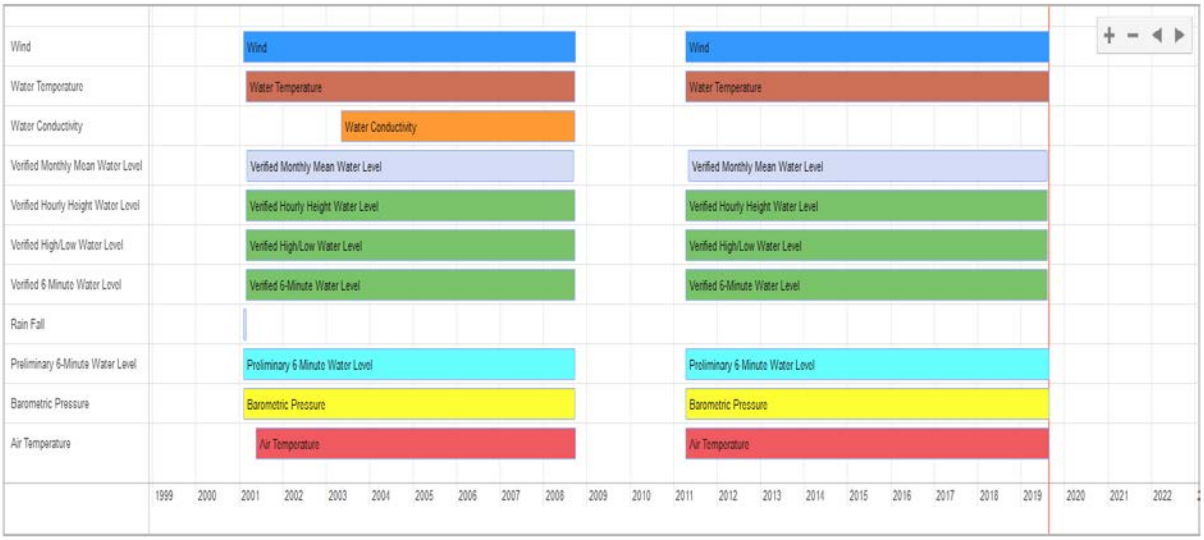

Figure 4.1.5.4 Galveston Bay Entrance Station available data

According to the Gulf of Mexico bathymetric map, Figure 4.1.5.5, the depth around High Island 10L is 20 meters. Furthermore, the terrain at High Island 10L is essentially flat, Figure 4.1.5.6.

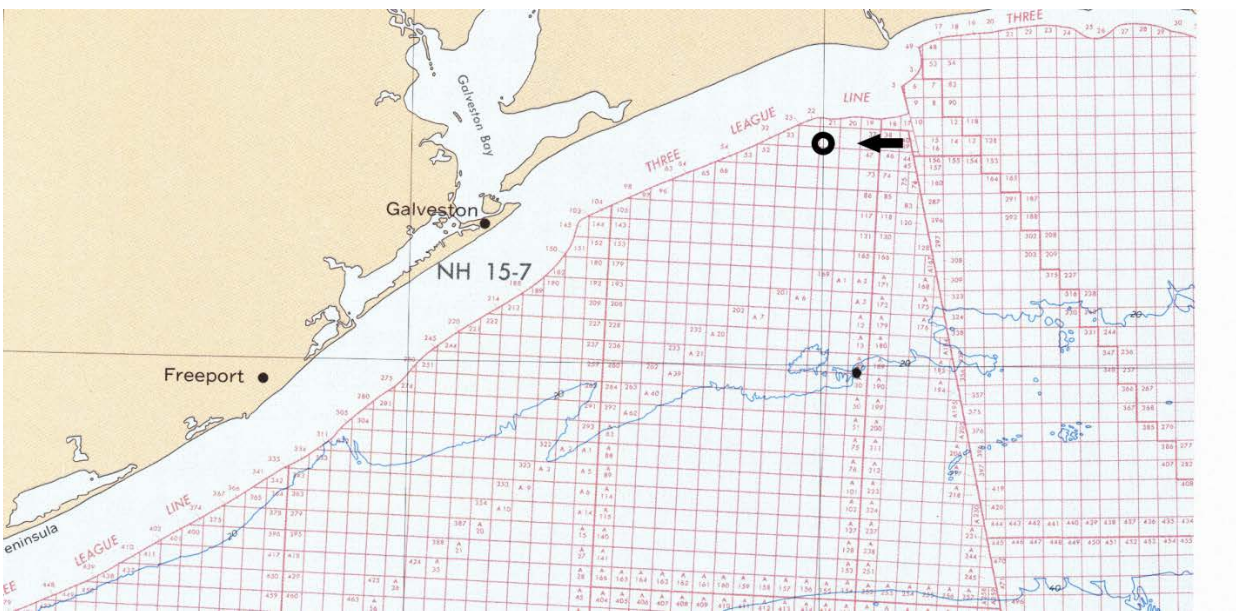

Figure 4.1.5.5 Gulf of Mexico Bathymetric Map, High Island 10L Location

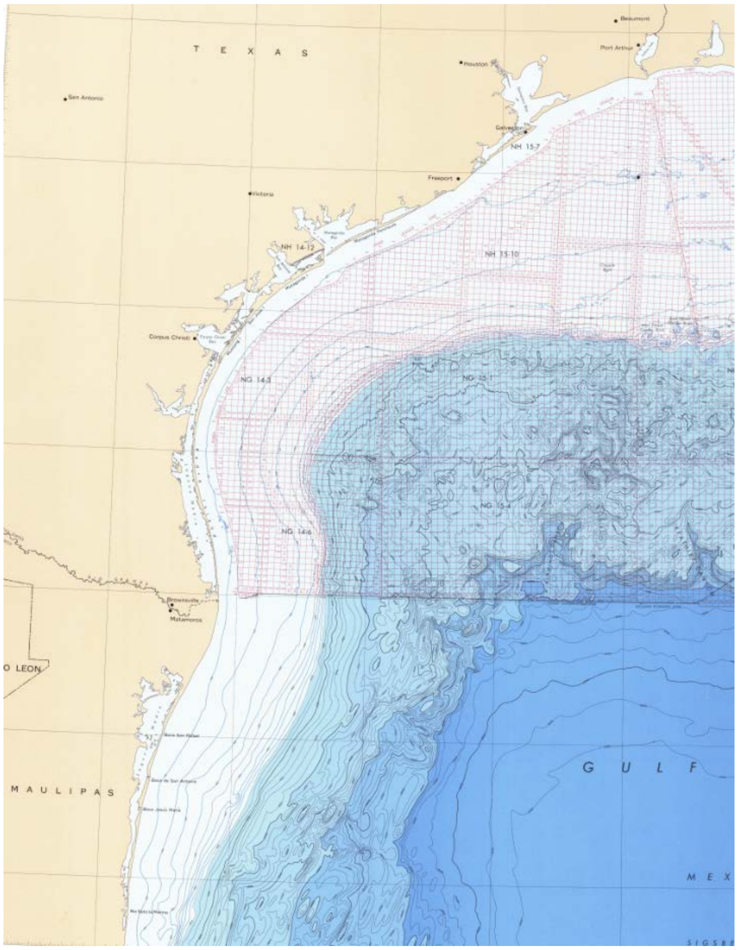

Figure 4.1.5.6 Gulf of Mexico Bathymetric Map [3]

We acknowledge useful interactions with GoMCarb team members, Curtis Oldenburg at the Lawrence Berkeley National Laboratory (LBL) and Anthony Knap at the Texas A& M University (TAMU) regarding marine environmental data near 10L and 24L lease blocks in Texas State Waters.

[1] *http://gis.rrc.texas.gov/gisviewer/*

[2] *https://tidesandcurrents.noaa.gov/map/index.html*

[3] https://maps.ngdc.noaa.gov/viewers/fishmaps/

Subtask 4.2: Plans for Testing of MVA Technologies

Subtask 4.2.1 Priority list for MVA Technologies and testing methods

No activity during this quarter.

TASK 5.0: Infrastructure, Operations and Permitting

Subtask 5.1: CO_2 Transport and Delivery

A key component of Trimeric's effort under Task 5 includes the assessment of existing infrastructure for re-use in CO_2 transport and storage applications. The objective of Subtask 5.1 (CO_2 Transport and Delivery) is to define what is known about infrastructure re-use and identify data gaps. The intent is to develop a screening tool that can be used to assess the potential of infrastructure assets (such as wells, platforms, and pipelines) for reuse. Trimeric is then applying these infrastructure screening criteria to assets in the High Island Large Block 10 region as a test case. In this way, a more detailed and practical understanding of the infrastructure reuse will be developed for the context of an overall CO_2 capture, transport, and storage project.

The work accomplished by Trimeric in support of Subtask 5.1 is described herein. Trimeric reviewed various literature sources and talked with industry experts about offshore infrastructure and its reuse, as listed in the references section of this quarterly report.

A summary of findings and Trimeric's plans to incorporate this information into the infrastructure screening criteria are now summarized.

Project Meetings with UT BEG

Trimeric met with UT BEG on July 19, 2019 to discuss progress to date and to receive guidance on path forward. As part of this discussion, UT BEG mentioned interest in HI-24L assets, as this block has active wells (as compared to HI-10L, which consists of dry holes and plugged wells). Therefore, during this quarter, Trimeric extended its queries to HI-24L for development of well screening methodologies.

Trimeric presented project findings on infrastructure re-use to the project team during a project team meeting held in Pittsburgh, PA on August 27, 2019 in conjunction with DOE-NETL's 2019 Carbon Capture, Utilization, Storage, and Oil and Gas Technologies Integrated Review Meeting. In attendance were UT BEG, DOE-NETL, and most of the project partners. Trimeric received feedback from project partners that will be used to help shape the infrastructure screening methodology.

General

Trimeric reviewed literature on infrastructure reuse for other offshore CO_2 storage or utilization projects (Zhou 2014, UK 2019). Takeaways included:

- The UK 2019 Consultation suggested prioritization of infrastructure for re-use as follows: depleted oil and gas reservoirs are the most important in terms of potential savings for having a well-characterized subsurface; trunk pipelines represent a significant savings advantage, with several EU projects reusing or contemplating their reuse; wells were less likely to be reused, with concerns about meeting standards for CO_2 use and concerns about corrosion; platforms were the least likely to be reused with only site specific circumstances justifying their reuse.
- The Zhou 2014 report drew heavily upon the Kingsnorth and Longannet projects, both of which have since been halted. Trimeric will work with the UT BEG to identify experts directly involved with these projects to help us identify and adapt learnings to the Gulf of Mexico.

Pipelines

- The Zhou 2014 report described the importance of designing the CO_2 pipeline for resistance to running ductile fracture; this concern was also expressed by one of the project's industrial experts during the August project team meeting. Because CO_2 depressurizes slowly, a longitudinal rupture of a pipeline could propagate for long distances; in contrast, crack propagation is not a concern for natural gas service because natural gas depressurizes quickly. For CO_2 service, the pipeline must be designed with periodic crack arrestors, such as joints of pipe with greater wall thickness [IEAGHG 2013].

Platforms

- Trimeric worked with UT BEG to identify the Texas General Land Office (GLO) as a source for platform data in Texas state waters. Trimeric is preparing a platform data request list to present to GLO, as the data do not appear to be readily available in a public online database.
- Trimeric reviewed a six-part series published by the Louisiana State University Center for Energy Studies on shallow structures in the Gulf of Mexico [Kaiser 2018]. The number of active structures in shallow waters (water depth < 400 ft) in the Gulf of Mexico rose steadily from the mid-1950s until reaching its peak in the late-1980s. The inventory of active structures plateaued throughout the 1990s (i.e., installation rates matched decommissioning rates), then declined from the mid-2000s to the present day. Based on the data presented in Kaiser (2018), Trimeric surmises the average lifetime of platforms in the shallow Gulf of Mexico waters is approximately 25 years, which agrees well with the typical platform lifespan of 20 to 30 years cited in Chakrabarti (2005).
- Dr. Elena Keen's PhD dissertation at the Hart Research Institute for Gulf of Mexico Studies at Texas A&M University in Corpus Christi, TX focused on platform assets in federal Gulf waters. Trimeric talked with Dr. Keen; her thesis is under embargo until 2020. Trimeric will review the dissertation when it becomes public. Dr. Keen recommended the Bureau of Safety and Environmental Enforcement (BSEE) as a source of information for assets in federal waters.
- Zhou (2014) discussed the platform equipment typically required for CO_2 processing: CO_2 process filters to remove rust particles picked up in the pipeline, CO_2 flow measurements and leak detection meters, injection manifold to route CO_2 to individual wells, well kill manifold supplied with seawater, a choke valve to control flow into the reservoir, and electrical heater (if needed, see next bullet point). Each well has its own flow line, well heater (if needed), well injection meter, and choke valve. A CO_2 vent line is directed downward toward sea, with no automatic venting of topside facilities, to avoid safety hazard to personnel.

Wells

- Trimeric worked with UT BEG to reconcile well information between the Texas Railroad Commission's (TX RRC's) database and the databases available to UT (IHS Enerdeq, IHS Petra, and Lexco OWL 7). There were several wells with incomplete information (e.g., missing API numbers) in the TX RRC database; UT used geographical coordinates to match the wells to the ones in the UT databases. The UT databases provided more complete and more easily accessible data than the TX RRC databases. In future, Trimeric will use the TX RRC data as a very quick initial screen to understand the assets present in an area, and will rely upon UT's databases to look at the details of any individual wells.
- UT BEG determined the steps required to obtain well completion data from TX RRC archives. The HI-10L area was not searchable by API number, so UT BEG had to consult the RRC archives to find the Oil/Gas Lease ID numbers for each well and searched by that ID number. Many wells had multiple ID numbers because of recompletions and changes from oil to gas

production. Review of these completion records is a manual process in which each lease ID is typed into the RRC online database query, and then the completion documents are viewed page by page. Trimeric is currently working with industry experts to determine the information that is of potential interest from these records. The team will then work to identify this information for a few example wells, in order to test out the well screening methodology.

- Trimeric reviewed the well assets in HI-24L, another block in High Island Large Block that is of interest to UT BEG. HI-24L contains 24 inactive (shut-in) wells, all owned by a single company, and all orphaned. The wells have been inactive anywhere from 2 to 21 years. HI-24L has 24 inactive wells, the most of any block in the High Island Large Block; there are 22 inactive wells in the remainder of the High Island Large Block, and no inactive wells in HI-10L. Trimeric will incorporate a well's shut-in status (i.e., its 14(b)(2) compliance) into the screening methodology.
- Trimeric talked with an industry expert who identifies opportunities to redevelop onshore oilfields and who had career experience with well completions in the Gulf of Mexico in the 1980s and 1990s. He suggested that we refine our screening criteria for the age of the wells. Our current criterion is for wells to be constructed after 1970 to ensure modern well construction; this date is important as a preliminary indicator of the integrity of wells within the field. However, he advises we will want much younger wells if we are going to reuse a well for injection. Therefore, we will need to know the lifetime of our CO_2 storage project as well as the projected start date for injection, as that will determine the age of assets that will make the most likely candidates for reuse. For example, if we have a 10-year project that will commence injection two years from now, and we assume a 25-year average life for assets, then we would target reusing assets that are currently approximately 13 years old or younger. This expert also cautioned that when he has wells that must be re-entered for re-work, he includes a significant line item in the budget for this work due to the uncertainty of well conditions. He also emphasized the importance of reviewing all available records for a field and reviewing even minute details within those records when vetting a field for development. Public records provide the data used for initial screening, but it is the owner's records that the most useful information will be found. Public records will typically not include mechanical issues encountered after a well is completed. An offer to acquire assets is typically contingent upon review of these records.
- Trimeric reviewed literature on well integrity concerns for CO_2 injection (Bachu 2009, Hawkes 2011, Sacuta 2015, Laumb 2017) to identify well construction parameters that might be included in a well screening methodology.
    - Bachu (2009) reviewed 31 wells for CO_2 injection and 48 wells for disposal of produced gas in Alberta, Canada for risk of leakage. Incidence of well failure was greater for converted wells than for purpose-drilled wells. Failures due to CO_2 injection were mostly from tubing and packing failures and were easily detected and repaired. More common were failures due to general causes encountered in the general well population, e.g., casing failure due to external corrosion. The authors noted that the failure rate of wells decreased for wells constructed after 1994 regulations for injection and disposal wells in Alberta, Canada went into effect. A well screening methodology for the Gulf of Mexico could likewise take into account any regulatory changes over the course of the time period in which wells were drilled in the target reservoir or could compare the regulations applied in Alberta to those applicable in the Gulf of Mexico to highlight potential issues.
    - The most important indicator of wellbore integrity is cement integrity according to Hawkes (2011). Laboratory tests showed that CO_2 attack on the porosity of the cement is unlikely to cause significant wellbore failure in well-cemented wellbores using

cements with relatively low porosities or water-to-cement ratios. Cementing issues which leave gaps between the bond interfaces and poor cementing practices which allow cement channeling are the main cause for concern. A well screening methodology for the Gulf of Mexico could likewise include review of well records for cementing practices used for well completion and well plugging.

- In Sacuta (2015), the authors reviewed wellbore integrity in the Weyburn-Midale field. The parameters most likely to affect integrity of wells were determined by investigating well records. These parameters included cementing, debonding between casings and wall rock, and channeling in the cement itself. The authors recommended ranking wells in order of importance for monitoring and investigation, with priority given to the cement plugs and sheaths of abandoned wells. The authors recommended that new wells used for CO_2 injection use CO_2-resistant cement across the whole injection zone. While the CO_2 may have very low moisture levels, the storage zone itself may have significant moisture. If required, remediation might be required prior to injection or might be deferred if the CO_2 plume will take time to reach the wellbore; the authors state that remedial operations should focus on the injection zone only.
- Laumb (2017) assessed wellbore corrosion and failure in the Weyburn Field. Well history was assembled based on available data, including completion reports and notes. Casing leaks were identified by failed pressure tests. The primary challenge to identifying and evaluating wellbore integrity degradation was the sparse time-lapse corrosion and cement evaluation data. Casing and cement evaluation logs are typically only run when there is an indication of an issue within a wellbore, and data are only collected in the zone where an issue is expected to exist. The authors postulated that the lack of data may be an indication that overall wellbore conditions were generally sufficient in the Weyburn field. The well screening criteria for the Gulf of Mexico could include pressure test results; Trimeric is determining how to obtain these data.

References

[Bachu 2009]
Bachu, S. and T. Watson. "Review of failures for wells used for CO_2 and acid gas injection in Alberta, Canada." Proceedings of GHGT-9 as published in Energy Procedia 1 (2009), p. 3531-3537. doi: 10.1016/j.egypro.2009.02.146

[Chakrabarti 2005]
Chakrabarti, S. editor. Handbook of Offshore Engineering, Volumes 1 and 2. Elsevier.

[Hawkes 2011]
Hawkes, C., C. Gardner, T. Watson, and R. Chalaturnyk. "Overview of wellbore integrity research for the IEA GHG Weyburn-Midale CO_2 Monitoring and Storage Project." Proceedings of the GHGT-10 as published in Energy Procedia 4 (2011), p. 5430-5437.

[IEAGHG 2013]
IEAGHG. "CO_2 Pipeline Infrastructure." 2013/18, December 2013.

[Interview 2019]
Interview with Undisclosed Expert, conducted by Joe Lundeen, Darshan Sachde, and Katherine Dombrowski of Trimeric Corporation, 27 September 2019.

[Kaiser 2018]
Kaiser, J. and S. Narra. "Review of shallow water GoM structure inventory offers preview of decommissioning requirements." Offshore Magazine, March – August 2018.

[Laumb 2017]
Laumb, J., K. Glazewski, J. Hamling, A. Azenkeng, N. Kalenze, and T. Watson. "Corrosion and failure assessment for CO_2 EOR and associated storage in the Weyburn Field." Proceedings of the GHGT-13 as published in Energy Procedia 114 (2017), p. 5173-5181.

[Sacuta 2015]
Sacuta, N., A. Young, and K. Worth. "International Energy Agency (IEA) Greenhouse Gas (GHG) Weyburn-Midale CO_2 Monitoring and Storage Project." Final Technical Report by the Petroleum Technology Research Centre for DOE-NETL Project DE-FE0002697, 22 December 2015.

[UK 2019]
UK Department for Business, Energy and Industrial Strategy. "Re-use of Oil and Gas Assets for Carbon Capture Usage and Storage Projects: Consultation." July 2019.

[USEPA 2012]
USEPA. "Underground Injection Control (UIC) Program Class VI Well Construction Guidance." EPA 816-R-11-020, May 2012.

[USEPA 2018]
USEPA. "Underground Injection Control (UIC) Program Class VI Implementation Manual for UIC Program Directors." EPA 816-R-18-001, January 2018.

[Zhou 2014]
Zhou, D, Y. Zhang, and S. Haszeldine. "Engineering Requirements for Offshore CO_2 Transportation and Storage: A Summary Based on International Experiences." UK-China (Guangdong) CCUS Centre. Accessed at https://www.era.lib.ed.ac.uk/bitstream/handle/1842/15769/Engineering%20Requirements%20for%20Offshore%20CO2%20Transportation%20and%20Storage%20GDCCUS%20Zhou%20Zhang%20Haszeldine%20March%202014.pdf?sequence=1&isAllowed=y

<u>Subtask 5.1.2 Evaluate feasibility of subsea template in GoM</u>

(See Task 1, note on Aker Solutions.)

Subtask 5.1.3 Preliminary Risk Assessment of CO2 Release from Truck/Barge Transfer Operations

No activity this quarter.

Subtask 5.1.4 Site Leasing

In September, co-PI, Tip Meckel, met with Robert Hatter and George Martin at the GLO (Texas General Land Office) to discuss CCUS developments, including an update of 45Q and implications for developing CCUS projects on lands owned and managed by the GLO. The meeting resulted in a better understanding of leasing concepts for CO_2 storage projects, easements for pipeline development, and comparisons with lease structures for wind and solar projects.

Subtask 5.2: Scenario Optimization

Trimeric Corp.

During the most recent quarter, Trimeric continued outreach efforts along the Texas Gulf Coast, including contact with project personnel on a new LNG facility along the Texas Gulf Coast. The GoMCarb project background was shared with the contact who has forwarded on the information to project leadership. The project is not identified at this time since Trimeric has not received a response to the initial inquiry at the time of this writing.

In addition, to facilitate outreach and scenario optimization, Trimeric developed a basic block flow diagram of an LNG facility and the potential integration of CO_2 storage into the existing process. As noted previously, LNG facilities represent an important source along the Gulf Coast for the following reasons:

- CO_2 is already separated from the incoming natural gas to facilitate the liquefaction process – this leads to a potentially large, high purity CO_2 source.
- The CO_2 is often sent to an incinerator as part of the gas separated from the natural gas. CO_2 (an inert in the combustion process) increases the cost of the incineration process. Diverting CO_2 from the incinerator would potentially provide benefits to the LNG facility.
- LNG facilities are near the coastline, simplifying transport logistics for storage.

Figure 5.2.1 depicts a generic LNG pre-treatment process including potential integration and benefits of CO_2 storage.

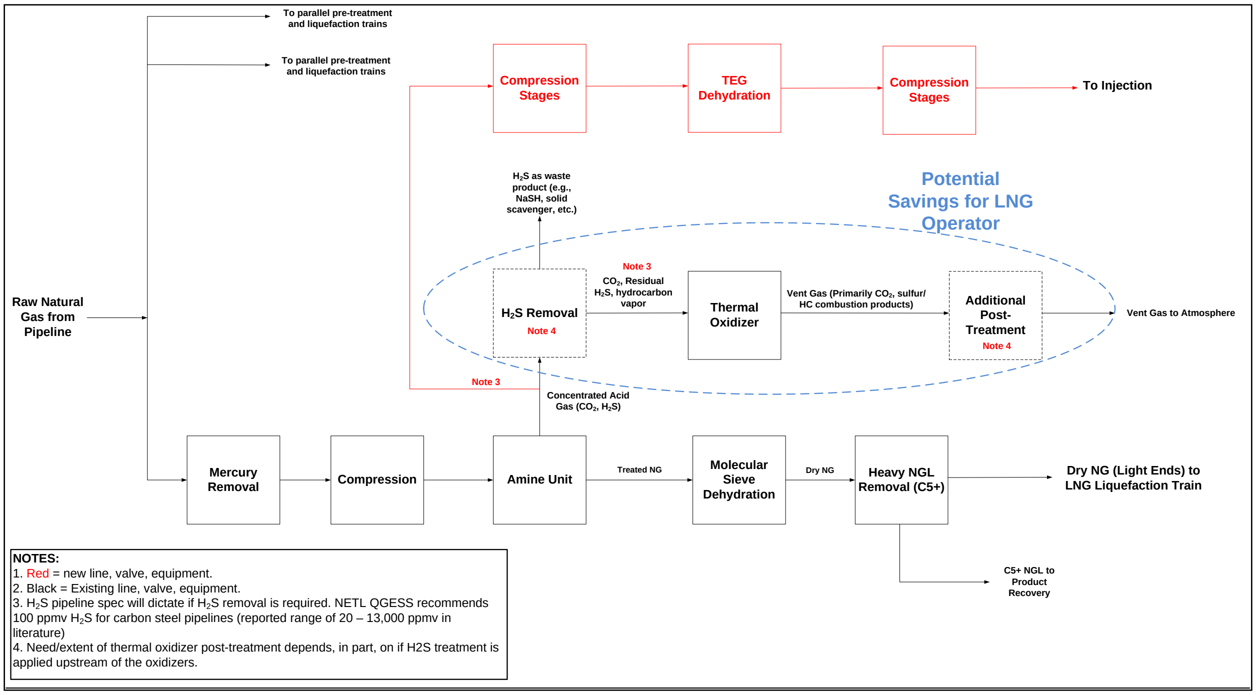

Figure 5.2.1 - Overview of LNG Liquefaction Pre-Treatment Train and Potential CO_2 Storage Project Integration/Benefits

Lamar University

This research study identifies the most efficient and cost-effective strategy for the compression of CO_2 captured from the major CO_2-producers found at a refinery. There can be various point sources of CO_2 (i.e. furnaces, boilers, fluidized catalytic crackers, methane steam reformers, and electric power generators). Van Straelan et al. (2010) attempted to identify and classify the key sources of CO_2 from a refinery into 4 major categories (Table 5.2.1). The feasibility of capture from auxiliary sources is based on the available amine technology used for CO_2 separation (i.e. capture). Attempting to capture from smaller CO_2 producers could result in higher operating expenses (OPEX). With the current technology, it is predicted that of the total refinery CO_2 emissions, 40% of those emissions occur from these point sources.[1]

Table 5.2.1- Description of Unit Operations within a typical Petroleum Refinery that produces CO_2

CO_2 Producer	***Description***
Furnaces and Boilers	Heat required for separating liquid feed and provide heat of reaction for processes such as reforming and cracking
Fluid Catalytic Cracker	CO_2 generated when a low hydrogen feed is upgraded to produce more valuable products
Hydrogen Generation Units	Most Hydrogen production processes also produce CO_2 as a by-product (i.e. Steam Methane Reformer)

Utilities	CO_2 generated from production of electricity and steam at the refinery

In this research, Aspen Plus™ is used to simulate the various CO_2 point sources. These process models are then used to size compressors needed for CO_2 delivery to a pipeline. Since there is no “one size fits all” design for refineries, factors to be included in the Aspen simulations are 1) refining capacity (250,000 – 700,000 bbl/day), 2) quality of crude oil (API gravity and PONA), and 3) final products (gasoline, diesel, jet fuels, lubricants). These variables will lead to the design and deployment of optimized compressions strategies. The different compression strategies that will be taken under consideration are:

a) Compression of CO_2 to liquid phase

    a. *Using individual compressors to compress CO_2*

This strategy deploys the individual smaller compressors at every CO_2 point source in the refinery and transport the CO_2 in super-critical (SC) phase to the offshore site for CO_2 injection.

    b. *Single on-site compressor*

This strategy would first collect all the captured CO_2 from every point source as it is in the gas phase, and then combine all the sources to compress them to liquid phase on the site, which will then be transported offshore for CO_2 injection

b) Compression of CO2 to super critical state

    a. *Using individual compressors to compress CO_2*

This strategy deploys the individual smaller compressors at every CO_2 point source in the refinery and transports the CO2 in super critical phase to the offshore site for CO_2 injection.

    b. *Single on-site compressor*

This strategy would first collect all the captured CO_2 from every point source as it is in the gas phase, and then combine all the sources to compress them to SC phase on the site, which will then be transported offshore for CO_2 injection

c) No Compression

    a. This strategy deals with the transport of CO_2 gas using pipelines to the offshore site where it will be compressed to supercritical state before injection.

The economic feasibility of all the three compression strategies will be studied and tailored to suit the needs of the refineries in Southeast Texas. Valero Refinery, in partnership with Air Products, Inc., have captured approximately 4 million tons of CO_2 from the two steam Methane Reformers present in the refinery. Hence, the first model to be simulated using Aspen will be the Steam Methane Reformer.

Aspen Simulation of Steam Methane Reformer

Steam Methane Reformation

Hydrogen production via Methane Steam Reforming (SMR) involves the reaction of methane with steam in a 1:3 molar ratio to form Carbon Monoxide and Hydrogen (or Syngas).[2,3] This is a two-step process where the first reaction is the Methane Steam Reforming (MSR) which occurs in the presence of nickel-alumina catalyst. It is an endothermic reaction operating at ~700 ^oC. The two main reactions occurring in SMR reactor are:

1. $CH_4 + H_2O \rightarrow CO + 3H_2 \qquad \Delta H\ (298K) = 206.1\ KJ/mol$
2. $CH_4 + 2H_2O \rightarrow CO_2 + 4H_2 \qquad \Delta H\ (298K) = 165\ KJ/mo$

A third reaction occurring in the process is called the Water Gas shift reaction. It is a reversible, exothermic reaction. An Fe-based catalyst or a copper-based catalyst is commonly used.

3. $CO + H_2O \rightarrow CO_2 + H_2 \qquad \Delta H\ (298K) = -41.15\ KJ/mol$

The rates of reactions for all the three equations are as follows[2]:

1. $r_1 = \dfrac{\frac{k_1}{P_{H_2}{}^{2.5}}\left(P_{CH_4}P_{H_2O} - \frac{P_{H_2}^3 P_{CO}}{K_1}\right)}{(DEN)^2}$

2. $r_1 = \dfrac{\frac{k_2}{P_{H_2}{}^{3.5}}\left(P_{CH_4}P_{H_2O}^2 - \frac{P_{H_2}^4 P_{CO_2}}{K_2}\right)}{(DEN)^2}$

3. $r_1 = \dfrac{\frac{k_3}{P_{H_2}{}^{3.5}}\left(P_{CO}P_{H_2O} - \frac{P_{H_2} P_{CO_2}}{K1}\right)}{(DEN)^2}$

Where $DEN = 1 + K_{CH_4}P_{CH_4} + K_{H_2}P_{H_2} + K_{CO}P_{CO} + \frac{K_{H_2O}P_{H_2O}}{P_{H_2}}$

In this work, the sizing of the SMR, and therefore the amount of CO_2 produced, is based on the refinery capacity and the quality of the crude oil. The range of H_2 needed is 300 – 700 SCF/bbl. In recent years, the Permian Basin has been supplying a considerable amount of crude oil to Southeast Texas refineries. Crude from the Permian Basin is a lighter crude (i.e., requiring less H_2 for upgrading) than many Middle Eastern crudes.

References

(1) van Straelen, J.; Geuzebroek, F.; Goodchild, N.; Protopapas, G.; Mahony, L. CO2 Capture for Refineries, a Practical Approach. *Int. J. Greenh. Gas Control* **2010**, *4* (2), 316–320.

(2) Xu, J.; Froment, G. F. Methane Steam Reforming, Methanation and Water-gas Shift: I. Intrinsic Kinetics. *AIChE J.* **1989**, *35* (1), 88–96.

(3) Amran, U. I.; Ahmad, A.; Othman, M. R. Kinetic Based Simulation of Methane Steam Reforming and Water Gas Shift for Hydrogen Production Using Aspen Plus. *Chem. Eng. Trans.* **2017**, *56* (March), 1681–1686.

Subtask 5.2.1 Analog Site Optimization

No activity during this quarter

Subtask 5.3: Communication

See Subtask 5.1.4, Site Leasing.

TASK 6.0: Knowledge Dissemination

Subtask 6.1: Stakeholder Outreach

University of Texas, Stan Richards School of Advertising & Public Relations

In July, the team finalized the interview guide and in-depth interviews for the focus groups mentioned in the previous report. We also recruited participants and scheduled meeting times for the interviews. The interviews were carried out by post-doctoral scholar Dr. Rachel Lim, Dr. Hilary Olson and Research Program Coordinator Emily Moskal over a three-day period from July 30 to Aug. 1 in Beaumont, TX. During Beaumont trip members of the team also attended the Port Arthur Chamber of Commerce Industry Show to network with relevant CCS stakeholders. Overall, the team connected with ~40 stakeholders in Winnie, Beaumont, and Port Arthur, TX.

The preliminary insights from these qualitative interviews were presented at the Gulf Coast Carbon Center's Summer 2019 Open House & Progress Review on August 6 in Houston. Dr. Lim presented a poster titled, "Benefit & Risk Communication Research In The Golden Triangle Area" co-authored with Dr. Lucy Atkinson, Dr. LeeAnn Kahlor, Dr. Olson and Ms. Moskal.

In September, the team continued to analyze the data from the qualitative interviews, relying on these insights to develop the questions and stimuli for the survey, to be fielded this fall. We also submitted a protocol to UT's Institutional Review Board to conduct the study and received approval in September. The group continues to finesse the questions and the stimuli to be included in the survey, which will be fielded among a sample of 900 residents of the Texas Gulf Coast area.

Lamar University

Performed in collaboration with UT team members (Hilary Olson, Emily Moskal, and Rachel Lim), focus group discussions were conducted at Lamar University (July 30 – Aug 1) to determine the extent of current knowledge by various stakeholder groups in the Southeast Texas area in regards to CO_2, its effects in the local environment, and people's concern for reducing CO_2 emissions.

Subtask 6.2: Technical Outreach

Dr. Curtis Oldenburg submitted the following abstract to the fall AGU (American Geophysical Union) meeting in San Francisco.

Four-region process modeling of offshore CO_2 well blowouts

C.M. Oldenburg, L. Pan, Y. Zhang, Q. Zhou

Energy Geosciences Division, LBNL

Interest in offshore geologic carbon sequestration is motivating risk assessment of subsea pipeline and well leakage in the Gulf of Mexico (GoMCarb project). In this study, we address whether rare offshore CO_2 blowouts result in CO_2 emissions at the sea surface. Four distinct regions or domains control CO_2 transport: (1) the CO_2-containing reservoir deep below the seafloor; (2) the well and pipeline system; (3) the water column; and (4) the atmosphere above the sea surface. We model these four regions by linking together three simulation models. The reservoir containing the CO_2 is tightly coupled to the well and pipeline and we use T2Well for modeling this coupled system. T2Well models two-phase flow in the porous medium and in the well-pipeline system based on Darcy's law and the drift-flux model, respectively. For CO_2 transport in the water column, we use TAMOC which models jet and buoyant plume flow in ambient seawater by discrete and Lagrangian particle and integral model approaches. For the atmospheric dispersion above the sea surface, we use the NRAP MSLR which is a simple nomograph approach derived from empirical data. Each upstream model feeds output to the next downstream model (one-way coupling). Preliminary T2Well simulations of a very rare large-scale CO_2 blowout scenario involving a 2-inch diameter hole in a pipeline feeding a CO_2 injection well results in 35 kg/s leakage rate at the seafloor. Using established methods, we predict that CO_2 emitted into the water column at this rate forms bubbles with an average size of ~0.5 mm which facilitates strong dissolution of CO_2 into the seawater. TAMOC results suggest that for a blowout in 50 m of water, less than 1% of the leaked CO_2 will make it to the sea surface, while in 10 m of water 94% of the CO_2 will arrive at the surface and further leak into the atmosphere. Using a 1% CO_2 concentration in air above the sea surface as the criterion for safety with a 1 m/s wind at an elevation of 10 m, the NRAP MSLR forecasts a downwind safety distance of 0.5 km for the 10 m case, and 90 m for the 50 m case. In general, our preliminary modeling finds that large CO_2 well blowouts, which will be very rare events, are unlikely to manifest as acute CO_2 emissions at the sea surface in deep water, while large blowouts in shallow water (<10 m) will result in strong emissions at the sea surface.

Plain language summary

Offshore geologic carbon sequestration entails risk of CO_2 well or pipeline leakage. We have developed a four-region model for assessing consequences of rare offshore CO_2 well or pipeline blowouts. Model results show that, for a scenario involving a large blowout from a 2-inch hole in a supply pipeline connected to an injection well, most of the CO_2 emitted from a deep (>50 m) offshore pipeline will dissolve before reaching the sea surface, while a large blowout in shallow water (<10 m) will result in a large leakage flux at the sea surface.

1. The following abstract was presented at the annual SEG (Society of Exploration Geophysicists) convention in San Antonio, Texas on September 16, 2019.

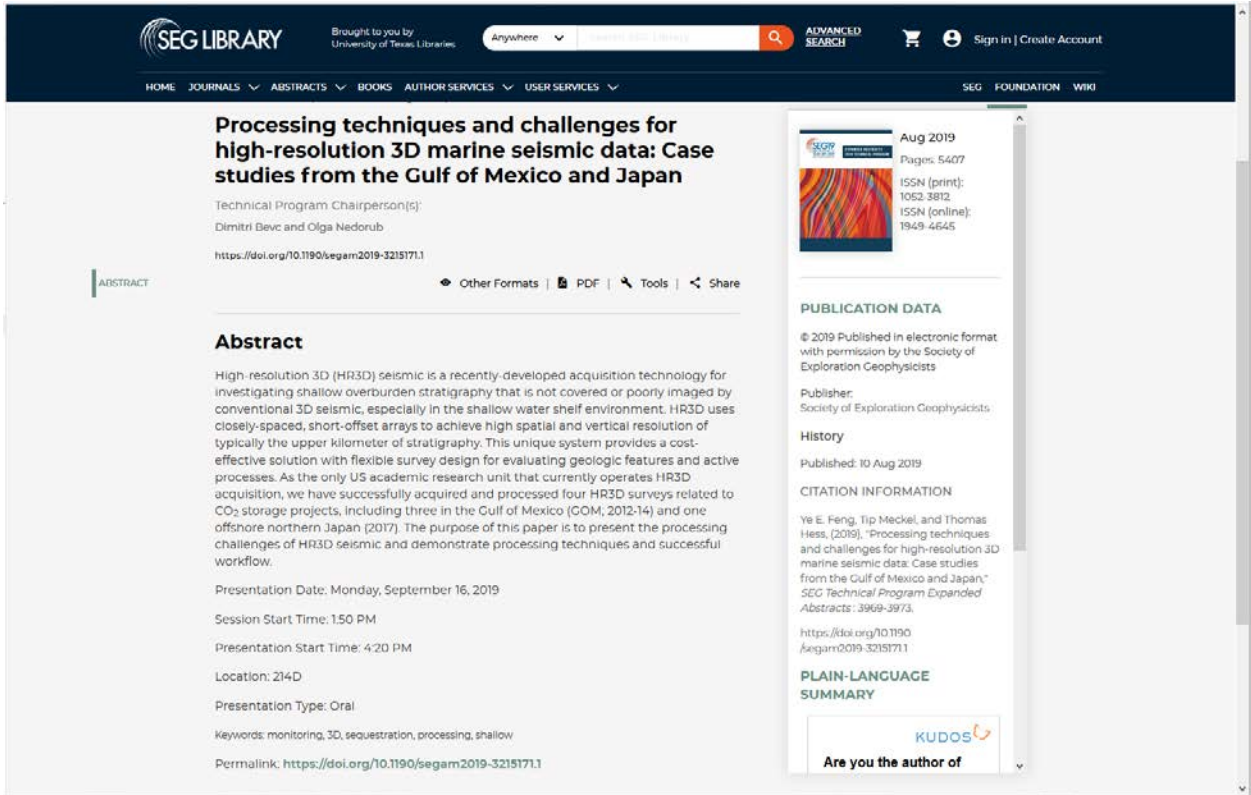

SEG LIBRARY
Brought to you by University of Texas Libraries
Anywhere
ADVANCED SEARCH
Sign in | Create Account
HOME JOURNALS ABSTRACTS BOOKS AUTHOR SERVICES USER SERVICES SEG FOUNDATION WIKI

Processing techniques and challenges for high-resolution 3D marine seismic data: Case studies from the Gulf of Mexico and Japan

Technical Program Chairperson(s):
Dimitri Bevc and Olga Nedorub

https://doi.org/10.1190/segam2019-3215171.1

ABSTRACT

Other Formats | PDF | Tools | Share

Abstract

High-resolution 3D (HR3D) seismic is a recently-developed acquisition technology for investigating shallow overburden stratigraphy that is not covered or poorly imaged by conventional 3D seismic, especially in the shallow water shelf environment. HR3D uses closely-spaced, short-offset arrays to achieve high spatial and vertical resolution of typically the upper kilometer of stratigraphy. This unique system provides a cost-effective solution with flexible survey design for evaluating geologic features and active processes. As the only US academic research unit that currently operates HR3D acquisition, we have successfully acquired and processed four HR3D surveys related to CO_2 storage projects, including three in the Gulf of Mexico (GOM; 2012-14) and one offshore northern Japan (2017). The purpose of this paper is to present the processing challenges of HR3D seismic and demonstrate processing techniques and successful workflow.

Presentation Date: Monday, September 16, 2019

Session Start Time: 1:50 PM

Presentation Start Time: 4:20 PM

Location: 214D

Presentation Type: Oral

Keywords: monitoring, 3D, sequestration, processing, shallow

Permalink: https://doi.org/10.1190/segam2019-3215171.1

Aug 2019
Pages: 5407
ISSN (print): 1052-3812
ISSN (online): 1949-4645

PUBLICATION DATA

© 2019 Published in electronic format with permission by the Society of Exploration Geophysicists

Publisher:
Society of Exploration Geophysicists

History

Published: 10 Aug 2019

CITATION INFORMATION

Ye E. Feng, Tip Meckel, and Thomas Hess, (2019), "Processing techniques and challenges for high-resolution 3D marine seismic data: Case studies from the Gulf of Mexico and Japan," *SEG Technical Program Expanded Abstracts* : 3969-3973.

https://doi.org/10.1190/segam2019-3215171.1

PLAIN-LANGUAGE SUMMARY

KUDOS

Are you the author of

2. The following poster (Figure 6.2.2) was presented at NETL's "Addressing the Nation's Energy Needs Through Technology Innovation – 2019 Carbon Capture, Utilization, Storage, and Oil and Gas Technologies Integrated Review Meeting" in Pittsburgh, PA on August 27 & 28.
3. In September the same poster (Figure 6.2.2) was presented at the 7th annual Bureau of Economic Geology Research Symposium (Figure 6.2.3).

Addressing the Nation's Energy Needs Through Technology Innovation — 2019 Carbon Capture, Utilization, Storage, and Oil and Gas Technologies Integrated Review Meeting, August 26th–30th, Pittsburgh, PA

Partnership for Offshore Carbon Storage Resources and Technology Development in the Gulf of Mexico

Reynaldy Fifariz, Tip Meckel, Ramon Trevino, Omar Ramirez Garcia, Izaak Ruiz, Mike DeAngelo, Dallas Dunlap
Gulf Coast Carbon Center, Bureau of Economic Geology, The University of Texas at Austin

1. Abstract

The primary goal of the "Partnership for Offshore Carbon Storage Resources and Technology Development in the Gulf of Mexico" (**GoMCarb**) is to develop an Offshore Carbon Storage Partnership that is similar in structure to the existing Regional Carbon Sequestration Partnerships (RCSPs) Characterization Phase, but focused on sub-seafloor geologic storage in the northwestern Gulf of Mexico. **GoMCarb**'s Offshore Storage Resource Assessment task has specific geographic areas of interest including the nearshore waters of the upper Texas coast (i.e., the High Island blocks of the Texas state waters and neighboring Offshore Continental Shelf (OCS) federal waters.

To that end, two oil and gas fields, High Island 10L and 24L, have been assessed for their potential CO_2 storage resources based on 3D seismic, well data and hydrocarbon production data. Lower Miocene sandstone reservoirs beneath the regional transgressive Amphistegina B (aka "Amph B") shale were targeted in the assessments. Sequence stratigraphic analysis, correlations, and mapping between marine flooding surfaces, MFS-9 to MFS-10, demonstrate how transgressive and regressive events resulted in a relatively thick package of stacked sandstone reservoirs, increasing the overall potential of the CO_2 storage resources. Geo-cellular models were then generated to populate volumetric properties for both sites.

Estimating CO_2 storage resources with various methods and comparing the results from both sites, provide better insight to how geological interpretations and volumetric parameters on a site-scale can influence the potential CO_2 storage resources. Ultimately, the main goal of the research is to test an improved workflow for assessing CO_2 storage sites.

2. Global Context

Global CCS Institute (2018)

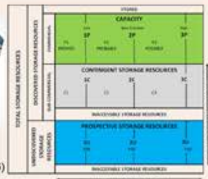

SRMS (2016)

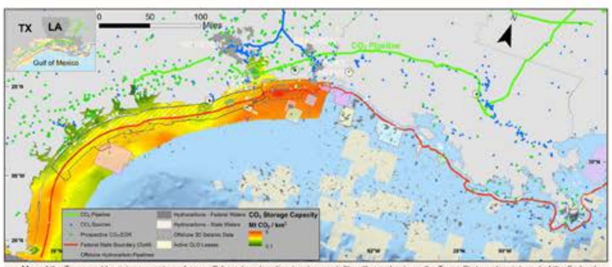

Map of the Texas and Louisiana coasts and near offshore (see location inset upper left), with emphasis on the Texas State waters inboard of the Federal-State boundary (solid red line). Extensive CO_2 storage resources estimation for Miocene stratigraphy: a total of 129 Gt (Wallace et al., 2013).

3. Regional Setting

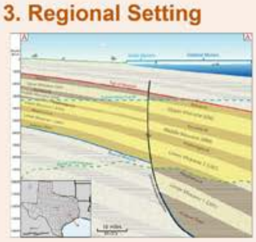

Wallace et al. (2013)

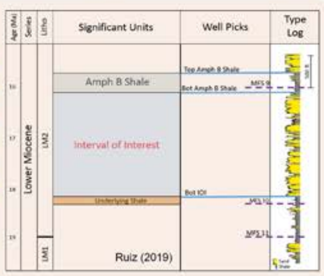

Ruiz (2019)

4. Site Assessment

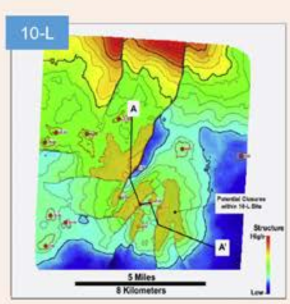

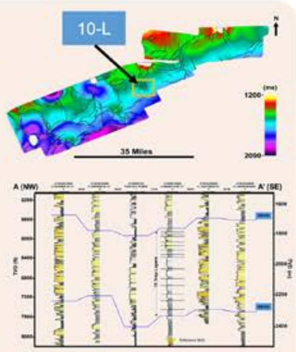

Using volumetric-based deterministic method: 10-L site (stacked storage) resulted in approximately **50 MT** of CO_2 storage resources.

DeAngelo et al. (2019)

5. Current Status

CO_2 storage sites characterization, modeling, and assessment of CO_2 storage resources have been performed for two existing fields in High-Island block within a 3D seismic dataset. In addition to the 3D seismic (1,200 mi^2 or 3,100 km^2), data included 72 well-log suites (all with SP logs and 12 with density/neutron porosity logs).

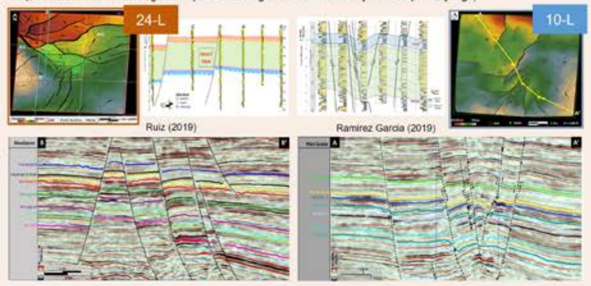

Seismic data owned or controlled by Seismic Exchange, Inc.; Interpretation is that of the Bureau of Economic Geology

6. Geo-cellular Modeling

Define grid geometry from framework → Upscale properties to grid cells → Variogram modeling → Run facies and porosity modeling

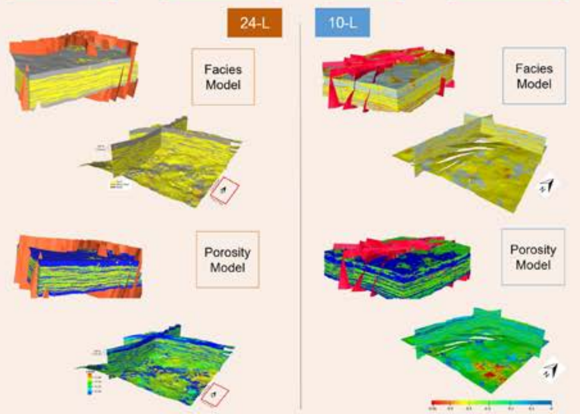

Ruiz (2019)

Ramirez Garcia (2019)

7. CO_2 Storage Resources Estimation

$$G_{CO2} = A \cdot h_{net} \cdot \phi_{eff} \cdot \rho \cdot E_{saline}$$ (Goodman et al., 2011)

	24-L			10-L		
	P10	P50	P90	P10	P50	P90
E_{saline} = Ev*Ed (Unspecified)	7.40%	14%	24%	7.40%	14%	24%
3D Model [Mt]	57	108	186	12	24	41
E_{saline} = Ev*Ed (Shallow shelf)	11%	23%	41%	11%	23%	41%
CO_2 SCREEN [Mt]	85	179	317	17	39	72

8. References

1. CO_2 Storage Resources Management System (2016). Society of Petroleum Engineers.
2. DeAngelo, M. V., Fifariz, R., Meckel, T., & Treviño, R. H. (2019). A seismic-based CO_2-sequestration regional assessment of the Miocene section, northern Gulf of Mexico, Texas and Louisiana. *International Journal of Greenhouse Gas Control, 81*, 29-37.
3. Global CCS Institute (2018). The Global Status of CCS.
4. Goodman, A., Hakala, A., Bromhal, G., Deel, D., Rodosta, T., Frailey, S., ... & Huerta, N. (2011). US DOE methodology for the development of geologic storage potential for carbon dioxide at the national and regional scale. *International Journal of Greenhouse Gas Control, 5*(4), 952-965.
5. Ramirez Garcia, O. (2019). Geologic characterization and modeling for quantifying CO_2 storage capacity of the High Island 10-L field in Texas state waters, offshore Gulf of Mexico. The University of Texas at Austin, Master's thesis.
6. Ruiz, I. (2019). Characterization of the High Island 24L field for modeling and estimating CO_2 storage capacity in the offshore Texas state waters, Gulf of Mexico. The University of Texas at Austin, Master's thesis.
7. Trevino, R.H., and T.A. Meckel, Eds., 2017, Geological CO2 Sequestration Atlas of Miocene Strata, Offshore Texas State Waters, Report of Investigations #283, Bureau of Economic Geology, Austin, TX.
8. Wallace, K.J., T.A. Meckel, D.L. Carr, R.H. Trevino, and C. Yang, 2013, Regional CO2 sequestration capacity assessment for the coastal and offshore Texas Miocene interval, Greenhouse Gases Science and Technology, 4:53-65, DOI 10.1002/ghg.

9. Acknowledgement

This material is based upon work supported by the U.S. Department of Energy – National Energy Technology Laboratory, under award agreement **DE-FE0031558**

Figure 6.2.2 – Poster presented at "Addressing the Nation's Energy Needs Through Technology Innovation – 2019 Carbon Capture, Utilization, Storage, and Oil and Gas Technologies Integrated Review Meeting" in Pittsburgh, PA

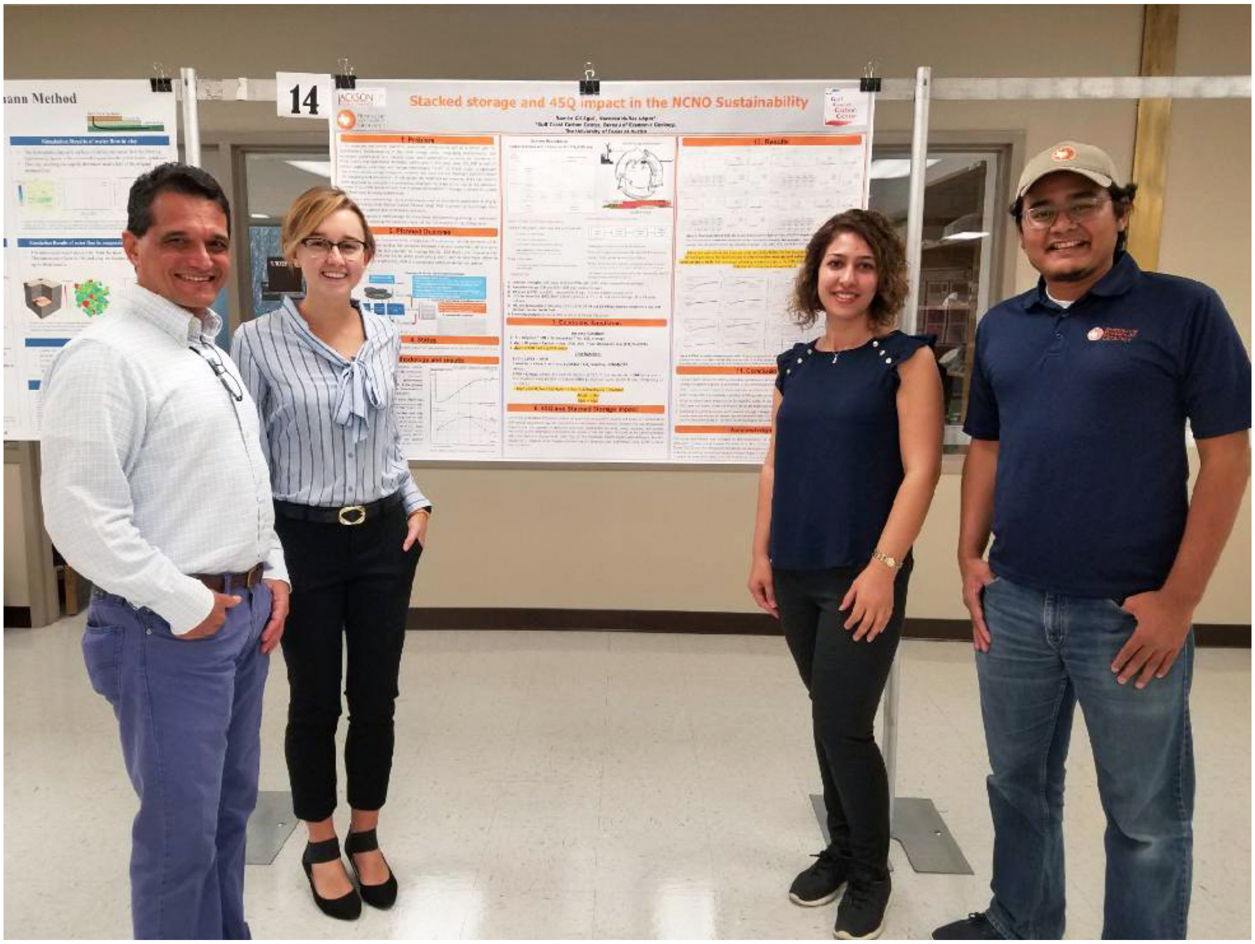

Figure 6.2.3 – The first author (far right) of the poster in figure 6.2.2 with colleagues at the 7th Annual Bureau of Economic Geology Research Symposium.

On August 27, PI, Dr. Susan Hovorka presented, a talk (Figure 6.2.4) summarizing the project's accomplishments during the previous year at NETL's "Addressing the Nation's Energy Needs Through Technology Innovation – 2019 Carbon Capture, Utilization, Storage, and Oil and Gas Technologies Integrated Review Meeting."

Figure 6.2.4 – Title slide of annual summary presentation given by project PI, Dr. Susan Hovorka.

Subtask 6.3: Advisory Committee

On August 27, 2019, some members of the GoMCarb advisory committee and members of the research and outreach ("RO") team met in Pittsburgh. Members attending in person were in Pittsburgh to attend NETL's "Addressing the Nation's Energy Needs Through Technology Innovation – 2019 Carbon Capture, Utilization, Storage, and Oil and Gas Technologies Integrated Review Meeting." The meeting was convened by Advisory Committee chair, Tim Dixon, and Katherine Dombrowski from Trimeric Corporation (Figure 6.3.1), provided a presentation on surface-level CCS infrastructure, including details on pipeline requirements.

In Person Attendees:

Joshua White (LLNL)

Katherine Dombrowski (Trimeric Corp.)

Ray McKaskle (Trimeric Corp.)

Curtis Oldenburg (LBNL)

Owain Tucker (Shell)

Daiji Tanase (Japan CCS Co. Ltd.)

Ramon Trevino (University of Texas)

Tip Meckel (University of Texas)

Susan Hovorka (University of Texas)
Emily Moskal (University of Texas)
Tim Dixon, Advisory Cmte. Chair (IEAGHG)
Katherine Romanak (University of Texas)
Reynaldy Fifariz (University of Texas)

Virtual Attendees
Darshan Sachde (Trimeric Corp.)
Joe Lundeen (Trimeric Corp.)
Robert Finley (Consultant)
Sean Brennan (USGS)
Jonathan Ajo-Franklin (Rice University)

Figure 6.3.1 – Katherine Dombrowski (far right by lectern and microphone) preparing to begin her presentation at the Advisory Committee and RO

PLANS FOR THE NEXT PROJECT QUARTER

In the next quarter, work will continue on:

Task 1

- Establish subcontract with Aker Solutions.
- Take possession of and test equipment ordered from Geometrics.

Task 2

Subtask 2.1:

Use the methodology (described in Subtask 2.1.1.2 Structural Interpretation) on the Offshore OBS mid-coast 3D and publicly available NAMSS seismic volumes that are deemed to have added value.

Subtask 2.1.3:

- Work to be done on HR3D datasets:

Re-processing of GOM2012 will be finished. GOM2013 and GOM2014 are prepped and reloaded with geometry and quality tested. Experiments have begun to see if the same or similar techniques used in GOM2012 will produce good results in the other two datasets. Once the parameters are optimized the same steps will quickly follow GOM2012 to completion.

	Data QC	Positional Corrections	Signal Processing	3D Statics and Balancing	Migration
GOM2012	Done	Done	Done	In Progress	In Progress
GOM2013	Done	Testing	Testing		
GOM2014	Done	Testing	Testing		

Task 3 Risk Assessment, Simulation and Modeling

- Subtask 3.2:

Work on the subtask's final report including the Mobility ratio sensitivity for the 2-fluid case (i.e., any f value: sealed, partially sealed or open outlet boundary) but with 2 fluids, "so we can change viscosity to have different mobility."

Task 4 Monitoring Verification and Assessment

- Subtask 4.1.4: Continue design of a controlled source for continuous DAS imaging in the water column and near-seafloor sediment

Task 5 Infrastructure, Operations and Permitting

- Subtask 5.1: Continued development of existing infrastructure "database" for High Island region. Trimeric will be seeking data on the existing wells, platforms and pipelines.
- Subtask 5.1: Continued development of methodology to evaluate existing infrastructure for re-use in CO_2 transportation with a focus of gathering and assessing industry expertise/experience on the subject. Continue to survey selected industry experts as they are identified.
- Subtask 5.2: Continued development of CO_2 source list along the Texas and Louisiana coast, including outreach and education of industry in the region.

Subtask 5.2: Add existing infrastructure data to CO_2 source data (in maps and database/spreadsheets) to provide first steps for longer-term scenario optimization

Task 6

- Field stakeholder survey in southeast Texas.
- Dr. Curtis Oldenburg will present a paper at the fall AGU (American Geophysical Union) meeting in San Francisco.
- Present topics in CCS to audiences of opportunity.

3. PRODUCTS

Publications, conference papers, and presentations.

Websites

http://www.beg.utexas.edu/gccc/research/gomcarb

Technologies or techniques

None generated to date.

Inventions, patent applications, and/or licenses

None generated to date.

Other products

None to date.

4. PARTICIPANTS & OTHER COLLABORATING ORGANIZATIONS

The University of Texas at Austin

Bureau of Economic Geology, GCCC (Gulf Coast Carbon Center)
Name: Susan Hovorka, PhD
Project Role: Principal Investigator
Nearest person month worked: 1
Contribution to Project: Leadership in planning and negotiating

Name: Tip Meckel, PhD
Project Role: Co-Principal Investigator
Nearest person month worked: 1
Contribution to Project: Dr. Meckel oversaw geologic interpretation work

Name: Ramón Treviño
Project Role: Co-Principal Investigator (project manager)
Nearest person month worked: 1
Contribution to Project: Mr. Treviño provided project management and project reporting; he acted at the primary contact for the NETL project manager and contracting specialist.

Name: Michael DeAngelo
Project Role: Researcher (geophysicist seismic interpreter)
Nearest person month worked: 1
Contribution to Project: Mr. DeAngelo conducted structural interpretation of the “TexLa Merge,” “Texas OBS” and “Chandeleur Sound” regional 3D seismic datasets.

Name: Katherine Romanak, PhD
Project Role: sediment geochemist
Nearest person month worked: 1
Contribution to Project: Liaison with Texas A&M GERG

Name: Reynaldy Fifariz, PhD
Project Role: post-doctoral fellow,
Nearest person month worked: 1
Contribution to Project: geological and seismic interpreter; liaison with Lamar U. doctoral student.

UT Institute for Geophysics, GBDS (Gulf Basin Depositional Synthesis) Industrial Associates Program

Name: John Snedden
Project Role: Senior Research Scientist
Nearest person month worked: 1
Contribution to Project: Dr. Snedden provides expertise in seismic stratigraphy and siliciclastic depositional systems.

Name: Jon Virdell
Project Role: Project Manager
Nearest person month worked: 1
Contribution to Project: Mr. Virdell provides project and GIS data management support.

Name: Marcie Purkey Phillips
Project Role: Biostratigrapher
Nearest person month worked: 1
Contribution to Project: Mrs. Purkey Phillips contributed expertise in biostratigraphy and integrated well and seismic data in the Chandeleur 3D survey area.

Fugro Marine Geoservices, Inc.

Lamar University

Louisiana Geological Survey

Trimeric Corp.

Lawrence Berkeley National Laboratory

Lawrence Livermore National Laboratory

TDI-Brooks, Inc.

Texas A&M University GERG (Geochemical & Environmental Research Group)

U.S. Geological Survey (USGS)

5. IMPACT:

6. CHANGES/PROBLEMS

Changes in approach and reasons for change: **None**

Actual or anticipated problems or delays and actions or plans to resolve them: **None**

Changes that have a significant impact on expenditures: **None**

Change of primary performance site location from that originally proposed: **None**.

7. SPECIAL REPORTING REQUIREMENTS

Respond to any special reporting requirements specified in the award terms and conditions, as well as any award specific requirements. **None**

References Cited

Burke, L. A., Kinney, S. A., Dubiel, R. F., & Pitman, J. K. (2012). Regional Map of the 0.70 PSI/FT Pressure Gradient and Development of the Regional Geopressure-Grandient Model for the Onshore and Offshore Gulf of Mexico Basin, U.S.A. . *GCAGS Journal, 1* 97-106.

Pitman, J. K. (2011). Reservoirs and petroleum systems of the Gulf Coast: Depth to top overpressure [map]. In <*http://www.datapages.com/Services/GISUDRIL/OpenFiles/ReservoirsandPetroleumSystemsoftheGulfCoast.aspx*>: U.S. Geological Survey.